NATIONAL ADVISORY COMMITTEE FOR AERONAUTICS

WARTIME REPORT

ORIGINALLY ISSUED

January 1943 as
Memorandum Report

THE EFFECT OF AMPHIBIOUS FLOATS ON THE POWER-OFF

STABILITY AND CONTROL CHARACTERISTICS

OF A TWIN-ENGINE CARGO AIRPLANE

By Steven E. Belsley and Roy P. Jackson

Ames Aeronautical Laboratory
Moffett Field, California

NACA

WASHINGTON

NATIONAL ADVISORY COMMITTEE FOR AERONAUTICS

MEMORANDUM REPORT

for the

Materiel Command, U.S. Army Air Forces

THE EFFECT OF AMPHIBIOUS FLOATS ON THE POWER-OFF

STABILITY AND CONTROL CHARACTERISTICS

OF A TWIN-ENGINE CARGO AIRPLANE

By Steven E. Belsley and Roy P. Jackson

SUMMARY

Power-off wind-tunnel tests of a 1/11-scale model of
a twin-engine cargo airplane equipped with amphibious floats
are reported herein. The tests were conducted in the Ames
7- by 10-foot wind tunnel at the request of the Army Air
Forces Materiel Command. Longitudinal and lateral stability
and control characteristics were investigated for three flap
positions.

At any given angle of attack, the floats have a
negligible effect on the lift coefficient. The longi-
tudinal destabilizing effect of the floats is equivalent
to a 2-percent M.A.C. shift of the neutral point. The
floats-on full-load stability is, however, greater than
the floats-off full-load stability because of a 3-percent
M.A.C. shift forward of the full-load center of gravity
when the floats are added. The directional stability is
reduced by the floats an amount equal to $\Delta dC_n/d\psi = 0.0004$.
Three of four tail variations tested to compensate for this
loss in directional stability proved satisfactory. The
floats do not change the control characteristics of either
the elevator or rudder. The measured drag increment due to
the floats is $\Delta C_{D_p} = 0.0095$. The test results indicate
that, if one of the three skid fins is added, the

longitudinal and lateral stability and control characteristics of the airplane will be as satisfactory floats on as floats off.

INTRODUCTION

At the request of the Army Air Forces Materiel Command, tests were conducted in the Ames 7- by 10- foot wind tunnel on a 1/11-scale model of a twin-engine cargo airplane. The purpose of the tests was to determine the effect of amphibious floats on the power-off longitudinal and lateral stability and control characteristics of the airplane and to determine the drag increment of the floats and the float gear.

The stability and control characteristics of the airplane in the floats-off condition were taken as a measure of satisfactory characteristics for the floats-on condition. Accordingly, corresponding floats-off and floats-on tests were made. The tests included yaw runs with several additions of tail area to improve the directional stability.

The tests were conducted during the period of November 14 to November 30, 1942, inclusive. All the data included herein previously have been transmitted in preliminary form.

MODEL

A 1/5-scale model of a two-engine cargo airplane was used in these tests. The full-scale dimensions of the airplane are given in table I. No attempt was made to check the model dimensions. The configuration key of the model, corresponding to the data presented, is given in table II. A three-view drawing of the airplane showing the relative positions of the normal gear, the floats, and the float gear is presented in figure 1. The model mounted in the tunnel is shown in the standard configuration, less tail, in figure 2, and in the standard configuration, floats on, in figure 3. Figure 4 shows the detail of the flaps and the float gear.

COEFFICIENTS AND CORRECTIONS

All results are presented in the form of standard NACA coefficients referred to the stability axes, a mutually

perpendicular system with the origin at the center of
gravity. In this system, the Z-axis lies in the plane of
symmetry and is perpendicular to the relative wind direction;
the X-axis is also in the plane of symmetry and is perpen-
dicular to the Z-axis; and the Y-axis is perpendicular to
the plane of symmetry. A definition of coefficients and
notation used in this report follows:

C_L lift coefficient $\left(\dfrac{\text{lift}}{qS} = \dfrac{\text{force along the Z-axis}}{qS} \right)$

$C_D{'}$ $\dfrac{\text{force along the X-axis}}{qS}$

C_D $C_D{'}$ at zero yaw

$C_Y{'}$ Lateral-force coefficient $\left(\dfrac{\text{lateral force}}{qS} \right.$

$\left. = \dfrac{\text{force along the Y-axis}}{qS} \right)$

$C_m{'}$ pitching-moment coefficient $\left(\dfrac{\text{pitching moment}}{qS\bar{c}} \right.$

$\left. = \dfrac{\text{moment around Y-axis}}{qS\bar{c}} \right)$

C_m $= C_m{'}$ at zero yaw

C_n yawing-moment coefficient $\left(\dfrac{\text{yawing moment}}{qSb} \right.$

$\left. = \dfrac{\text{moment around Z-axis}}{qSb} \right)$

$C_l{'}$ rolling-moment coefficient $\left(\dfrac{\text{rolling moment}}{qSb}\right.$

$\left. = \dfrac{\text{moment about X-axis}}{qSb}\right)$

C_{D_P} parasite drag coefficient $\left(C_D - \dfrac{C_L{}^2}{\pi A}\right)$

q dynamic pressure $\left(\dfrac{1}{2}\rho V^2\right)$

S wing area

$\bar{c}$ mean aerodynamic chord (M.A.C.)

b wing span

A aspect ratio (b^2/S)

Subscript

$(\ )_t$ due to tail

The prime is used to denote coefficients referred to stability axes that differ from coefficients referred to wind axes.

All tests were run at a dynamic pressure q of 75 pounds per square foot corresponding to a Reynolds number (based on M.A.C.) of 1,700,000.

Tares were obtained on the model by mounting it in the tunnel in the inverted position with a strut image system (fig. 5). The tares were taken as the change in the coefficients resulting from the addition of the image system. Stream-inclination corrections were also determined by use of the image system. Tunnel-wall corrections are defined in the appendix.

RESULTS AND DISCUSSION

The center-of-gravity (c.g.) locations and weights of
the twin-engine cargo airplane are presented in figure 6 for
the standard and empty cargo condition, with floats on and
floats off. A summary of figure 6 is given as follows:

Condition		Gross weight (lb)	Horizontal position from M.A.C. leading edge	Vertical position from M.A.C. leading edge	Vertical position from thrust line
Floats on	Standard cargo	29,000	20.80	-9.95	-2.68
	Empty cargo	20,277	11.85	-16.75	-9.48
Floats off	Standard cargo	26,000	23.40	1.06	8.34
	Empty cargo	16,600	18.85	-1.69	5.59

Note: The c.g. position is measured parallel and perpen-
dicular to the fuselage reference line in percent
of the M.A.C.

From the preceding table it is seen that the addition
of the floats shifts the c.g. position (airplane loaded)
about 3 percent M.A.C. forward and about 9 percent M.A.C.
down. For this reason the longitudinal stability at zero
yaw is summarized in the discussion below with respect to
the two loaded c.g. locations. All data are presented with
respect to the floats-on c.g. location except in the summary
plot (fig. 10) wherein data are presented about the c.g.
location corresponding to both the fully loaded floats-off
and floats-on conditions.

The relocation of the c.g. position will have but a
negligible effect on control-surface effectiveness and on
the lateral-stability characteristics. The only noticeable

change in the C_m' vs ψ curves will be roughly a constant shift. (The amount can be obtained from the summary longitudinal stability characteristics at zero yaw.)

Longitudinal Stability and Control

Longitudinal stability at zero yaw.- The effect of the floats on the longitudinal characteristics at zero yaw is shown for flaps up in figure 7, for flaps down 15° in figure 8, and for flaps down 45° in figure 9. The stability is summarized in figure 10. Figure 11 presents the effect of the float gear with flaps down.

At any given angle of attack, the floats reduced the lift a very small amount ($\Delta C_L \cong 0.05$) at low values of C_L, flaps up and flaps down, while at values of C_L near $C_{L_{max}}$ the reduction in lift is $\Delta C_L \cong 0.03$ flaps up and zero flaps down (figs. 7 to 9, inclusive).

The effect of the floats about any fixed c.g. position is to reduce the stability by $\Delta dC_m/dC_L = 0.018$ flaps up, and $\Delta dC_m/dC_L = 0.024$ flaps down 15° and 45°.

The values of dC_m/dC_L of figure 10, for the respective c.g. positions floats on and off summarized in the following table, indicate that the airplane in the loaded condition will exhibit a greater degree of stability floats on than floats off since the full-load c.g. shift more than compensates for the decreased dC_m/dC_L previously noted.

Condition		dC_m/dC_L	c.g. position and loading
Flaps up	Floats off	-0.166	(3) of figure 6
	Floats on	-0.180	(1) of figure 6
Flaps down 15°	Floats off	-0.160	(3) of figure 6
	Floats on	-0.164	(1) of figure 6
Flaps down 45°	Floats off	-0.153	(3) of figure 6
	Floats on	-0.162	(1) of figure 6

Due to the floats, however, there is a negative shift in the C_m value at zero lift corresponding to approximately 1° of elevator.

The effect of the float gear on the stability (fig. 11) is small and is sensibly constant with C_L and with flap position. The pitching-moment increment added by the gear is $\Delta C_m = -0.005$.

Pitching-moment characteristics in yaw.- The effect of the floats on the forces and moments in yaw are shown for flaps up in figures 12 and 13, for flaps down 15° in figure 14, and for flaps down 45° in figure 15.

The increment of $C_m{}'$ added by the floats is independent of the angle of yaw within the yaw range obtainable with the rudder ($\psi = \pm15°$). Because the $C_m{}'$ increment in yaw due to the float gear was independent of the yaw angle and therefore may be obtained from figure 11, the results are not presented.

Longitudinal control at zero yaw.- The elevator effectiveness at zero yaw with floats off and floats on is presented for flaps up in figures 16 and 17, for flaps down 15° in figures 18 and 19, and for flaps down 45° in figures 20 and 21.

The addition of the floats with the flaps up and the flaps down 15° does not change the elevator effectiveness for deflections within the range normally used ($\delta_e = 0°$ to -20°) but the effectiveness at deflections greater than -20° appears to be a function of both flap position and floats (figs. 16 to 19, inclusive). With the flaps down 45°, the elevator effectiveness for the full range of elevator deflection ($\delta_e = 0°$ to -25°) remains unchanged by the addition of the floats.

In the $C_{L_{max}}$ region, flaps down 45°, the value of C_m ($\delta_e = 0°$), for the floats on c.g. location, is more positive floats on than floats off (fig. 9). This characteristic will remain unchanged for any given c.g. position. The allowable forward c.g. location on the standard airplane is 11 percent M.A.C. (reference 1), while the empty cargo, floats on, c.g. location is 11.85 percent M.A.C. (fig. 6). This more rearward c.g. position combined

with the fact that the floats do not affect the elevator effectiveness when the flaps are down 45°, indicate that the airplane will be as satisfactory in landing floats on as floats off. In addition, the ground effect will be less when landing with floats or float gear than when landing with normal gear.

Longitudinal control in yaw.- The elevator effectiveness in yaw with floats off and floats on is presented for flaps up in figures 22 to 25, for flaps down 15° in figures 26 and 27, and for flaps down 45° in figures 28 and 29.

For any of the three flap positions, the addition of the floats resulted in no change in elevator effectiveness in yaw. For the several values of C_L at which investigations were made, the change in trim due to the addition of floats is small and sensibly constant within the yaw range ($\psi = \pm 15^\circ$) to which the rudder will trim (figs. 12, 13, 14, and 15). For any given c.g. location that may be obtained on the airplane with floats on, the elevator characteristics in yaw should, therefore, be as satisfactory as on the standard cargo airplane.

Lateral Stability and Control

Lateral stability in yaw.- The effect of the floats on the lateral-stability characteristics in yaw is presented flaps up in figures 30 and 31, flaps down 15° in figure 32, and flaps down 45° in figure 33. Details of the four tail variations tested are shown in figure 34 and photographs of the tail variations mounted on the model are shown in figures 35(a) to 35(d). The directional-stability results are summarized in figure 36.

The roll stability while slightly increased is not adversely affected by the addition of the floats.

The destabilizing increment of directional stability due to the floats ($\Delta dC_n/d\psi \cong 0.0004$) was virtually independent of flap position, angle of attack, and tail (figs. 30 to 33, inclusive). The condition of least stability (climb, $C_L \cong 0.9$, flaps up) was chosen for determining the tail variations required to compensate for the loss.

In figure 36 the destabilizing effect of the floats, tail off, is $\Delta dC_n/d\psi = 0.00041$ and tail on is $\Delta dC_n/d\psi = 0.00034$. The yawing moment of the tail, floats off, is $dC_{nt}/d\psi = -0.00193$ and floats on is $dC_{nt}/d\psi = -0.00200$. On the basis of these results, an increase in tail area of 17 percent would be required if the aspect ratio, taper ratio, and tail length were held constant. As an alternative to an entirely new vertical tail, the modifications in figure 34 providing additional area were tested. Because of the low effectiveness of low aspect ratio surfaces, the areas added were somewhat more than twice $0.17 \, S_v$.

The remainder of the data of figure 36 indicates that any of the three skid fins tested will be adequate to compensate for the loss in directional stability.

The large rectangular skid fin tested had 33 percent more area than the small rectangular skid fin but did not add to the directional stability. The addition of the vertical fin extension actually reduced the stability from -0.00086 to -0.00080 (fig. 36). These characteristics may be accounted for by the change in effective tail length due to the addition of area ahead of the existing fin.

The reversal in the curve of C_n vs ψ near zero yaw (fig. 36) was not investigated, since it was not a result of the floats. It apparently is not causing undue difficulty in flight. The reversal may very well be a discontinuity in sidewash angle affecting the vertical tail, caused by a stall in the wing-fuselage juncture. At higher Reynolds numbers such a discontinuity would probably be decreased or eliminated.

Directional control in yaw.- The effect of the floats on the rudder effectiveness is shown for flaps up in figures 37 to 40, inclusive, for flaps down 15° in figures 41 and 42, and for flaps down 45° in figures 43 and 44. The rudder effectiveness with the several tail variations installed is shown in figures 45 to 48, inclusive.

The addition of floats with the normal tail made no change in rudder effectiveness (figs. 37 to 44, inclusive). The angles of yaw to which the rudder trimmed were slightly larger ($\Delta \psi = -1°$ at $\delta_r = 20°$) with the floats on because of

the reduction in stability caused by the floats.

Of the four tail variations tested, none makes any change in rudder effectiveness in the range of yaw angles to which the rudder will trim. For deflections within the unstalled rudder range, the rudder angles for trim in yaw with the tail additions in place are essentially the same as the floats-off normal tail, rudder angles for trim.

Drag Effects

When the floats are added to the airplane the tail wheel (which is nonretractable) will be removed. As shown on figure 49, substitution of the floats for the retracted main landing wheels causes a high-speed drag increment of $\Delta C_{D_p} = 0.0110$, while the drag decrement due to the removal of the tail wheel is $\Delta C_{D_p} = 0.0015$. Thus, the net increase in drag due to the change in the alighting gear is $\Delta C_{D_p} = 0.0095$.

The drag increment due to the extension of the four wheels in the float for land landings is $\Delta C_{D_p} = 0.0070$, as shown by the results of figure 11.

CONCLUSIONS

The conclusions drawn from the power-off tests of the 1/11-scale model of the twin-engine cargo airplane equipped with amphibious floats are:

1. At any given angle of attack, the floats have a negligible effect on C_L for all flap positions.

2. The longitudinal stability of the airplane for all flap positions is reduced by an amount equivalent to a 2-percent M.A.C. shift in neutral point by the addition of the floats.

3. The floats-on stability corresponding to full-load floats-on c.g. position is slightly greater ($\Delta dC_m/dC_L \cong 0.01$) than the floats-off stability corresponding to full-load floats-off c.g. position. Due to the floats, however, there is a negative shift in the C_m value at zero lift corresponding to approximately 1° of elevator.

4. The float gear added a negative increment to C_m, equivalent to 0.25° of elevator movement, which was constant in pitch and yaw.

5. The elevator effectiveness was unaffected by the floats. The airplane in landing should be as satisfactory floats on as floats off.

6. The directional stability was reduced by the floats ($\Delta dC_n/d\psi \cong 0.0004$), but three of the four tail variations tested compensated for the loss.

7. The rudder effectiveness was unchanged by the floats or the tail variations.

8. The drag increment due to the floats is $\Delta C_{D_p} = 0.0095$.

Ames Aeronautical Laboratory,
    National Advisory Committee for Aeronautics,
        Moffett Field, Calif.

APPENDIX

The tunnel-wall corrections are defined as follows:

$$\Delta a^\circ = (\delta_w + 0.017\ \bar{c})\frac{S}{C} C_L \times 57.3 = 0.94\ C_L$$

$$\Delta C_D = \frac{\delta_w C_L^2 S}{70} = 0.0143\ C_L^2$$

$$\Delta C_m = -\delta_t \frac{SC_L}{C} \frac{dC_{m_t}}{di_t} \times 57.3 = 0.019\ C_L$$

where

$\delta_w = 0.1235$

$\delta_t = 0.087$

$C = 70$ sq ft = tunnel cross-section area

$$\frac{dC_{m_t}}{di_t} = -0.033/\text{degree (computed)}$$

$$S = 8.16 \text{ sq ft}$$

$$\bar{c} = 1.047 \text{ ft}$$

REFERENCE

1. Anon.: Preliminary Handbook of Maintenance Instructions for the Douglas Commercial Model DC-3 Transport Airplane, Air Service Command, Air Force Section, Wright Field, Dayton, Ohio, May 15, 1942. (Technical Order No. 01-40NL-2)

TABLE I

FULL-SCALE DIMENSIONS OF THE TWIN-ENGINE CARGO AIRPLANE

Item	Wing	Horizontal Tail	Vertical Tail
Area	987 ft^2	206.5 ft^2	110.2 ft^2
Span	94.58 ft	26.7 ft	11.23 ft
Aspect ratio	9.06	3.45	1.145
M.A.C.	11.52 ft	--	--
Flap . . . . . (Type) . . .	Split	Simple (Balanced)	Simple (Balanced)
NACA Section	2215 root 2206 tip	Modified 0012	Modified 0012
Taper ratio	0.300	0.231	0.264

Length from c.g. to elevator hinge line, l_H = 39.7 ft

Length from c.g. to rudder hinge line, l_V = 38.3 ft

Item	Movable Surfaces		Flap (Split)
	Elevator	Rudder	
Area aft hinge. . .	62.2 ft^2	35.8 ft^2	83.5 ft^2
Span	26.7 ft	9.26 ft	41.5 ft
Total surface area affected by	176.6 ft^2	84.0 ft^2	552 ft^2
Chord	--	--	2.01 ft (const.)

TABLE II

MODEL CONFIGURATION KEY

Symbol	Item
W	. . . . Wing
B	. . . . Fuselage
N	. . . . Nacelles
E	. . . . Exhaust stacks
H	. . . . Horizontal tail
V	. . . . Vertical tail
V_1	. . . . Triangular skid fin
V_2	. . . . Small rectangular skid fin
V_3	. . . . Large rectangular skid fin
V_4	. . . . Vertical fin extension
F	. . . . Flaps
L	. . . . Main landing gear extended
L_R	. . . . Main landing gear retracted
L_T	. . . . Tail wheel
L_1	. . . . Front gear on floats, extended
L_2	. . . . Rear gear on floats, extended
L_{2R}	. . . . Rear gear on floats, retracted
p	. . . . Floats less main landing gear
S	. . . . Standard configuration, $WBNEL_RHVL_T$
a	. . . . Angle of attack of fuselage reference line with relative wind (corrected for wind-tunnel interference and stream angle)
a_u	. . . . Uncorrected geometrical angle of attack of fuselage reference line

It should be noted in the configurations tested that when the floats were installed, the main gear (L_R or L) and the landing wheel (L_T) were removed and a filler block was placed in the tail wheel hole (fig. 3(a)).
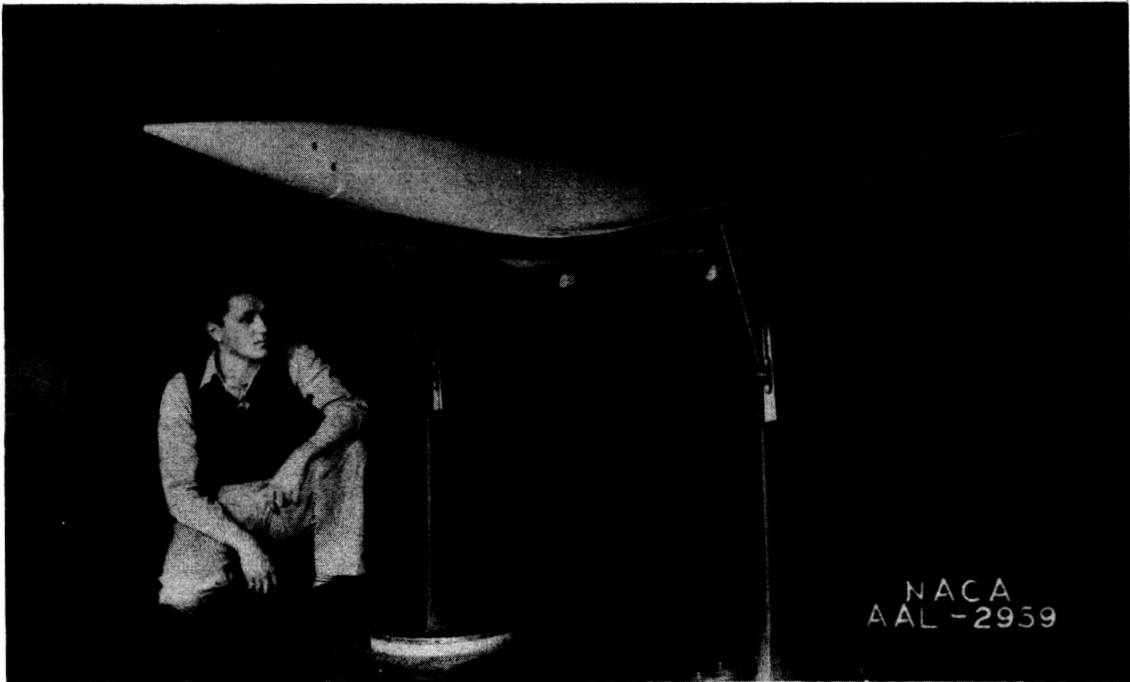
94.6'

17.5'

STA. 0

STA. 252.6 "

STA. 778.5 "

GROUND LINE
NORMAL GEAR
EXTENDED

41.7'

GROUND LINE
FLOAT GEAR
EXTENDED
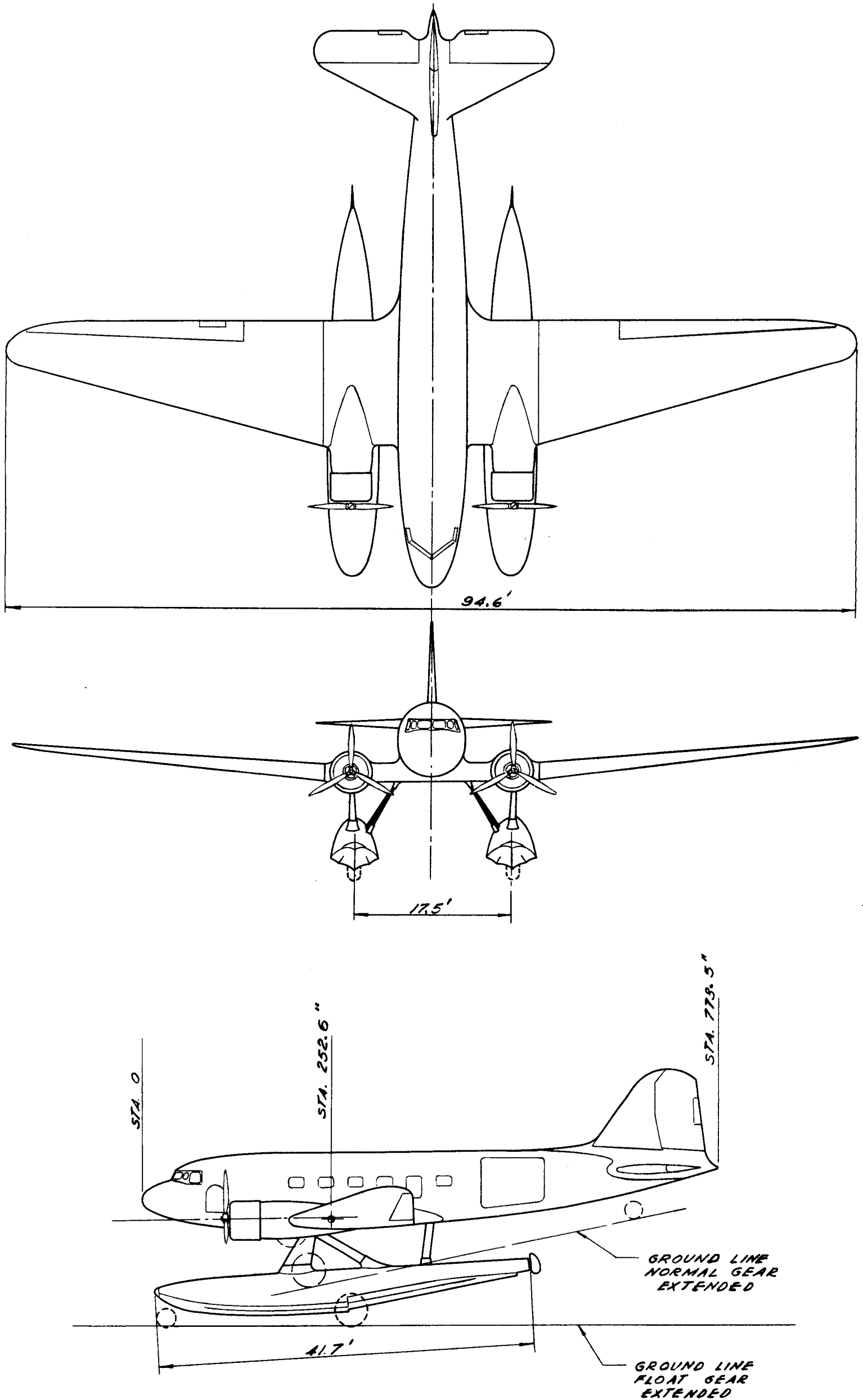
FIG. 1.- THREE VIEW DRAWING OF THE TWIN-ENGINE CARGO AIRPLANE
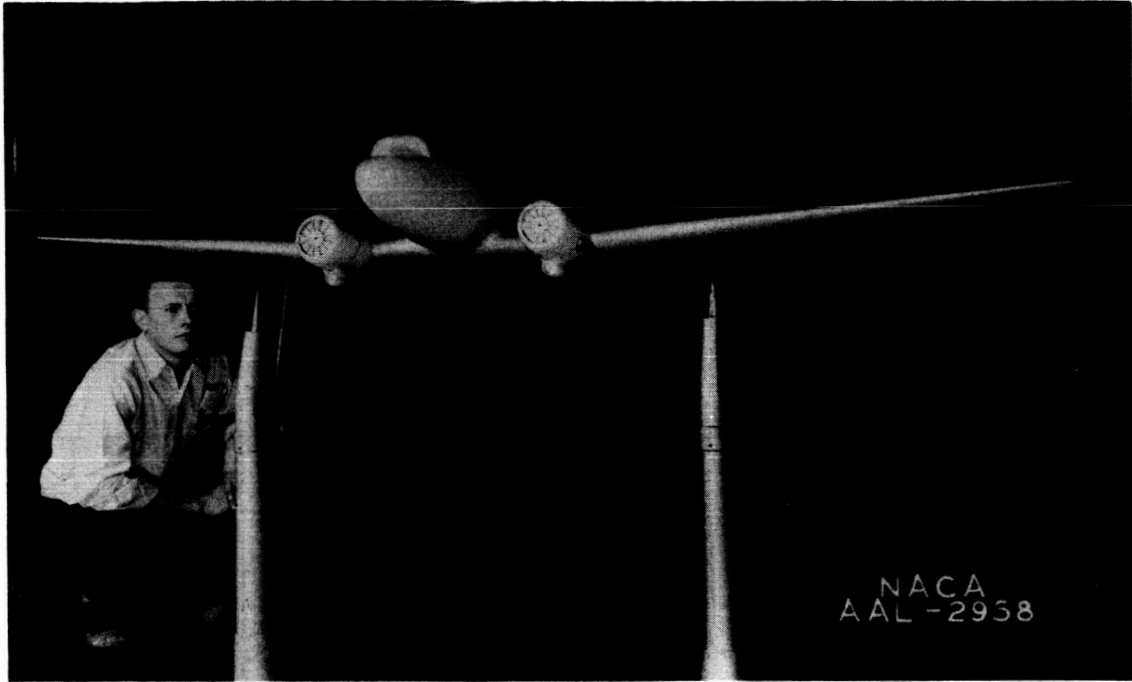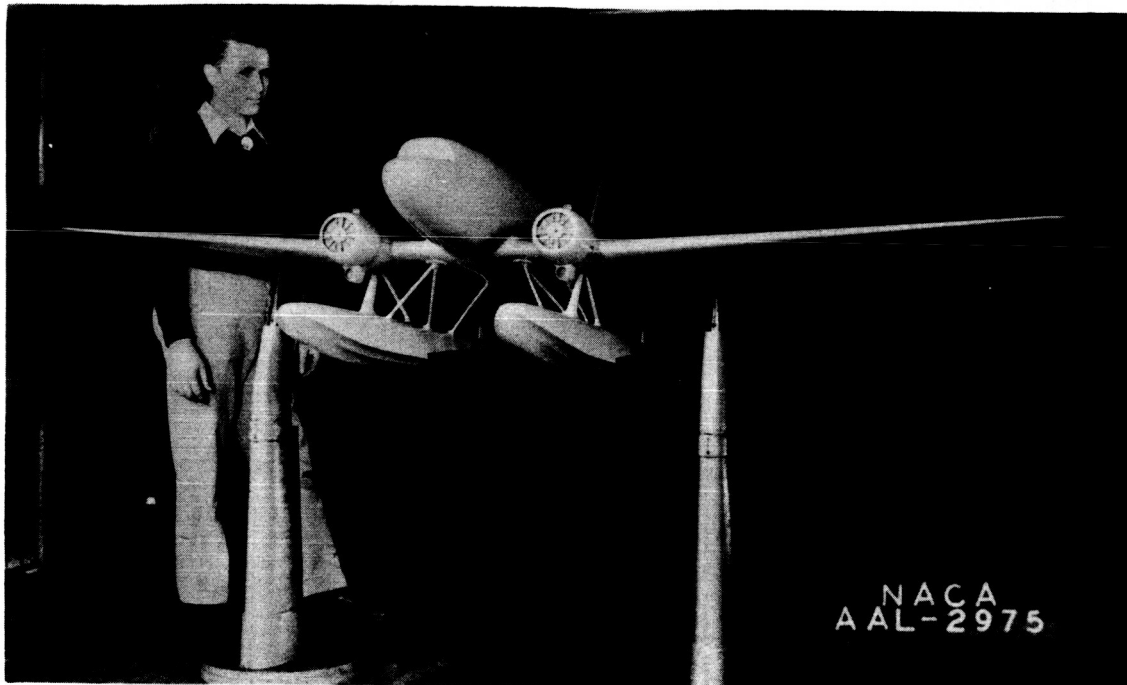
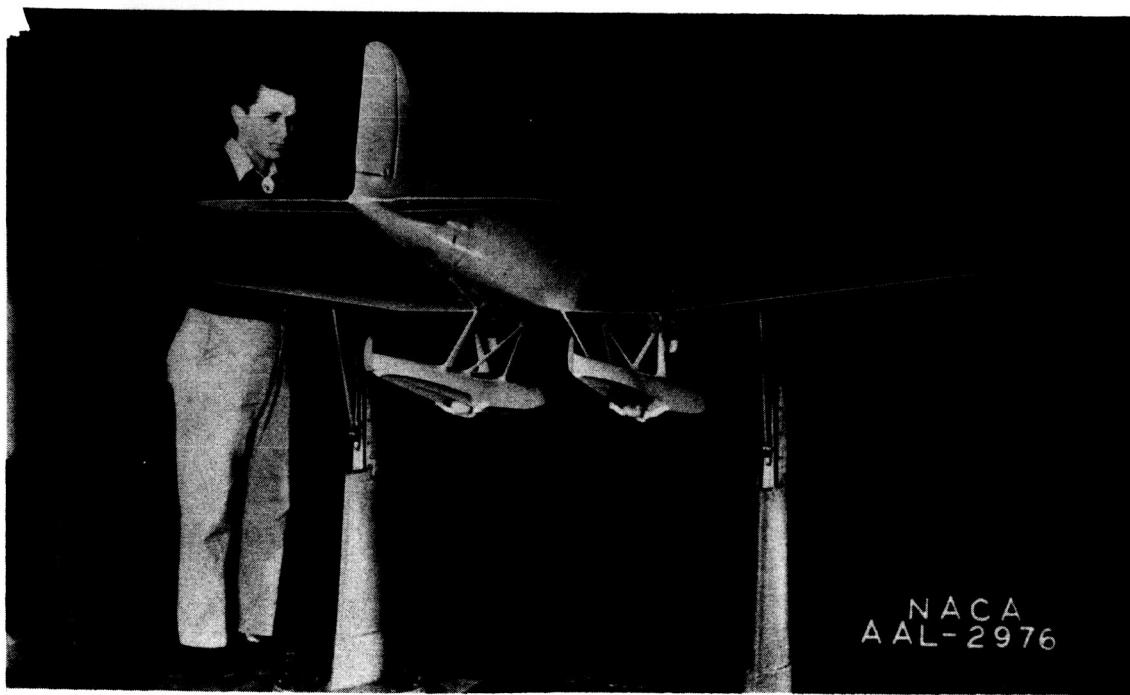Three-quarter front view

Three-quarter rear view

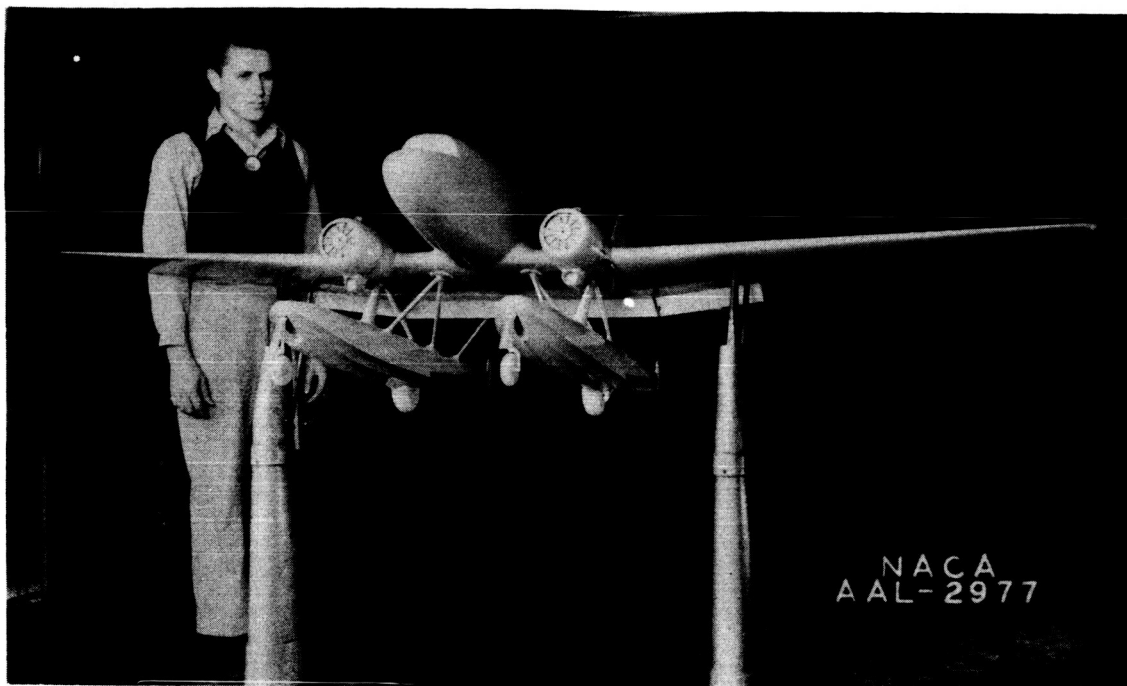Figure 2.- Model in the standard configuration less tail (S-HVI$_T$).
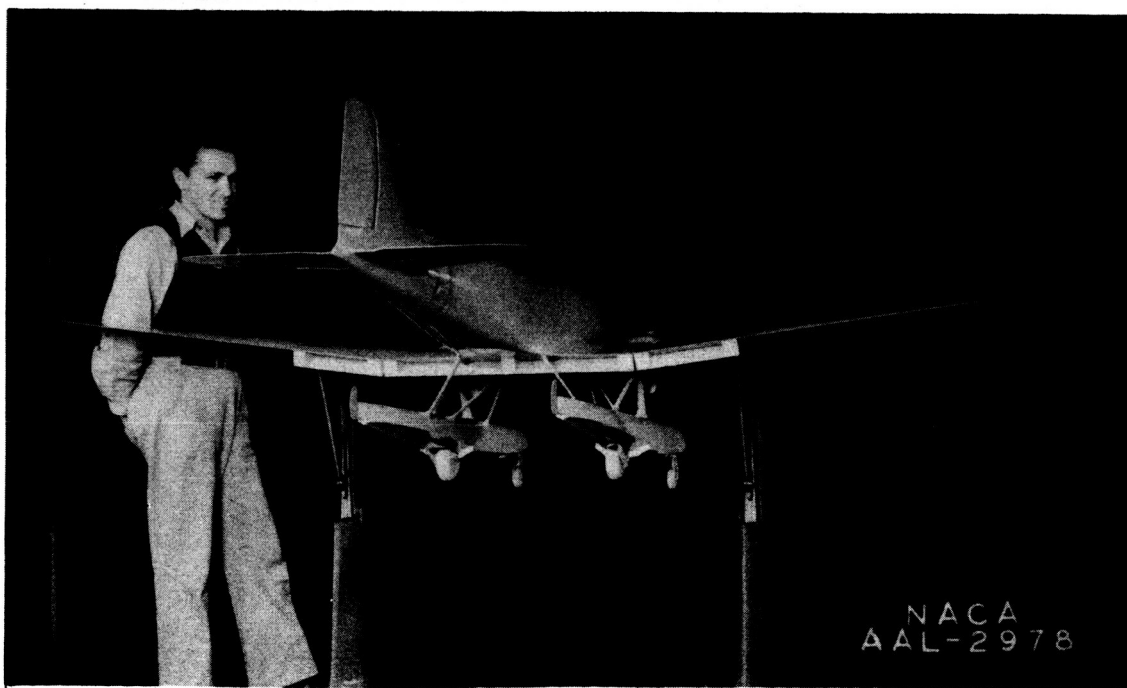
Three-quarter front view

Three-quarter rear view

Figure 3.- Model in the standard configuration plus floats (S-pL$_{2R}$-L$_T$).

Three-quarter front view.

Three-quarter rear view.

Figure 4.- Model showing detail of flaps and float gear $(S + pL_1L_2 + F^{45} - L_T)$.
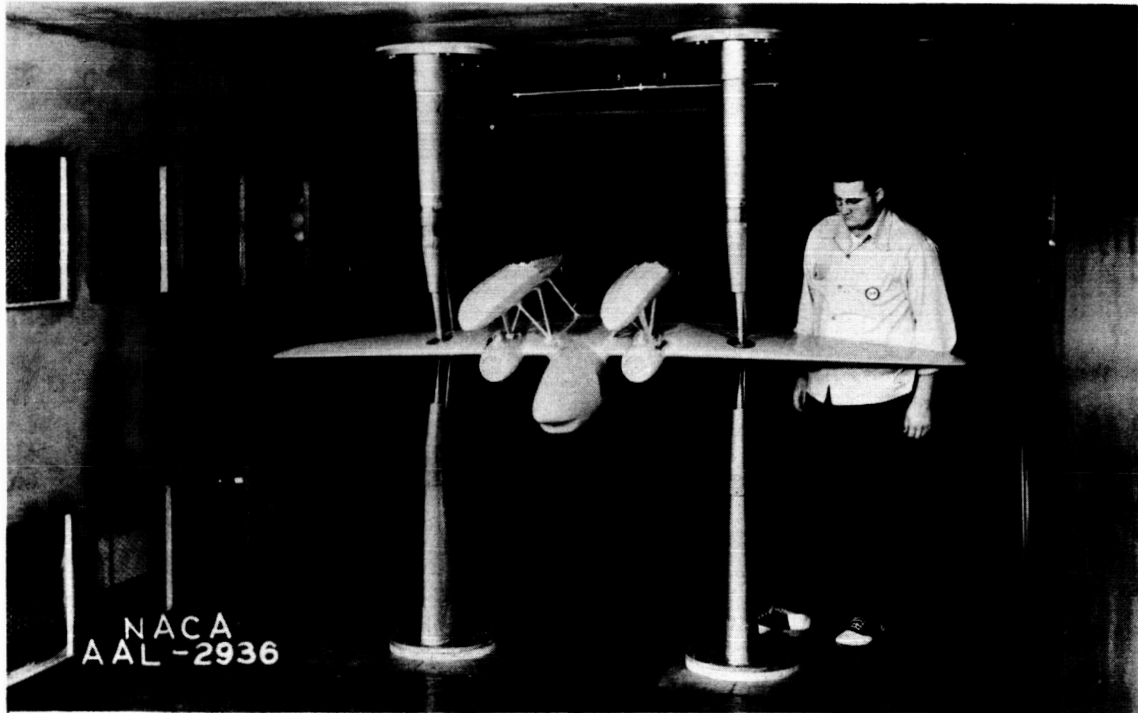
Figure 5.- Image strut system with model inverted.
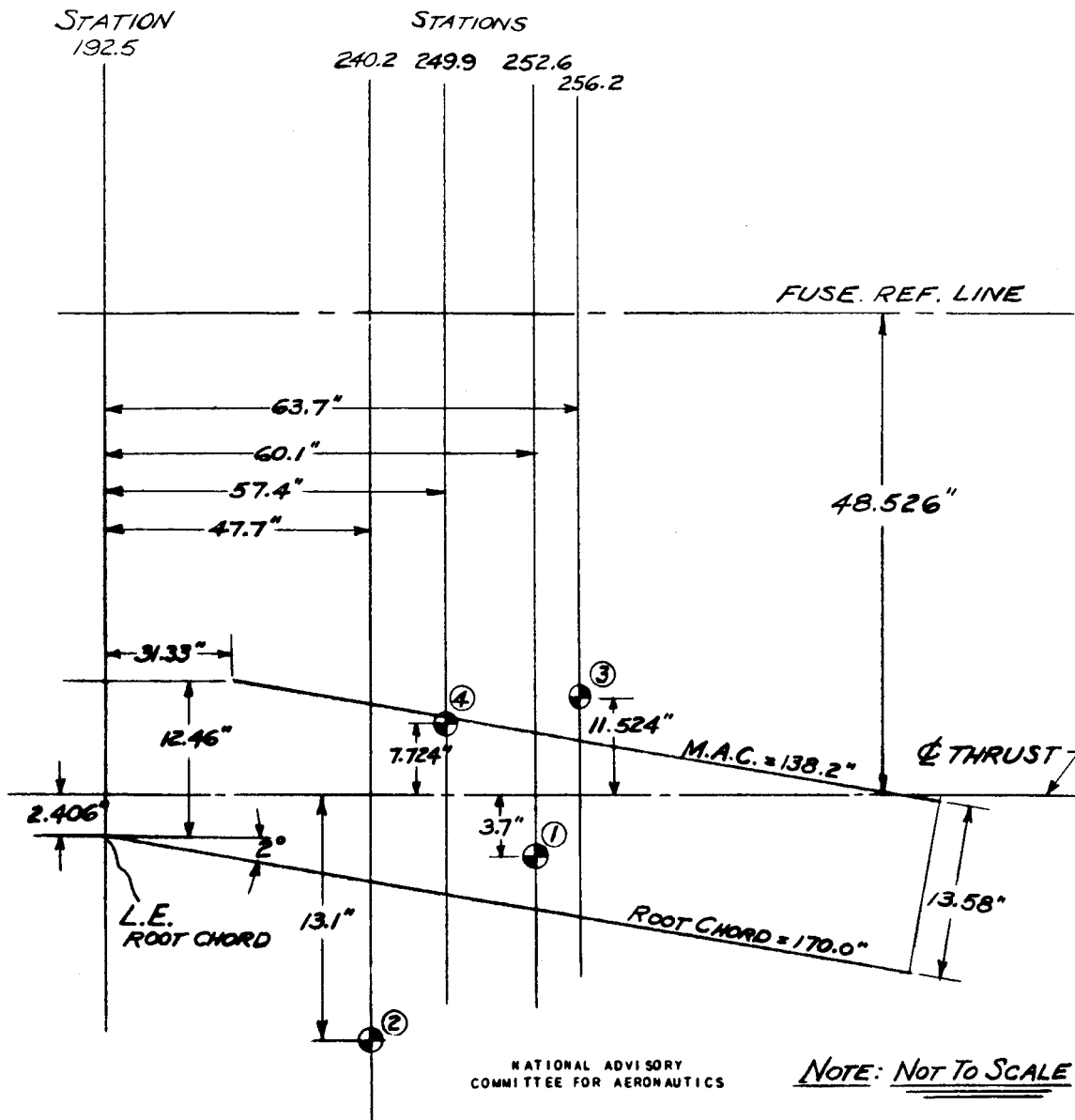
FIG. 6,-CENTER-OF-GRAVITY LOCATIONS FOR THE TWIN-ENGINE CARGO
AIRPLANE, FLOATS ON AND FLOATS OFF.

C_D

C_L

C_m

α

			FLOATS OFF - TAIL OFF
⦶	RUN 30	$S-HVL_T$	" "
▣	RUN 39	$S-HVL_T+PL_{aE}$	ON "
▲	RUN 33	S	OFF "
▼	RUN 36	$S+PL_{aE}-L_T$	ON "
			OFF = ON
			ON = "
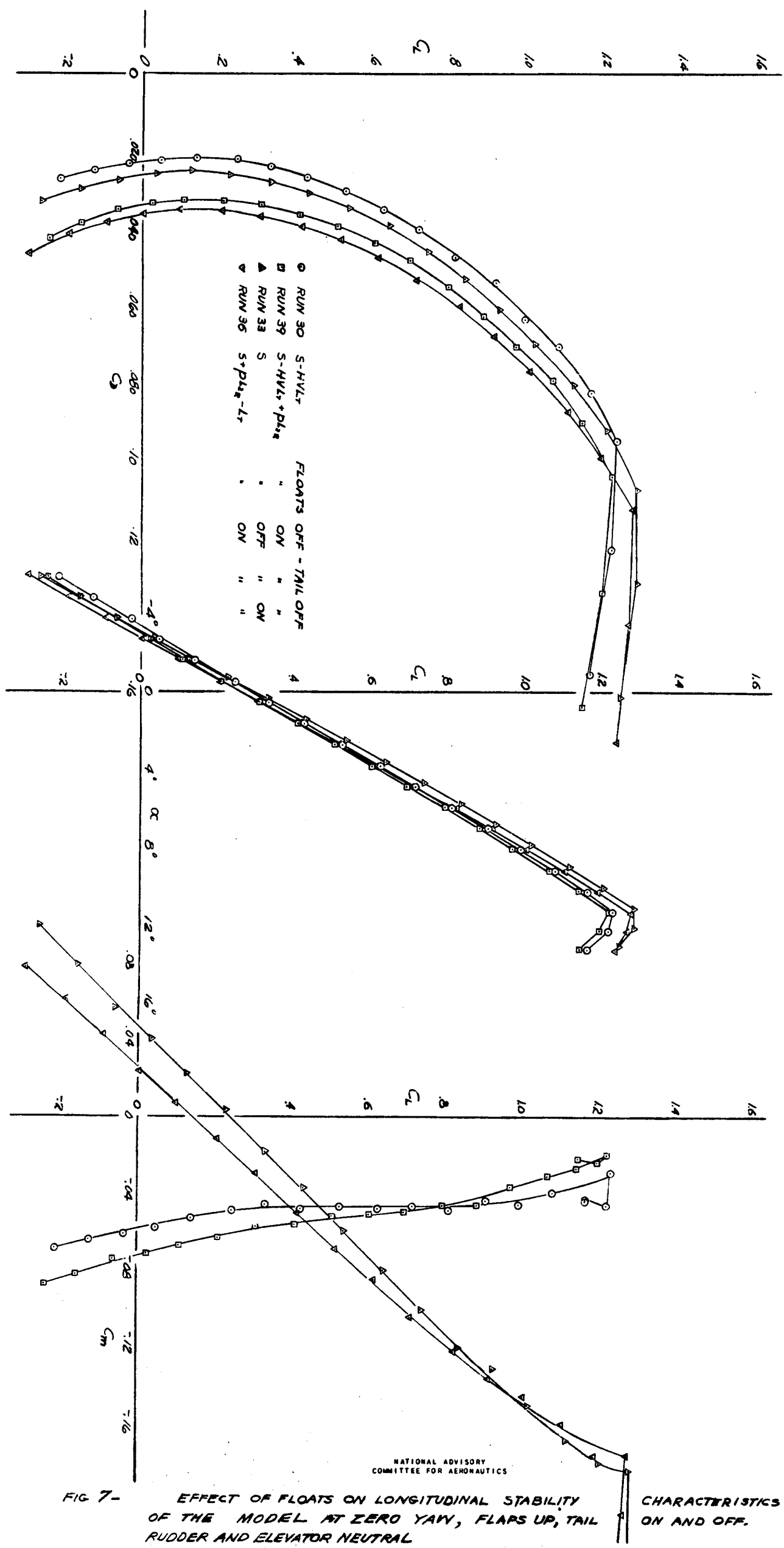
FIG 7-   EFFECT OF FLOATS ON LONGITUDINAL STABILITY   CHARACTERISTICS
OF THE MODEL AT ZERO YAW, FLAPS UP, TAIL   ON AND OFF.
RUDDER AND ELEVATOR NEUTRAL

			FLOATS OFF – TAIL OFF
○	RUN 46	S–HVLt+LF'S	FLOATS OFF – TAIL OFF
◻	RUN 44	S–HVLt+plr+F'S	" " ON
△	RUN 52	S+LF'S	" " OFF
▽	RUN 54	S+F'S+plr–Lt	" " ON
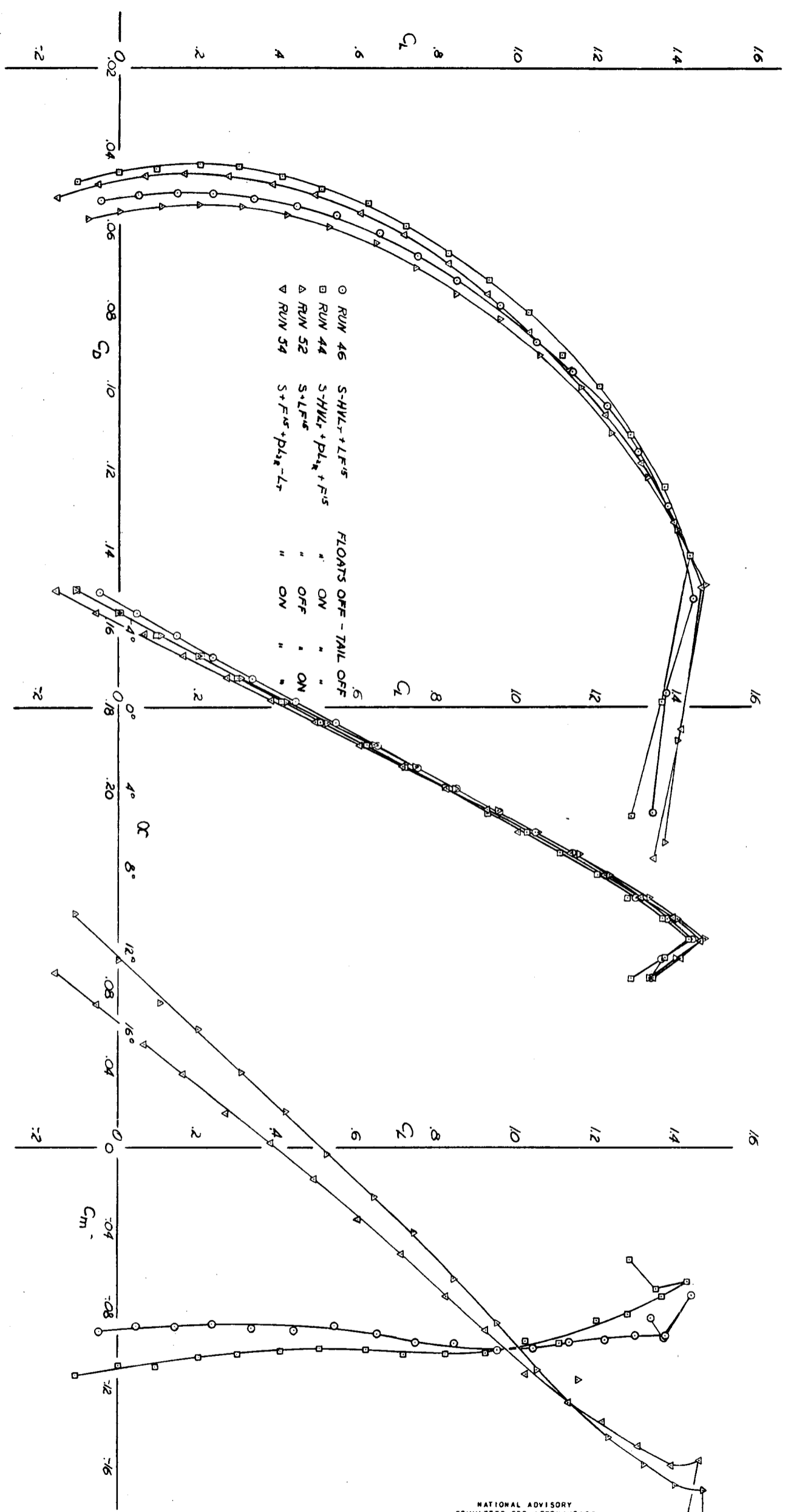
NATIONAL ADVISORY
COMMITTEE FOR AERONAUTICS

FIG. 8 – EFFECT OF FLOATS ON LONGITUDINAL STABILITY CHARACTERISTICS
OF THE MODEL AT ZERO YAW, FLAPS AT 15°, TAIL ON AND OFF,
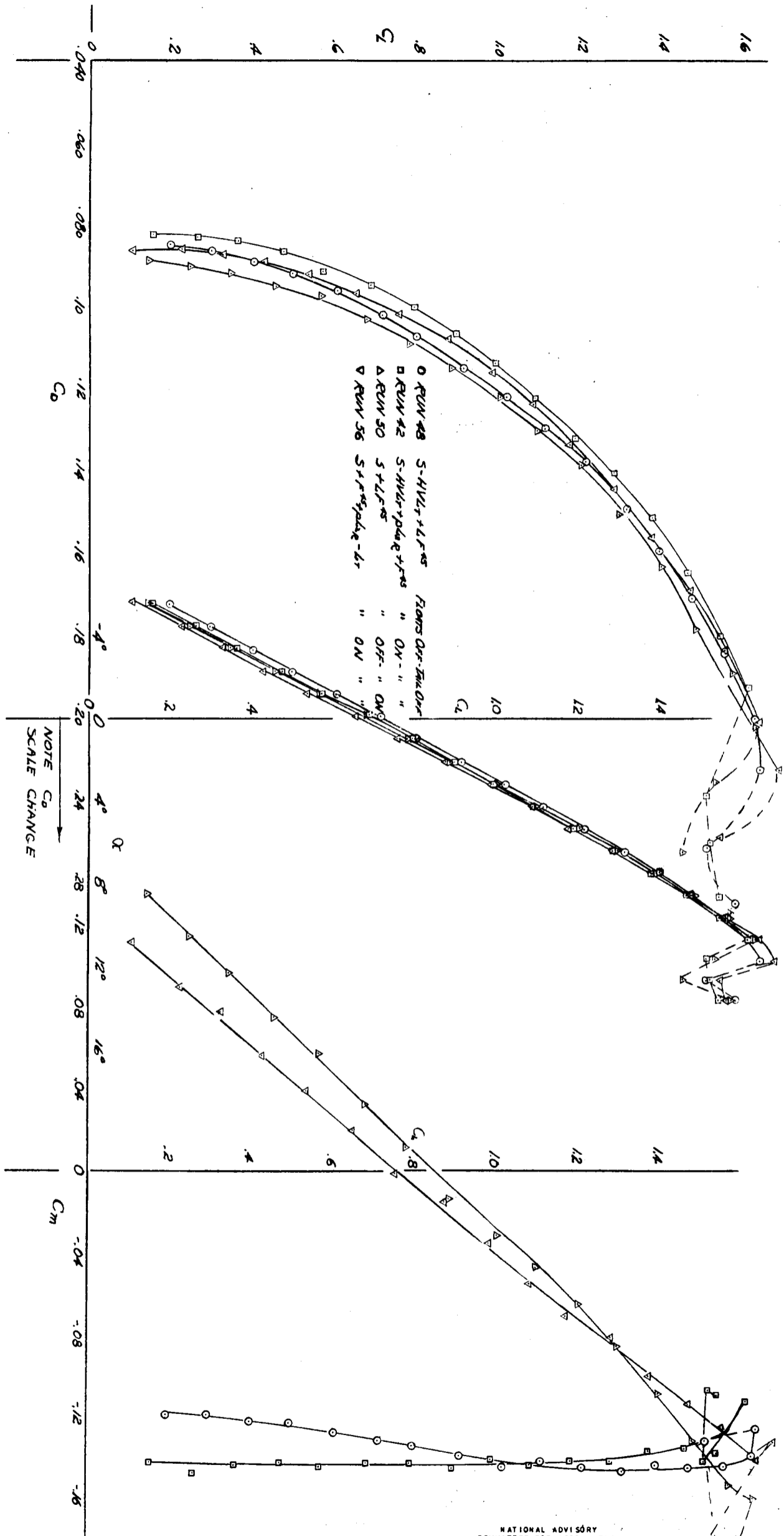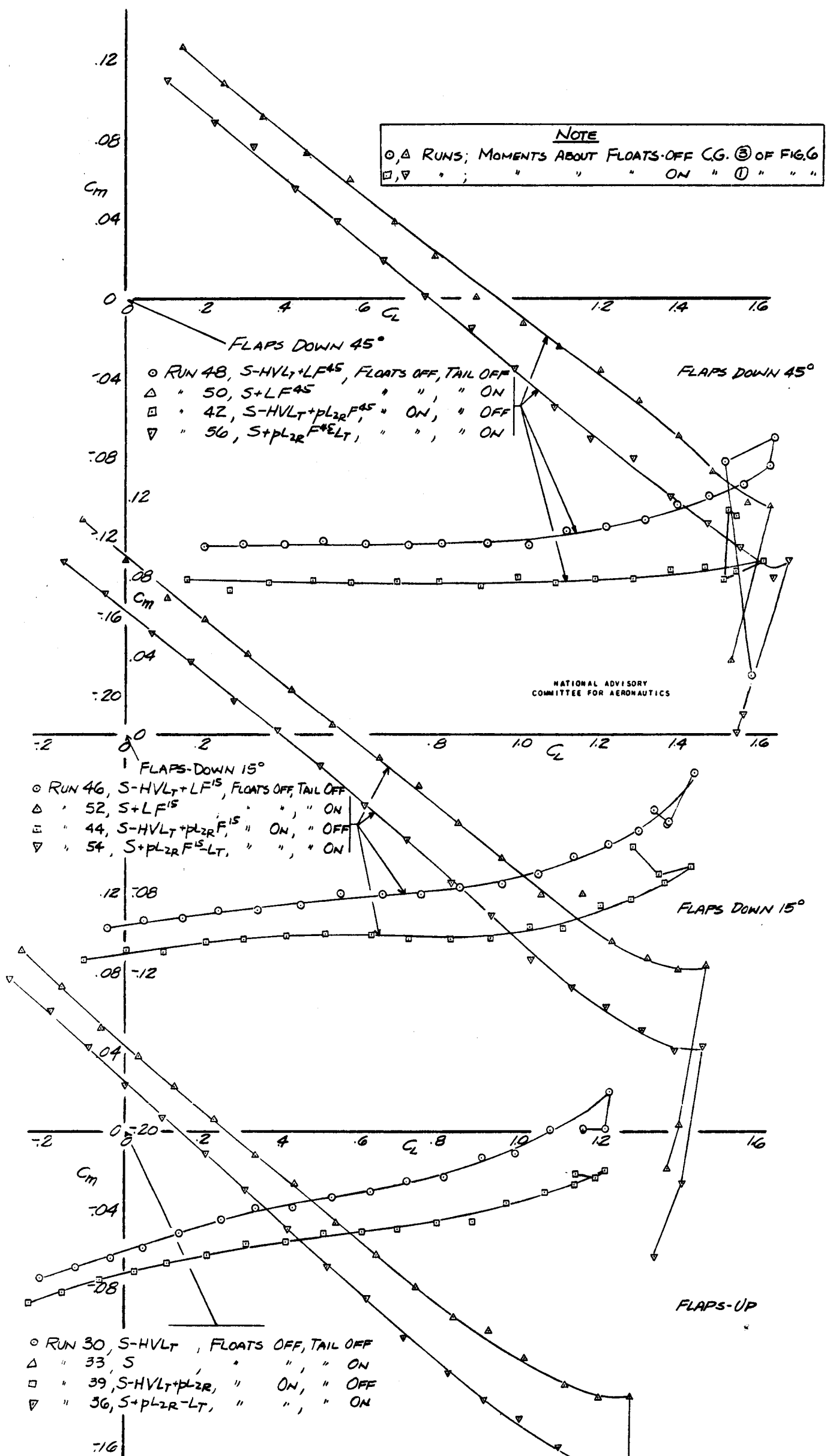RUDDER AND ELEVATOR NEUTRAL

A73

O RUN 48   S-HVL₊+LF 45   FLOATS OFF-TAIL OFF
□ RUN 42   S-HVL+TDR E+T45   " ON- "
△ RUN 50   S + LF 45   " OFF- " ON
▽ RUN 56   S + TDRₚₐₑ-Lₜ   " ON "

NOTE C_D
SCALE CHANGE

C_D

C_L

α

C_m

NATIONAL ADVISORY
COMMITTEE FOR AERONAUTICS

FIG 9 -   EFFECT OF FLOATS ON LONGITUDINAL STABILITY CHARACTERISTICS OF
THE MODEL AT ZERO YAW, FLAPS AT 45°, TAIL ON AND OFF.
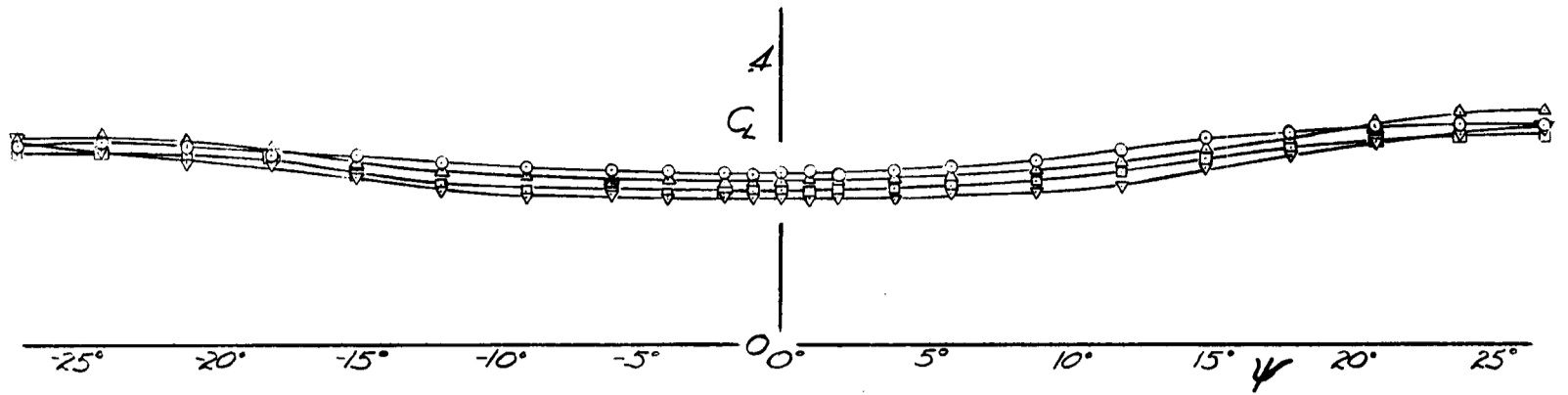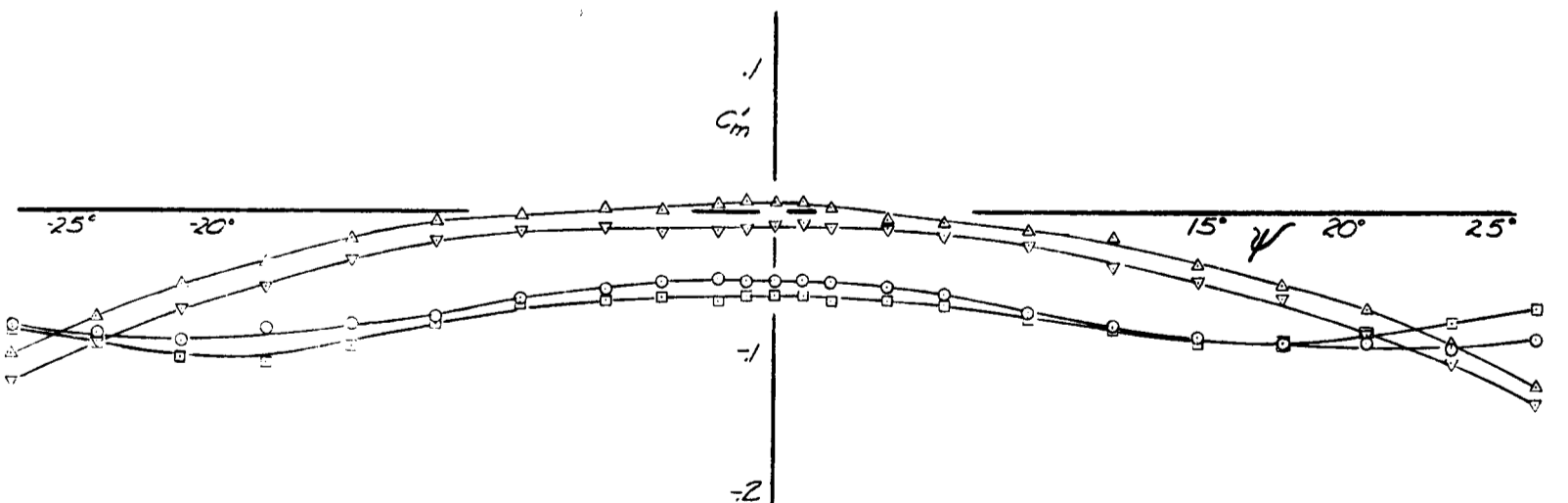RUDDER AND ELEVATOR NEUTRAL

C_m

.12
.08
.04
0
.2 .4 .6 C_L 1.2 1.4 1.6

FLAPS DOWN 45°

-.04
-.08

FLAPS DOWN 45°

○ RUN 48, S-HVL$_T$+LF^{45}, FLOATS OFF, TAIL OFF
△ " 50, S+LF^{45} " ", " ON
□ " 42, S-HVL$_T$+pL$_{2R}$F^{45} " ON, " OFF
▽ " 56, S+pL$_{2R}$F^{45}-L$_T$, " ", " ON

C_m

.12
.08
.04
0
-.04
-.08
-.12
-.16
-.20

-.2 0 .2 .8 1.0 1.2 1.4 1.6 C_L

FLAPS-DOWN 15°

○ RUN 46, S-HVL$_T$+LF^{15}, FLOATS OFF, TAIL OFF
△ " 52, S+LF^{15} " ", " ON
□ " 44, S-HVL$_T$+pL$_{2R}$F^{15} " ON, " OFF
▽ " 54, S+pL$_{2R}$F^{15}-L$_T$, " ", " ON

FLAPS DOWN 15°

NATIONAL ADVISORY
COMMITTEE FOR AERONAUTICS

C_m

.12
.08
.04
0
-.04
-.08
-.12
-.16
-.20

-.2 0 .2 .4 .6 C_L .8 1.0 1.2 1.6

FLAPS-UP

○ RUN 30, S-HVL$_T$, FLOATS OFF, TAIL OFF
△ " 33, S , " " , " ON
□ " 39, S-HVL$_T$+pL$_{2R}$, " ON, " OFF
▽ " 36, S+pL$_{2R}$-L$_T$, " " , " ON

FIGURE 10.— LONGITUDINAL STABILITY OF THE
MODEL AT ZERO YAW, FLOATS ON AND OFF, TAIL ON AND OFF,
MOMENTS ABOUT CENTER OF GRAVITY POSITION CORRESPONDING
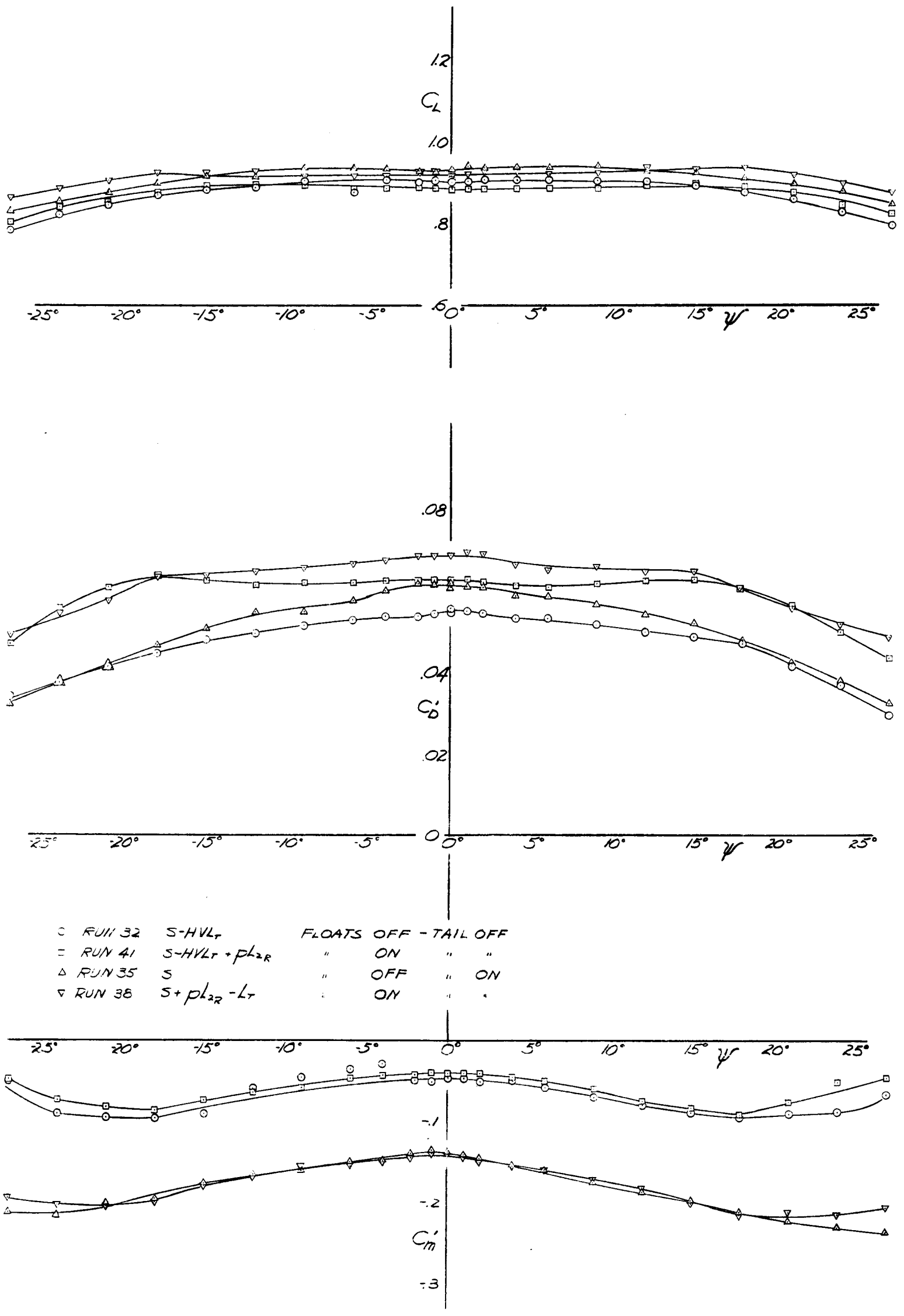TO THE FULL LOAD CONDITION, RUDDER AND ELEVATOR NEUTRAL

C_L

C_D

C_L

NOTE

NOTE C_D SCALE CHANGE

α

C_L

O RUN 54 $S+F^{15}+pl_{28}$ $-L_7$ FLOAT GEAR RET'D F^{15}
△ RUN 60 $S+F^{15}+pl_1L_2$ $-L_7$ "   "   EXT'D "
▽ RUN 56 $S+F^{45}+pl_{28}$ $-L_7$ "   "   RET'D F^{45}
□ RUN 58 $S+F^{45}+pl_1L_2$ $-L_7$ "   "   EXT'D "

C_m

FIG 11 -   EFFECT OF FLOAT GEAR ON LONGITUDINAL STABILITY
CHARACTERISTICS OF THE MODEL AT ZERO YAW, FLAPS
DOWN 15° AND 45°,   RUDDER AND ELEVATOR NEUTRAL.

o   RUN 64 , S-HVL$_T$, FLOATS OFF , TAIL OFF
□   "   65, S-HVL$_T$+pL$_{2R}$, " ON , "   "
△   "   62, S   ,   " OFF,   ON
▽   "   63, S+pL$_{2R}$-L$_T$, " ON ,   "
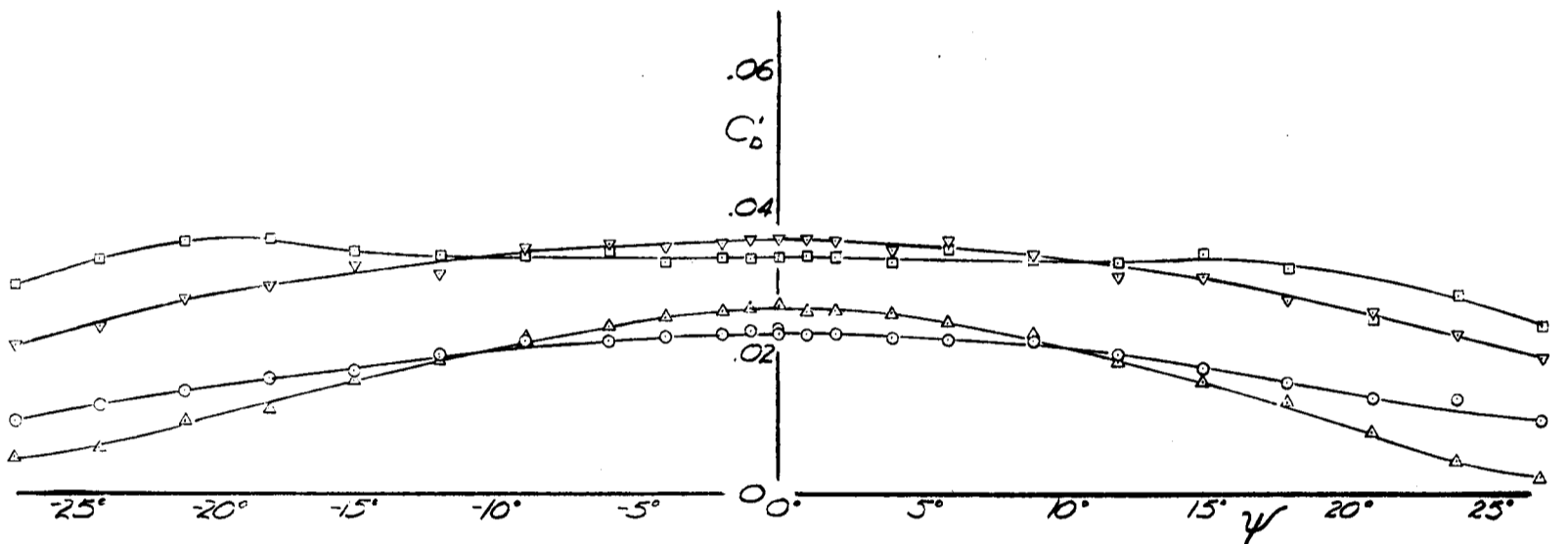
FIG 12 - EFFECT OF FLOATS ON C_L, C_D', AND C_m'.
            MODEL IN YAW, $\alpha_u = -1°$, FLAPS UP, TAIL ON AND OFF.
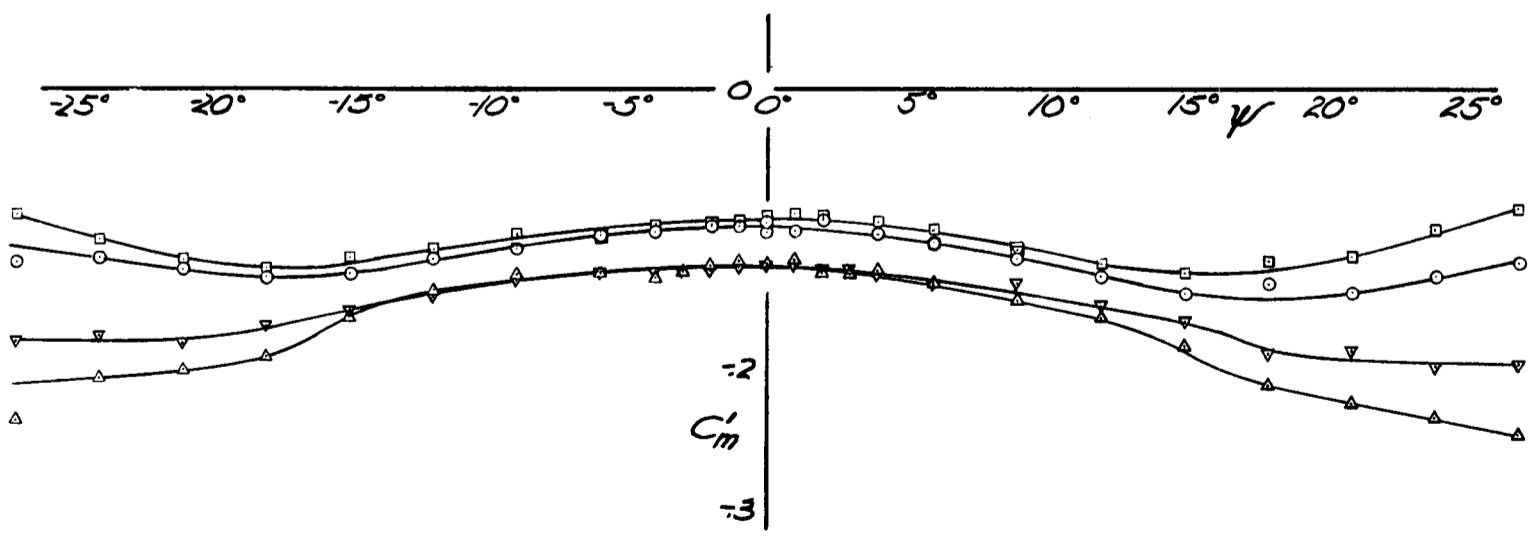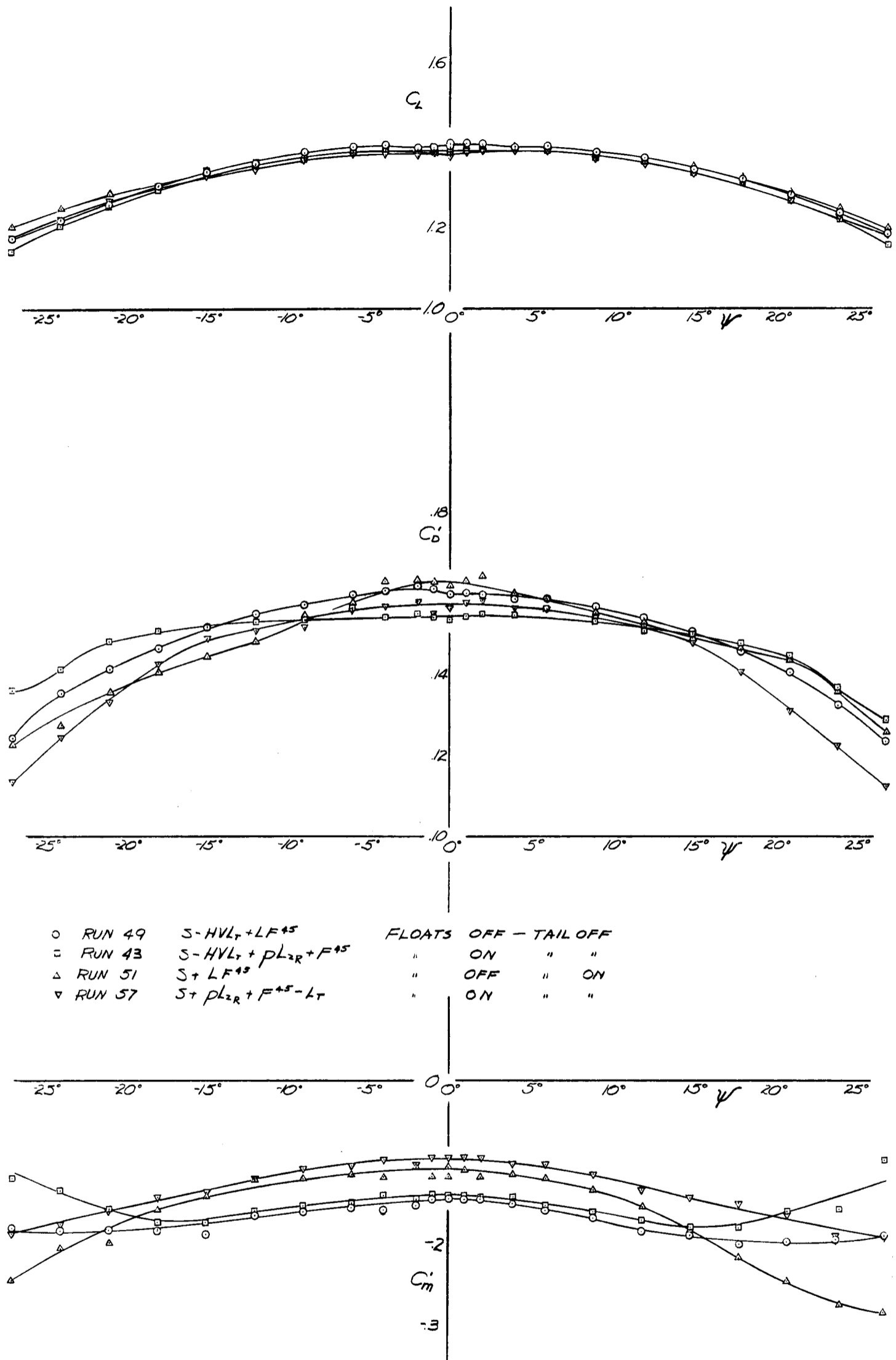   RUDDER AND ELEVATOR NEUTRAL

1.2

C_L

1.0

.8

-25° -20° -15° -10° -5° 0° 5° 10° 15° ψ 20° 25°

.08

.06

.04

C_D'

.02

-25° -20° -15° -10° -5° 0° 5° 10° 15° ψ 20° 25°

○	RUN 32	S-HVL$_T$	FLOATS OFF - TAIL OFF
□	RUN 41	S-HVL$_T$ + pl_{2R}	" ON " "
△	RUN 35	S	" OFF " ON
▽	RUN 38	S + pl_{2R} - L$_T$	" ON " "

-25° -20° -15° -10° -5° 0° 5° 10° 15° ψ 20° 25°

-.1

-.2

C_m'

-.3

FIG. 13 - EFFECT OF FLOATS ON C_L, C_D' AND C_m,
MODEL IN YAW, $\alpha_u = 6°$, FLAPS UP, TAIL ON AND OFF,
RUDDER AND ELEVATOR NEUTRAL

FIG. 14 - EFFECT OF FLOATS ON C_L, C_D' AND C_m',
MODEL IN YAW, $\alpha_U = 6°$, FLAPS DOWN 15°, TAIL ON AND OFF,
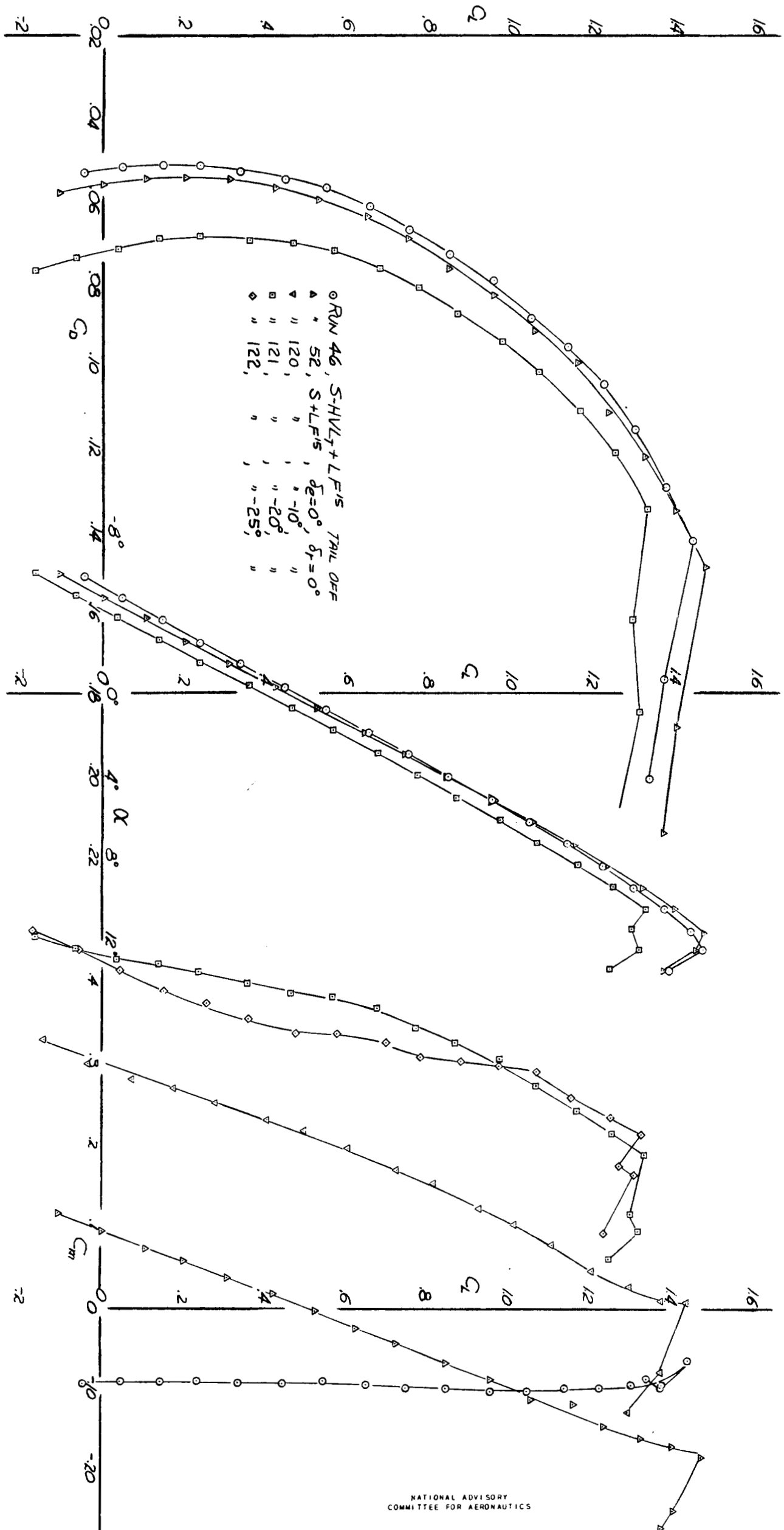RUDDER AND ELEVATOR NEUTRAL

FIG. 15 - EFFECT OF FLOATS ON C_L, C_D' AND C_m',
MODEL IN YAW, $\alpha_u = 6°$, FLAPS DOWN 45°, TAIL ON AND OFF.
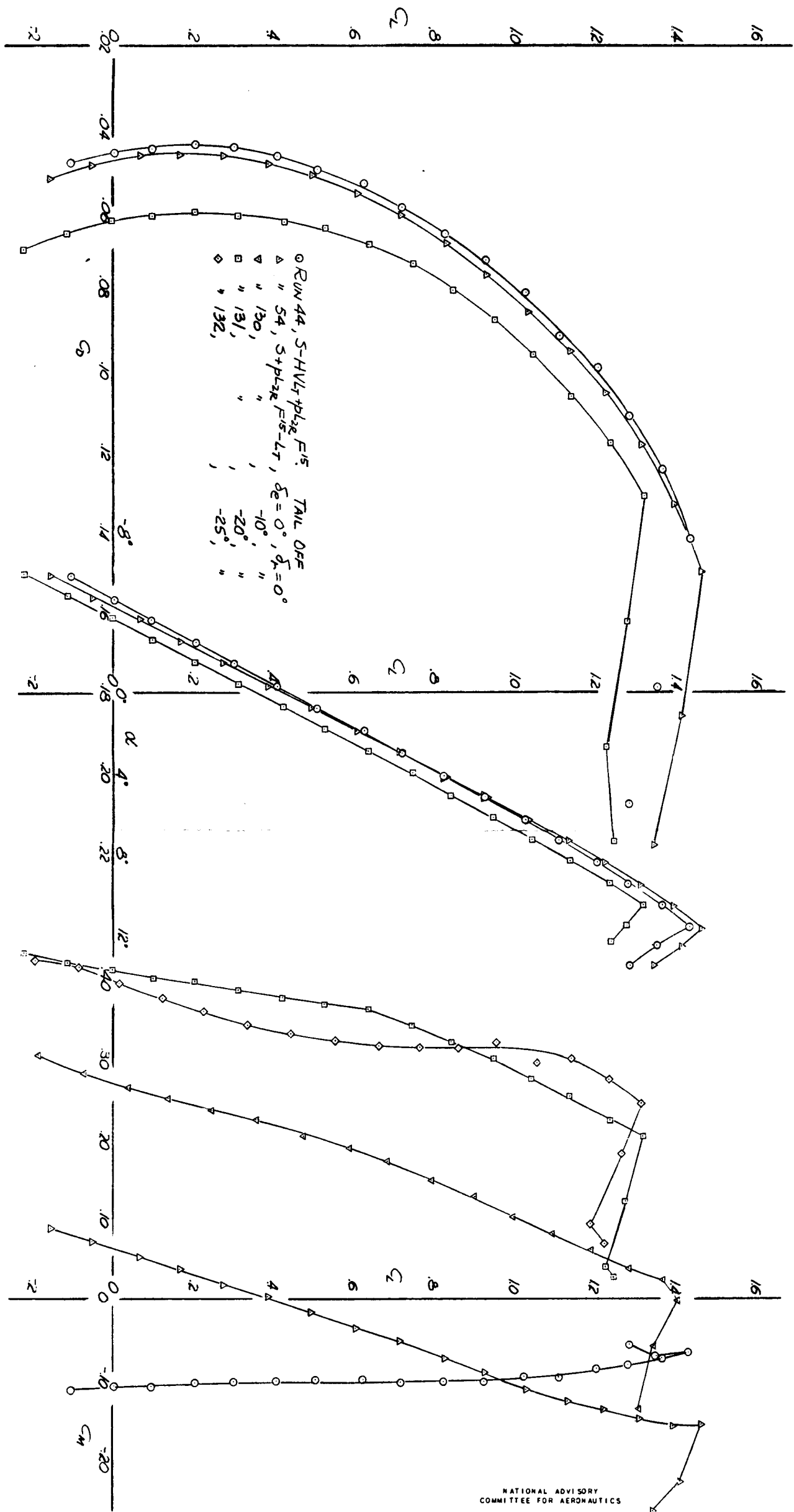RUDDER AND ELEVATOR NEUTRAL

O   RUN 49 $S-HVL_T+LF^{45}$ FLOATS OFF — TAIL OFF
□   RUN 43 $S-HVL_T+pL_{2R}+F^{45}$ "   ON   "   "
△   RUN 51 $S+LF^{45}$ "   OFF   "   ON
▽   RUN 57 $S+pL_{2R}+F^{45}-L_T$ "   ON   "   "

NATIONAL ADVISORY
COMMITTEE FOR AERONAUTICS

Legend:

	RUN 30	S-HVLr	TAIL OFF
⊙	RUN 33	S	δe=δf=0°
▲	RUN 103	"	δe=-10° δf=0°
▽	RUN 104	"	" -10° " "
◇	RUN 105	"	" -25° " "

C_L C_D α C_m

-4°   0°   4°   8°   12°

FIG. 16 – ELEVATOR EFFECTIVENESS, MODEL AT ZERO YAW,
FLOATS OFF, FLAPS UP, RUDDER NEUTRAL

Legend (within plot):

⊕ Run 39, S-HV(LT+pl$_{2R}$, Tail off
▲ " 36, S+pl$_{2R}$-LT, δ_e=0°, δ_r=0°
◀ " 86, " , -10° "
◻ " 87, " , -20° "
◇ " 88, " , -25° "

C_D C_L α C_m C_L

NATIONAL ADVISORY
COMMITTEE FOR AERONAUTICS

FIG 17 - ELEVATOR EFFECTIVENESS,   MODEL AT ZERO YAW,
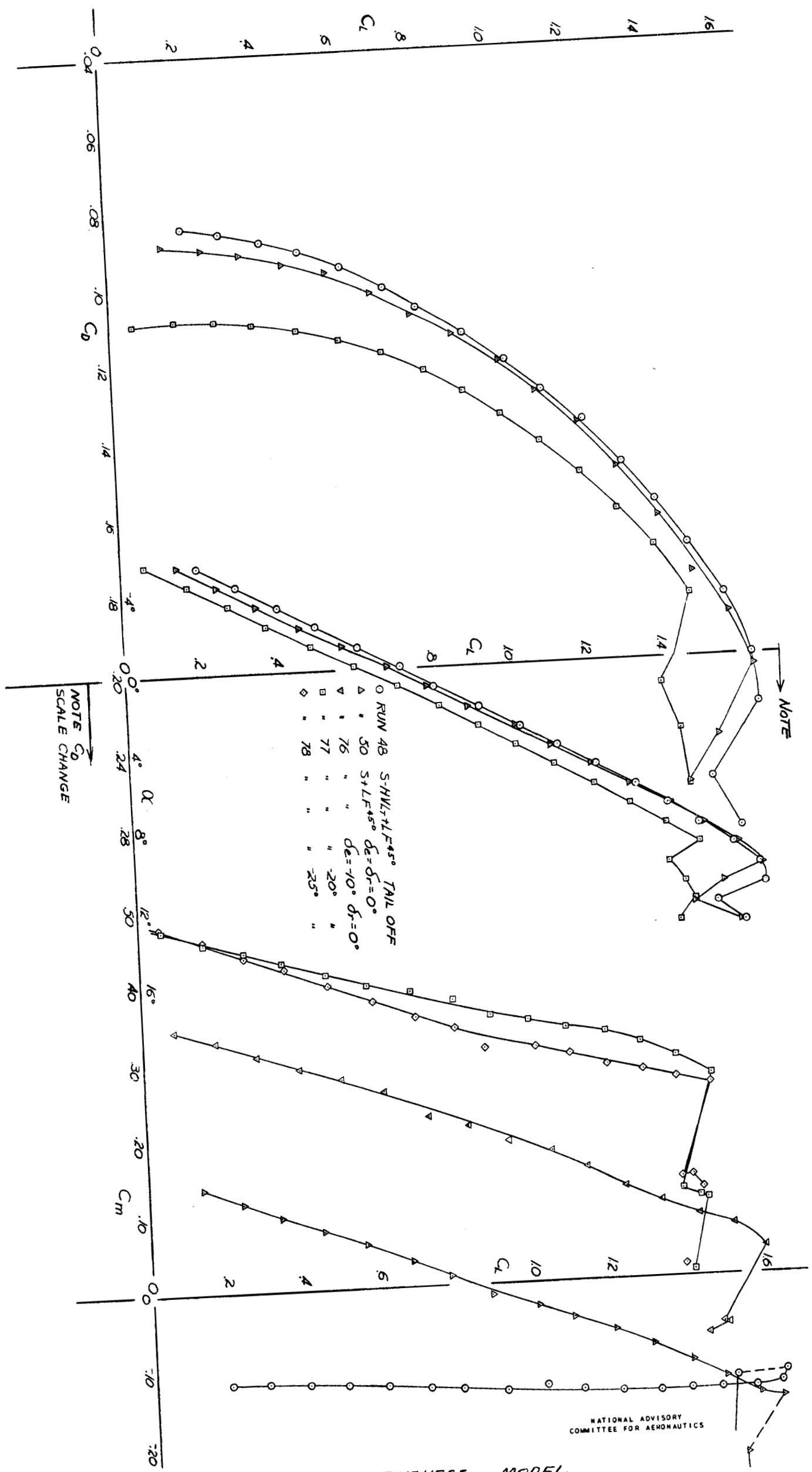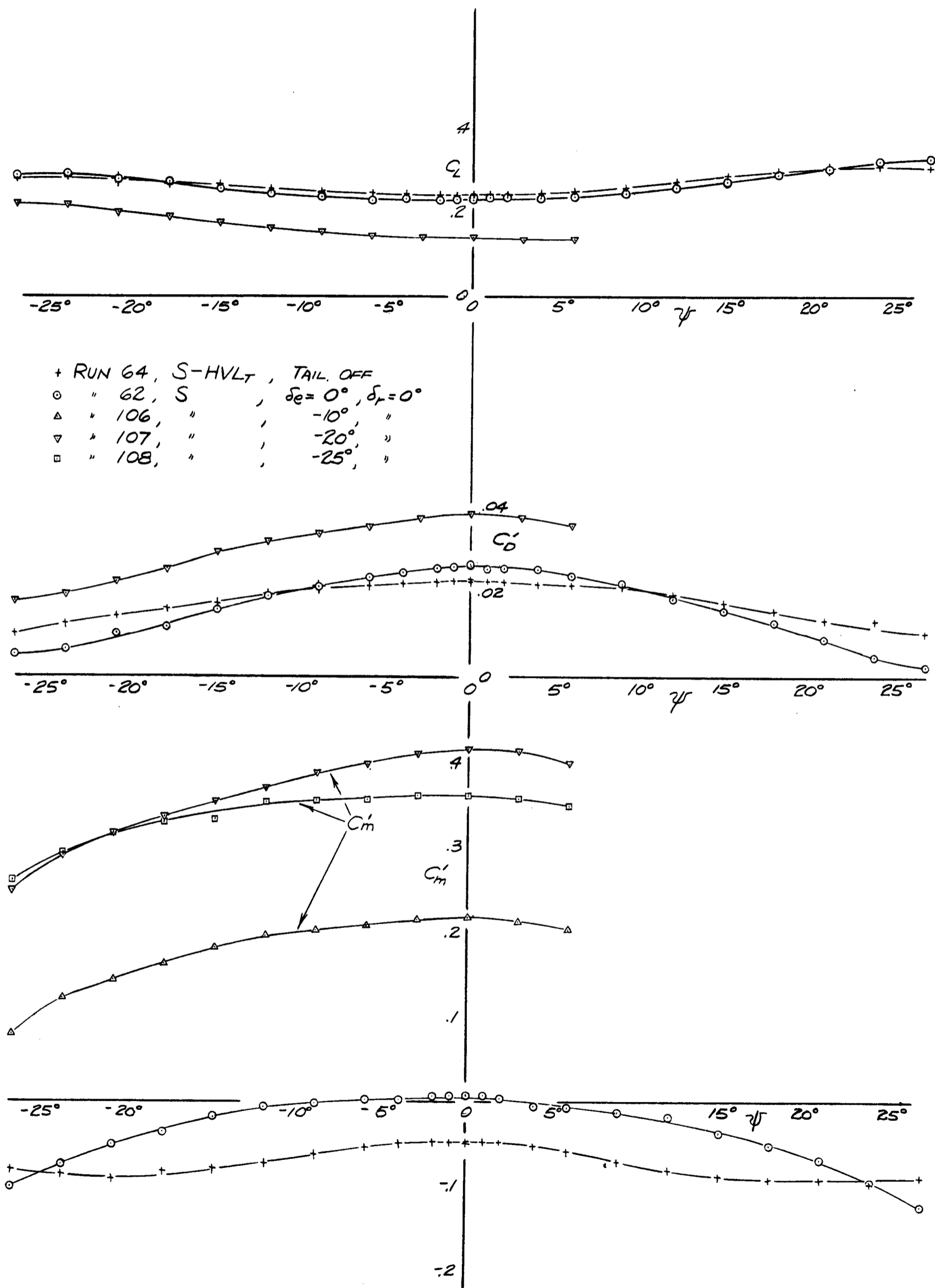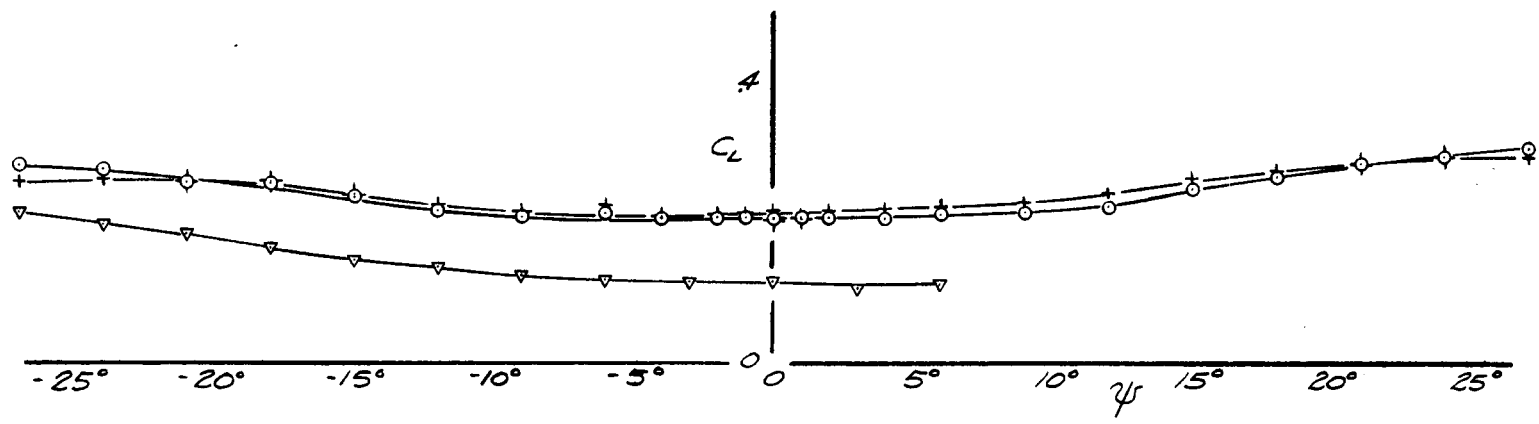FLOATS ON, FLAPS UP, RUDDER NEUTRAL.

○ Run 46, S-HV/L_T + LF's, TAIL OFF
▲ " 52, S+LF's , δe=0°, δr=0°
◀ " 120,   "   , " -10°, "
□ " 121,   "   , " -20°, "
◆ " 122,   "   , " -25°, "

FIG 18 - ELEVATOR EFFECTIVENESS,   MODEL AT ZERO YAW,
FLOATS OFF, FLAPS DOWN 15°, RUDDER NEUTRAL

Fig. 19 - ELEVATOR EFFECTIVENESS, MODEL AT ZERO YAW
FLOATS ON, FLAPS DOWN 15°, RUDDER NEUTRAL

Run 44, S-HV.L₁+p.L₂ₑ F¹⁵   TAIL OFF
  " 54, S+p.L₂ₑ F¹⁵-L.T., δₑ=0°, δᵣ=0°
  " 130,   "   "   "   -10°, "
  " 131,   "   "   "   -20°, "
  " 132,   "   "   "   -25°, "

FIG 20 - ELEVATOR EFFECTIVENESS, MODEL
AT ZERO YAW, FLOATS OFF, FLAPS DOWN 45°,
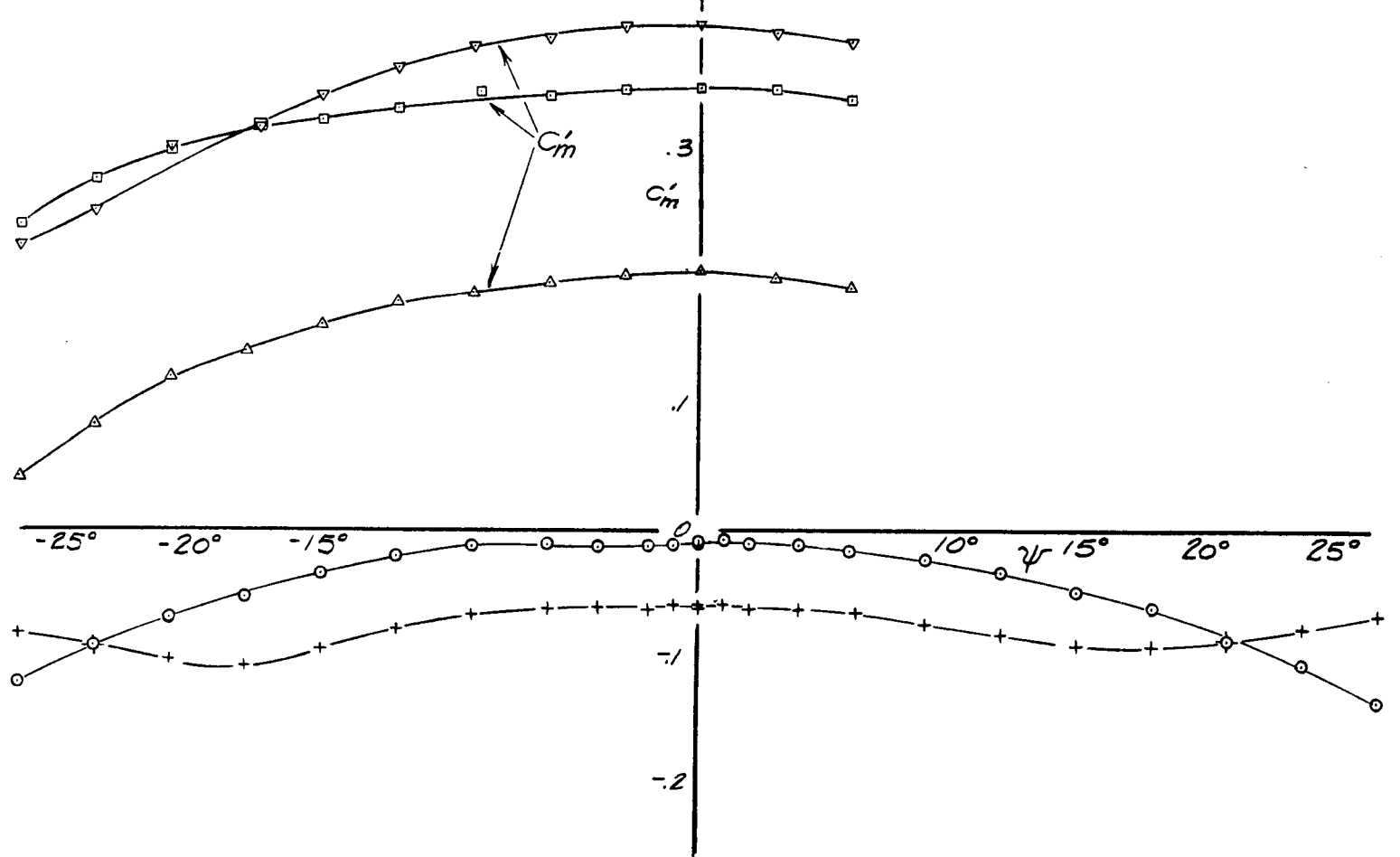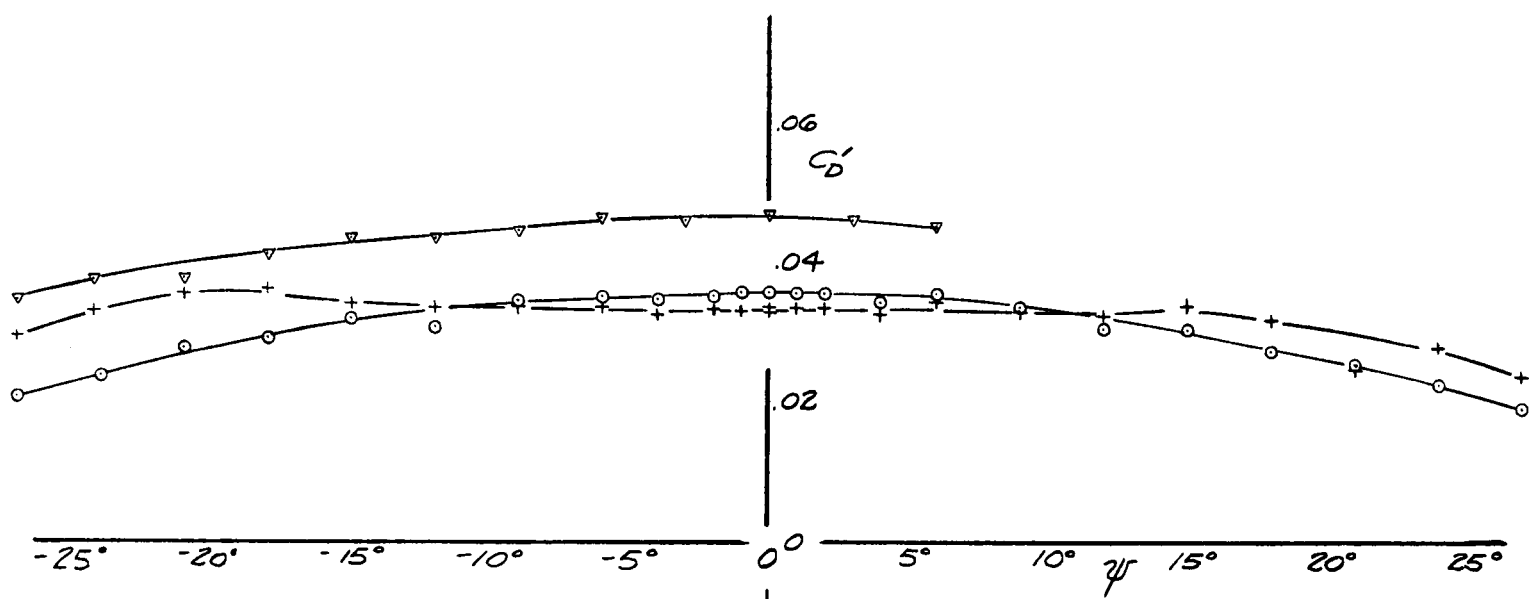RUDDER NEUTRAL

NATIONAL ADVISORY
COMMITTEE FOR AERONAUTICS

Legend:
- ⊙ Run 42, S-HV.Lt + pl₂ᵣ F⁴⁵ ; Tail Off.
- ▢ " 56, S+pl₂ᵣ F⁴⁵ δe=δr=0°
- ◄ " 66, " " δe=-10°, δr=0°
- ► " 67, " " -20°, "
- ◇ " 68, " " -25°, "

← Note Change in C_D Scale

Note.

NATIONAL ADVISORY
COMMITTEE FOR AERONAUTICS

FIG. 21 - ELEVATOR EFFECTIVENESS, MODEL AT ZERO YAW
FLOATS ON, FLAPS DOWN 45°, RUDDER NEUTRAL

Legend:
+ RUN 64, S-HVL_T, TAIL. OFF
⊙ " 62, S   , δe = 0° , δr = 0°
△ " 106, "   , -10°, "
▽ " 107, "   , -20°, "
□ " 108, "   , -25°, "

C_L

C_D'

C_m'

C_m'

FIG 22 - ELEVATOR EFFECTIVENESS OF THE MODEL IN YAW,
FLOATS OFF, FLAPS UP, $\alpha_u = -1°$, RUDDER NEUTRAL

+ RUN 65 , S−HVL$_T$+pL$_{2R}$ TAIL OFF
⊙   63 , S+pL$_{2R}$−L$_T$, δ_e= 0° , δ_r = 0°
△   89 ,   " ,   −10° , "
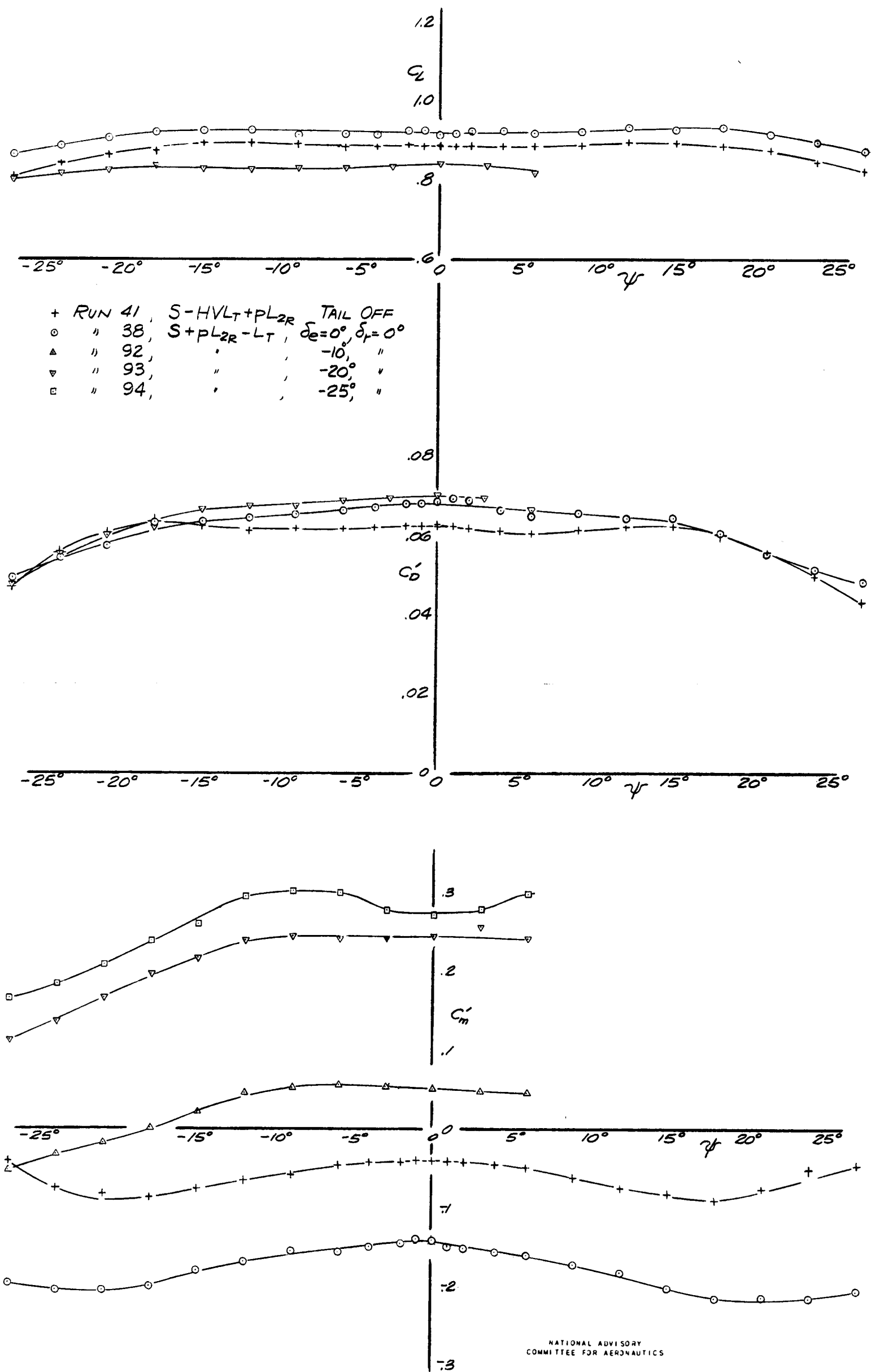▽   90   "   , −20° "
□   91   "   , −25° , "

FIG 23 -ELEVATOR EFFECTIVENESS OF THE MODEL IN YAW,
FLOATS ON , FLAPS UP, α_u=-1° , RUDDER NEUTRAL
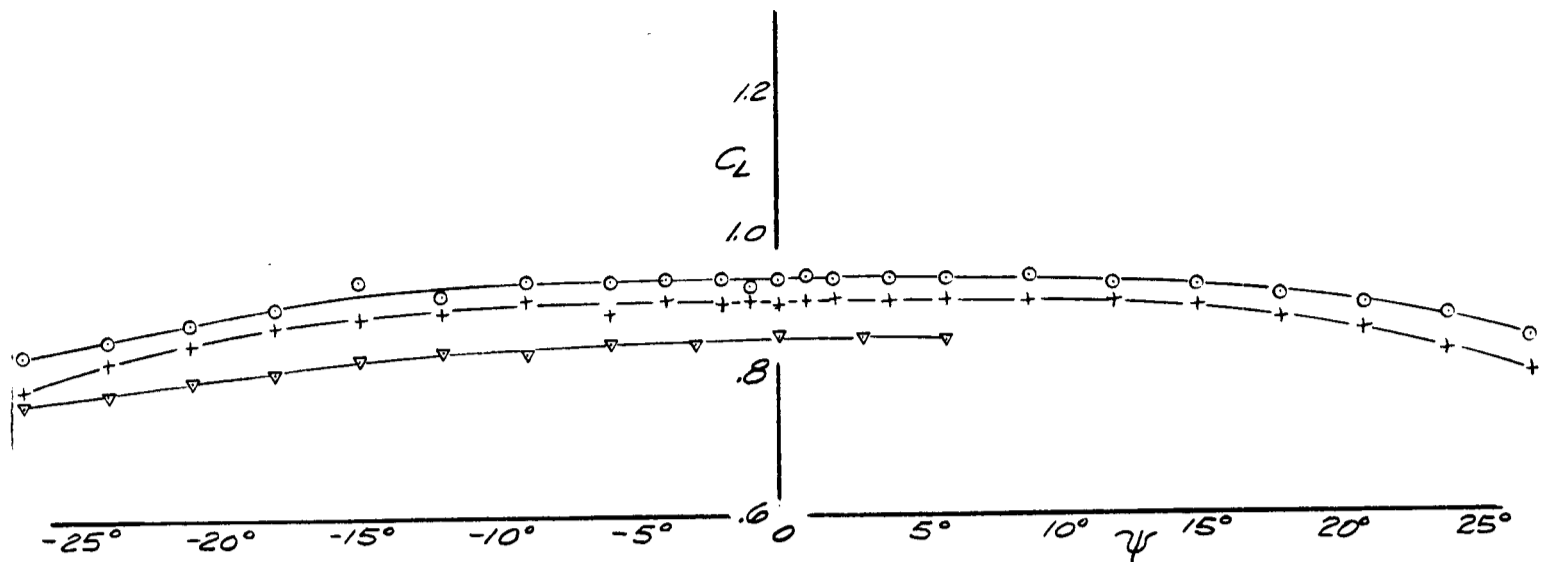
+   RUN 32 , S-HVL_T   TAIL OFF
⊙   "   35 , S $\delta_e = 0°$, $\delta_n = 0°$
△   "   109 , "   " -10° , "
▽   "   110 , "   " -20° , "
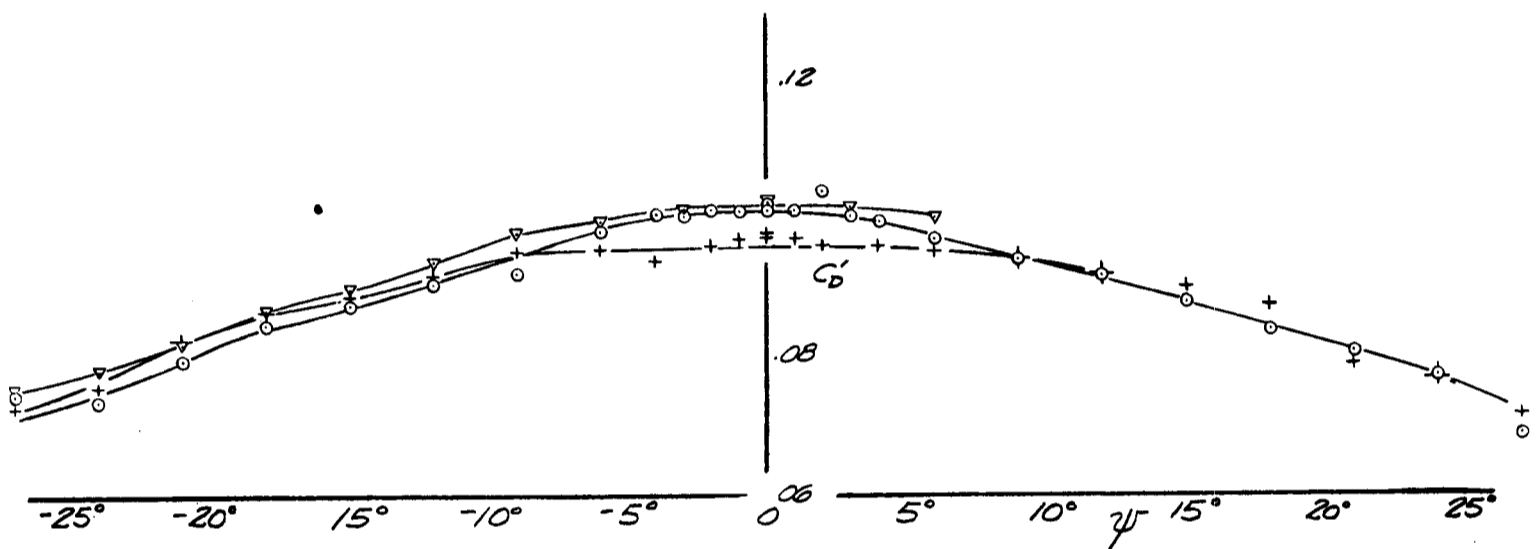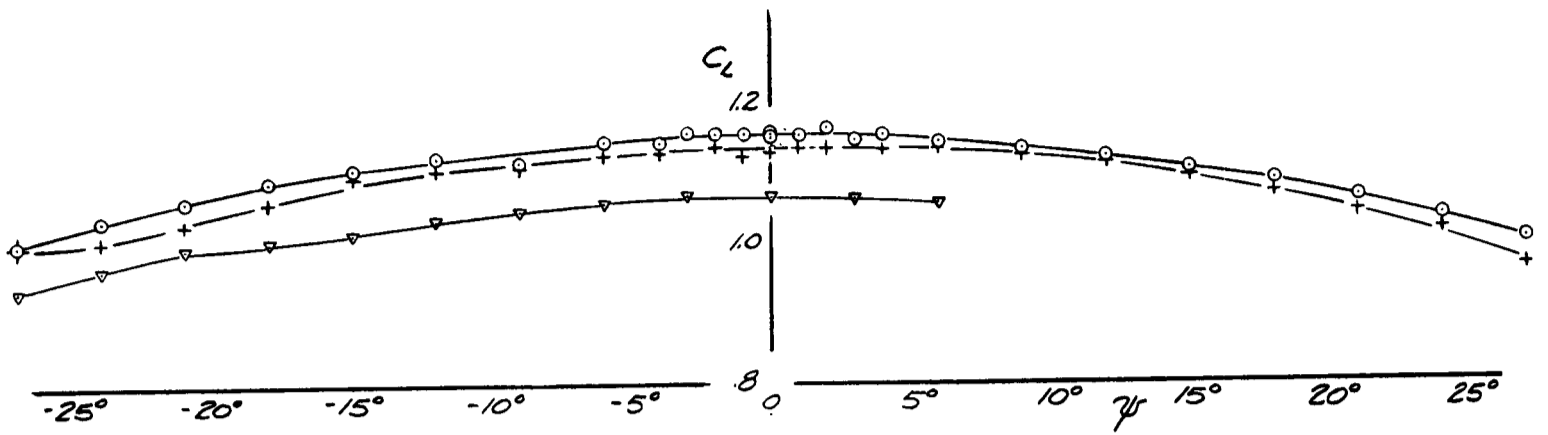⊡   "   111 , "   " -25° , "
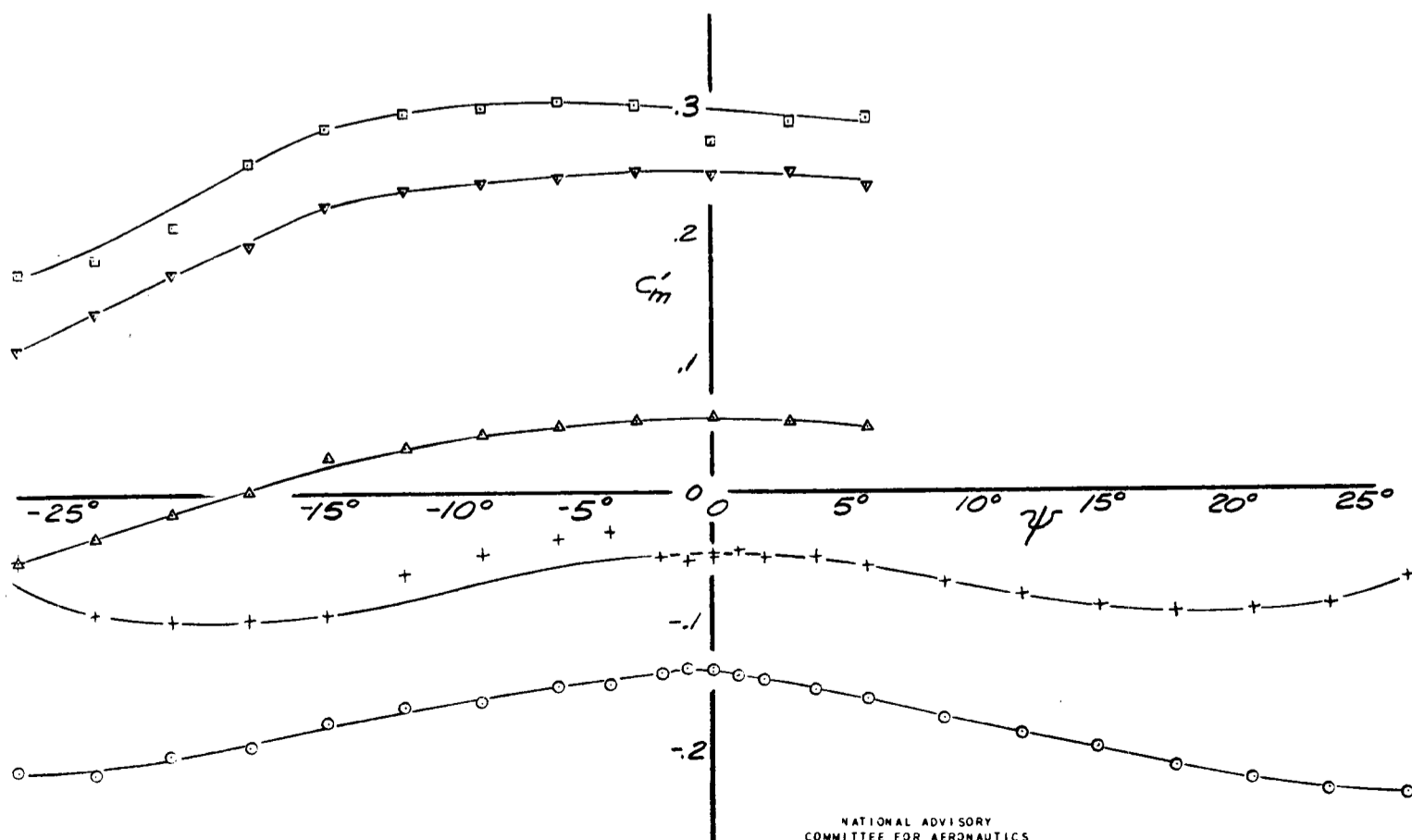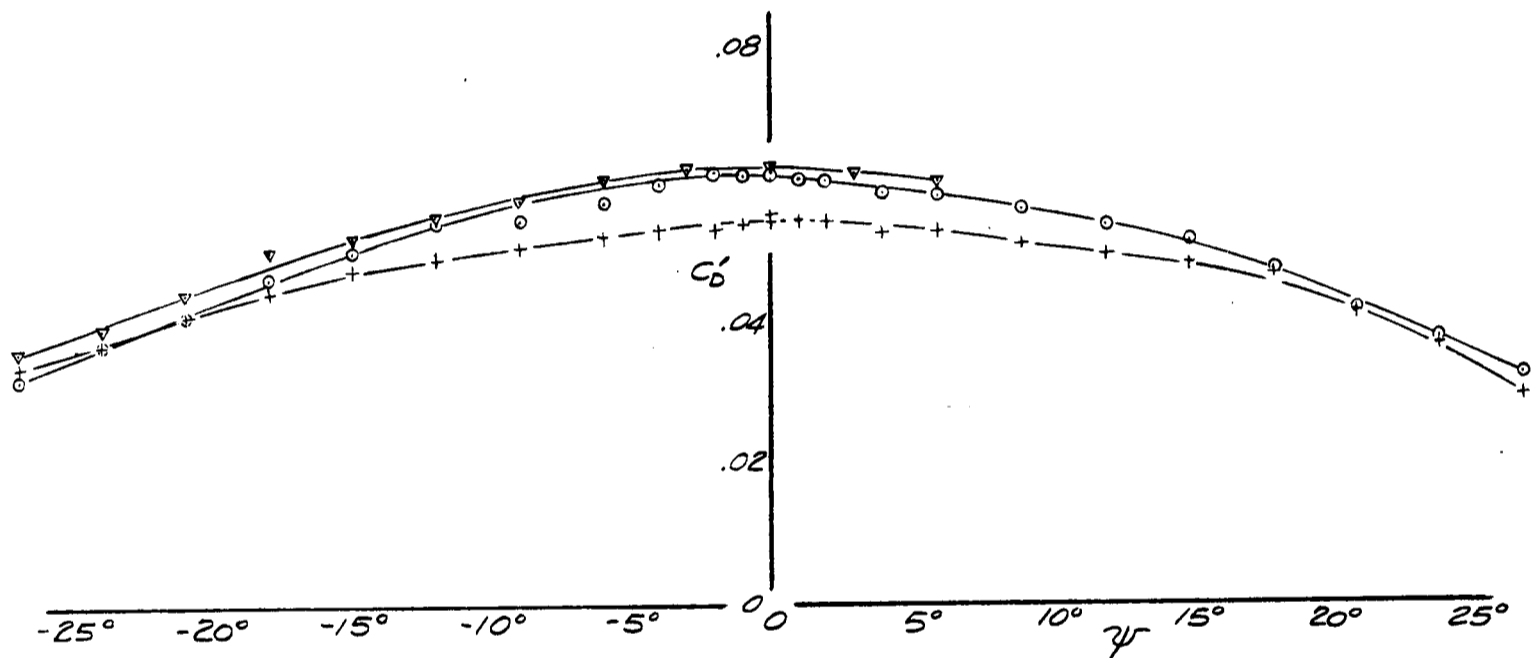
FIG. 24 - ELEVATOR EFFECTIVENESS OF THE MODEL IN YAW ,
FLOATS OFF , FLAPS UP , $\alpha_u = 6°$, RUDDER NEUTRAL

C_L

1.2

1.0

.8

.6

−25° −20° −15° −10° −5° 0 5° 10° ψ 15° 20° 25°

+ RUN 41 , S−HVL$_T$+PL$_{2R}$ TAIL OFF
⊙)) 38 , S+PL$_{2R}$−L$_T$, $\delta_e=0°$, $\delta_r=0°$
△)) 92 , " , −10° , "
▽)) 93 , " , −20° , "
□)) 94 , " , −25° , "

.08

.06

.04

.02

C_D'

0

−25° −20° −15° −10° −5° 0 5° 10° ψ 15° 20° 25°

.3

.2

.1

C_m'

−25° −15° −10° −5° 0 5° 10° 15° ψ 20° 25°

−.1

−.2

−.3

FIG. 25 − ELEVATOR EFFECTIVENESS OF THE MODEL IN YAW.
FLOATS ON, FLAPS UP , $\alpha_u=6°$, RUDDER NEUTRAL

C_L

.12

.10

.8
| -25° | -20° | -15° | -10° | -5° | 0 | 5° | 10° | ψ | 15° | 20° | 25° |

.12

C_D'

.08

.06
| -25° | -20° | 15° | -10° | -5° | 0 | 5° | 10° | ψ | 15° | 20° | 25° |

+ RUN 47 , S-HVL$_T$ + LF^{15} TAIL OFF
⊙   53 , S + LF^{15} , δ_e = 0° , δ_r = 0°
△   123 ,   "   ,   -10°   "
▼   124 ,   "   ,   -20°,   "
◨   125 ,   "   ,   -25°,   "
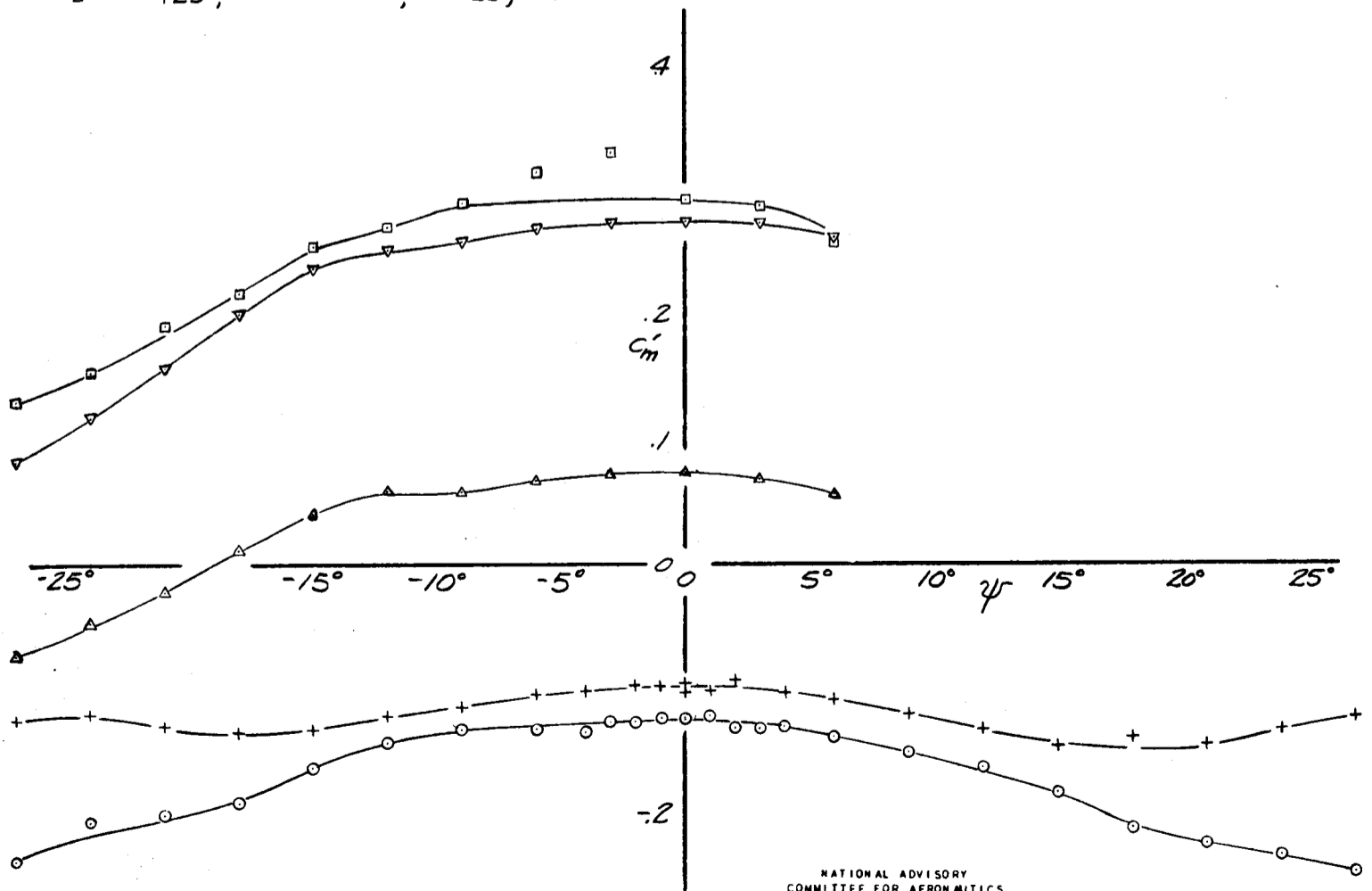
4

.2
C_m'

.1

| -25° | | -15° | -10° | -5° | 0 | 5° | 10° | ψ | 15° | 20° | 25° |

-.2

FIG. 26 - ELEVATOR EFFECTIVENESS OF THE MODEL IN YAW,
FLOATS OFF, FLAPS DOWN 15°, α_u = 6°, RUDDER NEUTRAL

+ RUN 45, $S-HVL_T +pL_{2R}F^{15}$ TAIL OFF
⊙ " 55, $S+pL_{2R}F^{15}-L_T$, $\delta_e=0°$, $\delta_f=0°$
△ " 133, " , -10°, "
▽ " 134, " , -20°, "
☐ " 135, " , -25°, "

FIG 27-ELEVATOR EFFECTIVENESS OF THE MODEL IN YAW,
FLOATS ON, FLAPS DOWN 15°, $\alpha_u=6°$, RUDDER NEUTRAL
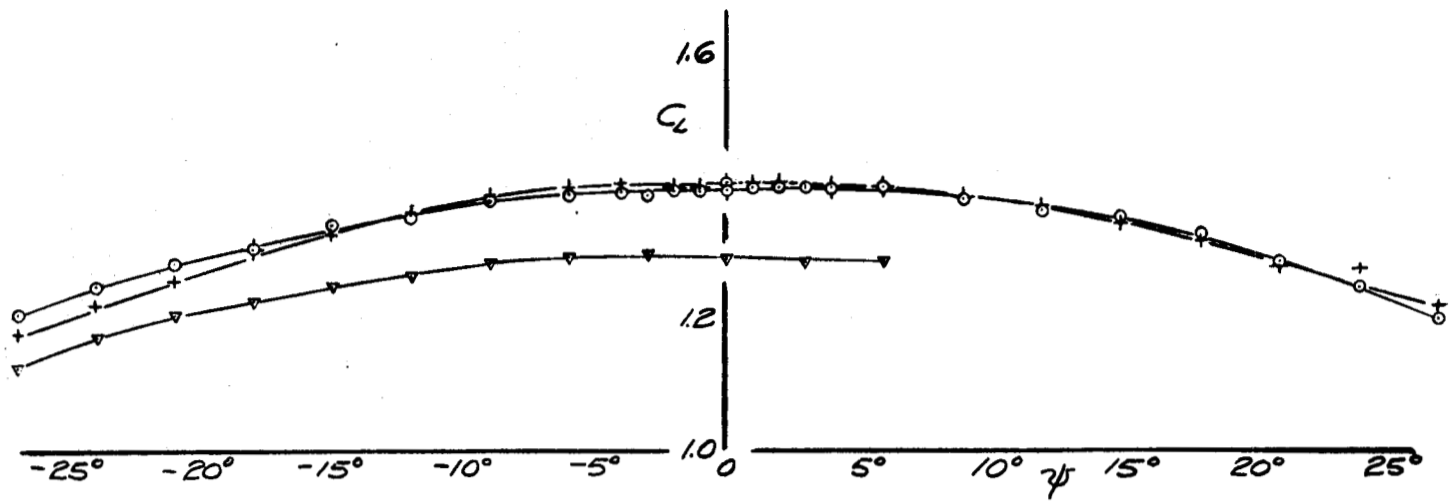
+ RUN 49, $S-HVL_T + LF^{45}$ TAIL OFF
⊙ " 51, $S + LF^{45}$, $\delta_e = 0$, $\delta_r = 0°$
▲ , 79,   "   ,   " −10°,   "
▼ , 80,   "   ,   " −20°,   "
▣ , 81,   "   ,   " −25°,   "
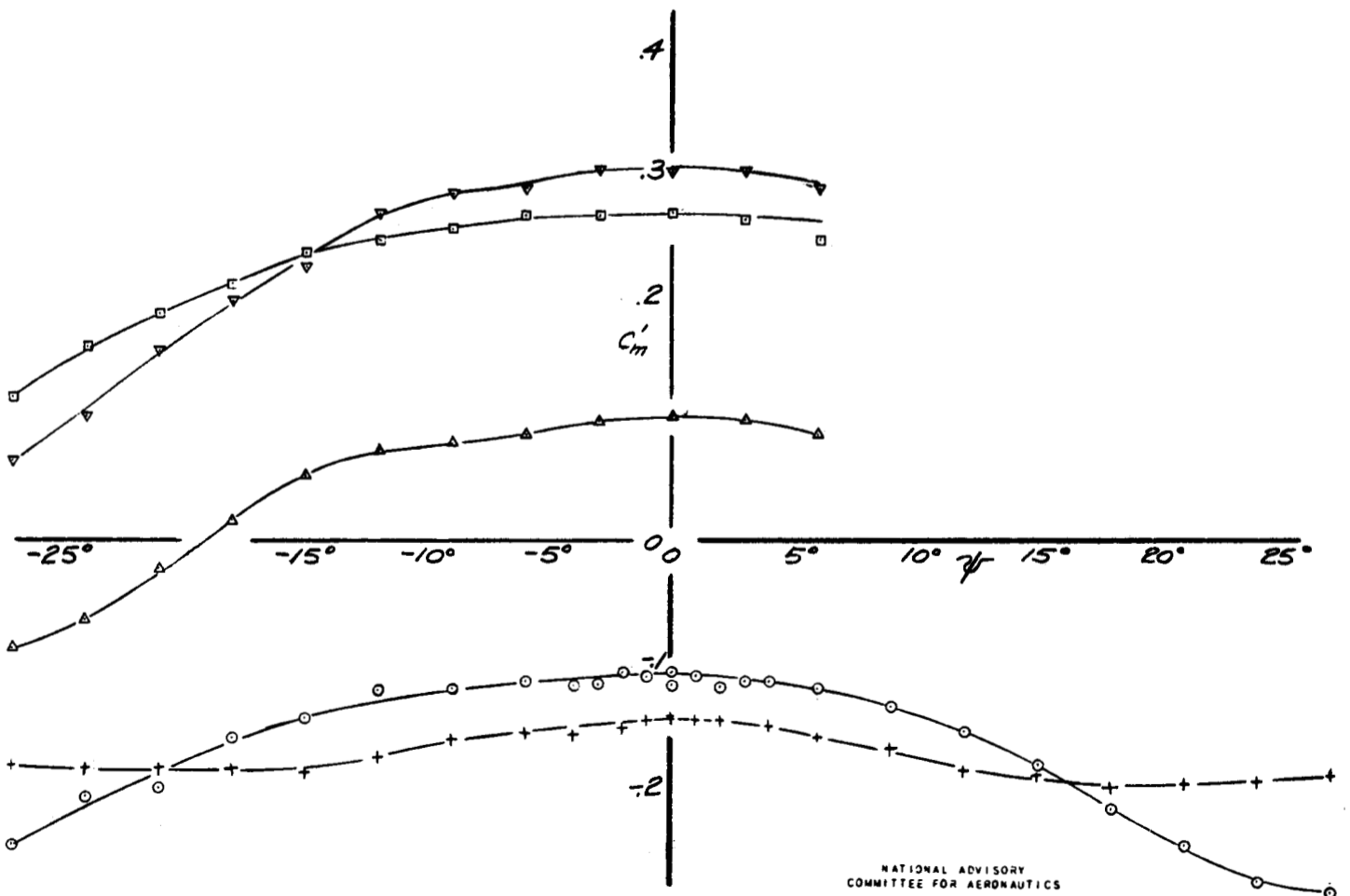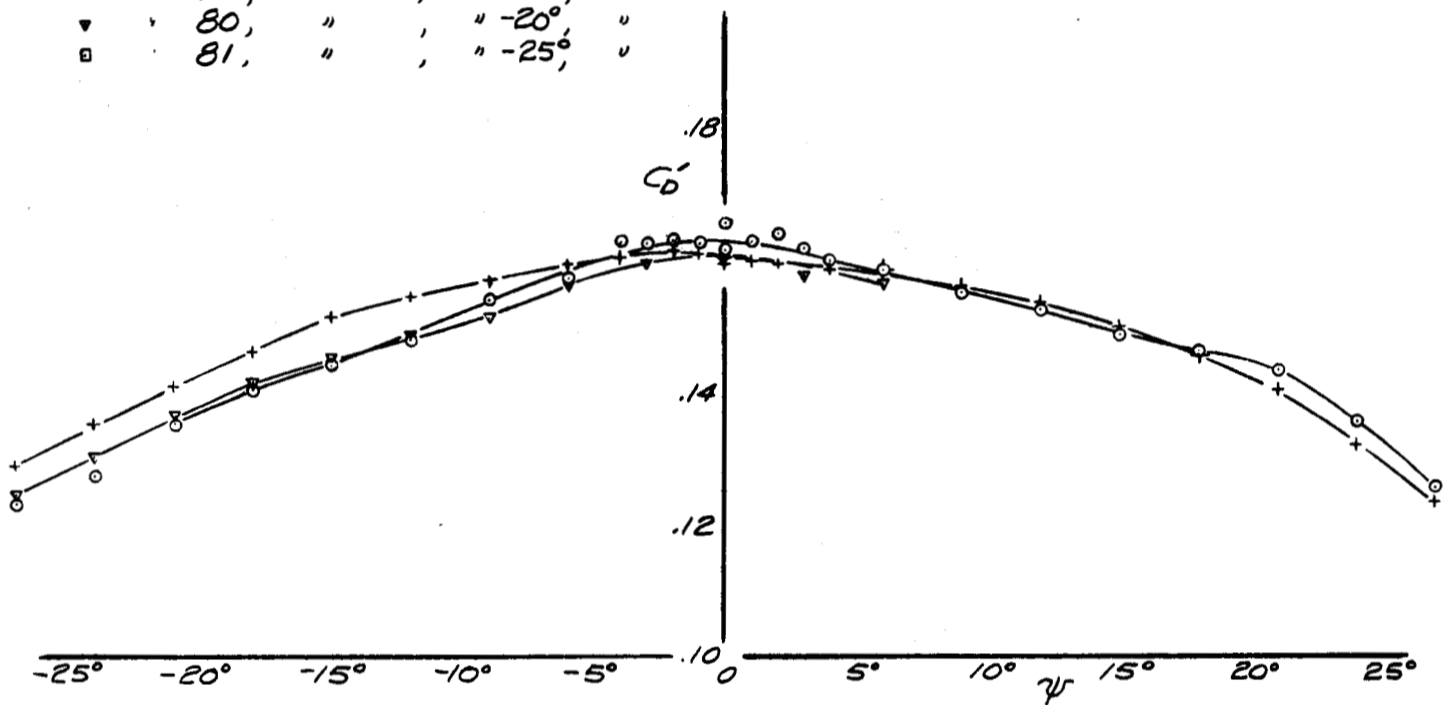
FIG. 28 - ELEVATOR EFFECTIVENESS OF THE MODEL IN YAW,
FLOATS OFF, FLAPS DOWN 45°, $\alpha_u = 6°$, RUDDER NEUTRAL

Legend (within middle plot):

+ Run 43, S-HVL$_T$+pL$_{2R}$F^{45} TAIL OFF
⊙ " 57, S+pL$_{2R}$F^{45}-L$_T$, δ_e=0°, δ_r=0°
▲ " 69,   "   ,   -10°, "
▼ " 70,   "   ,   -20°, "
☐ " 71,   "   ,   -25°, "

NATIONAL ADVISORY
COMMITTEE FOR AERONAUTICS

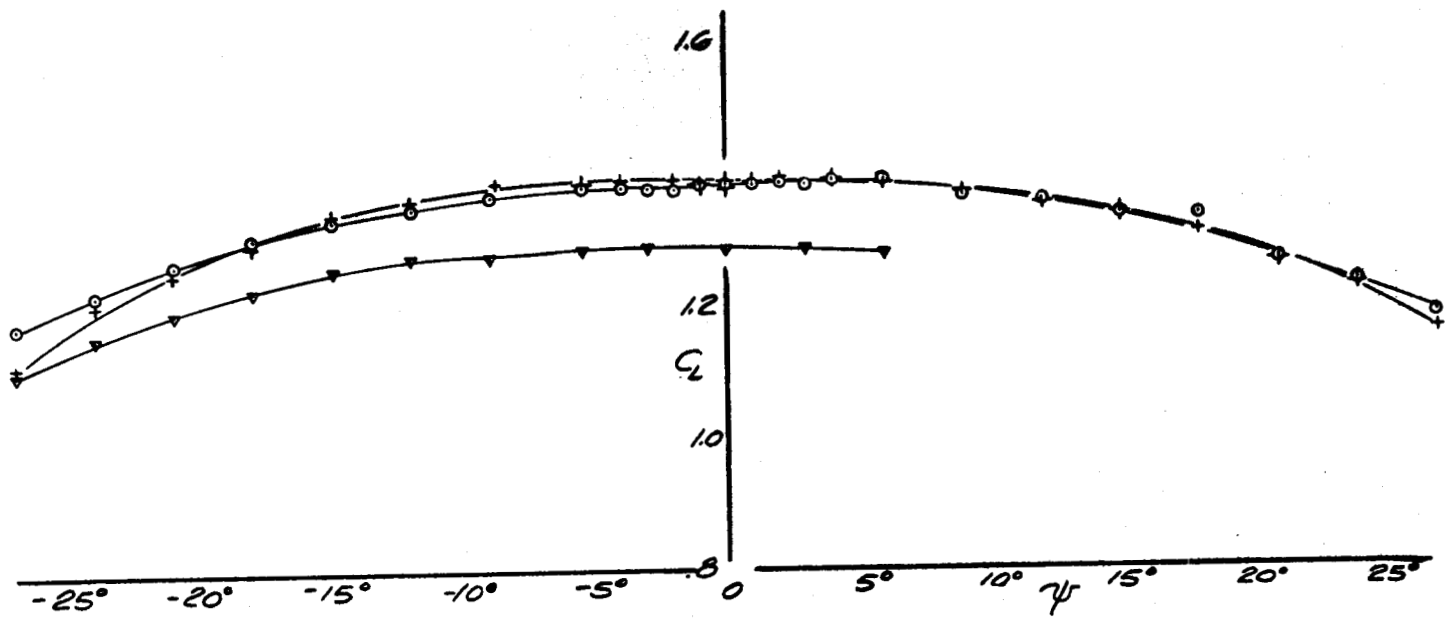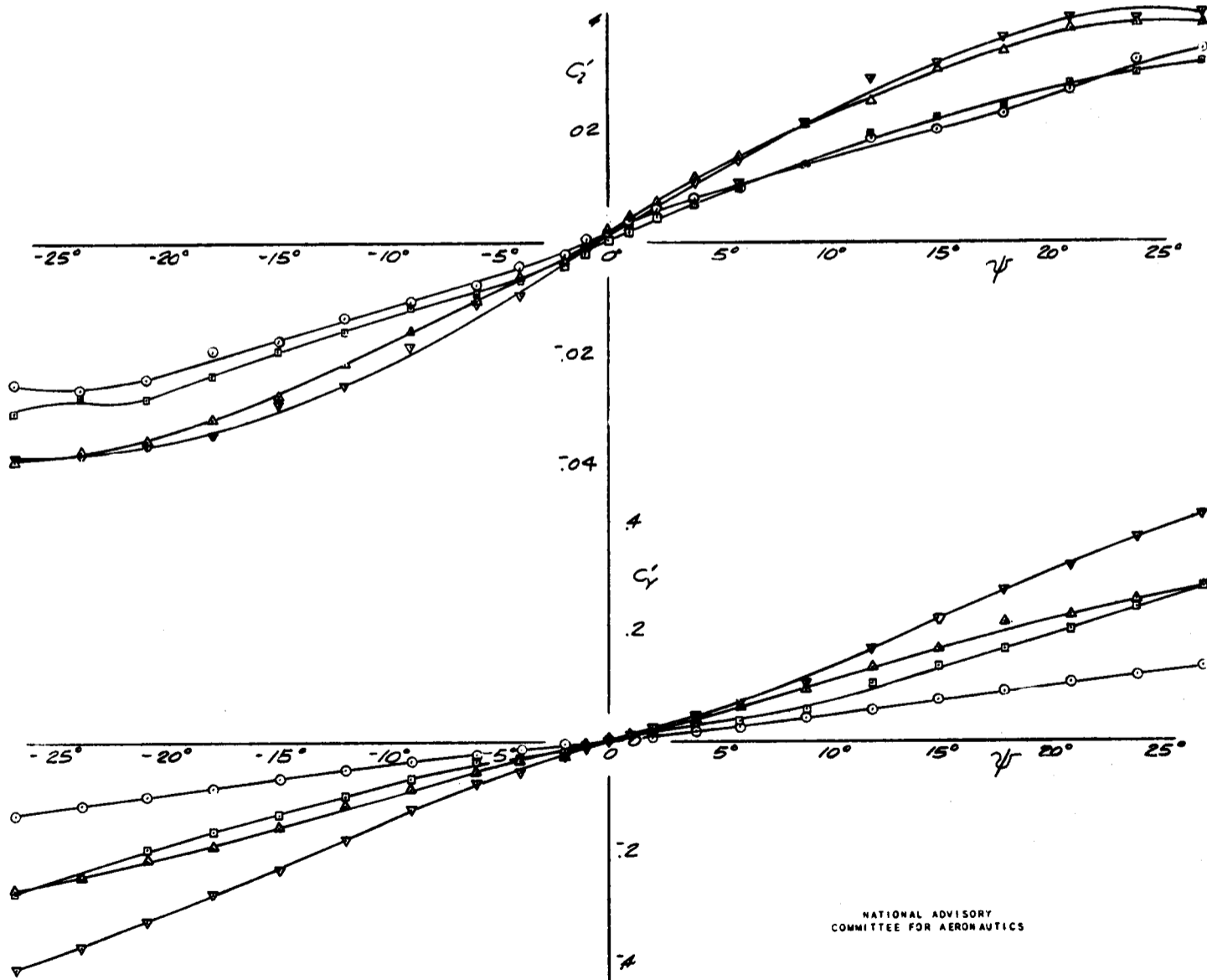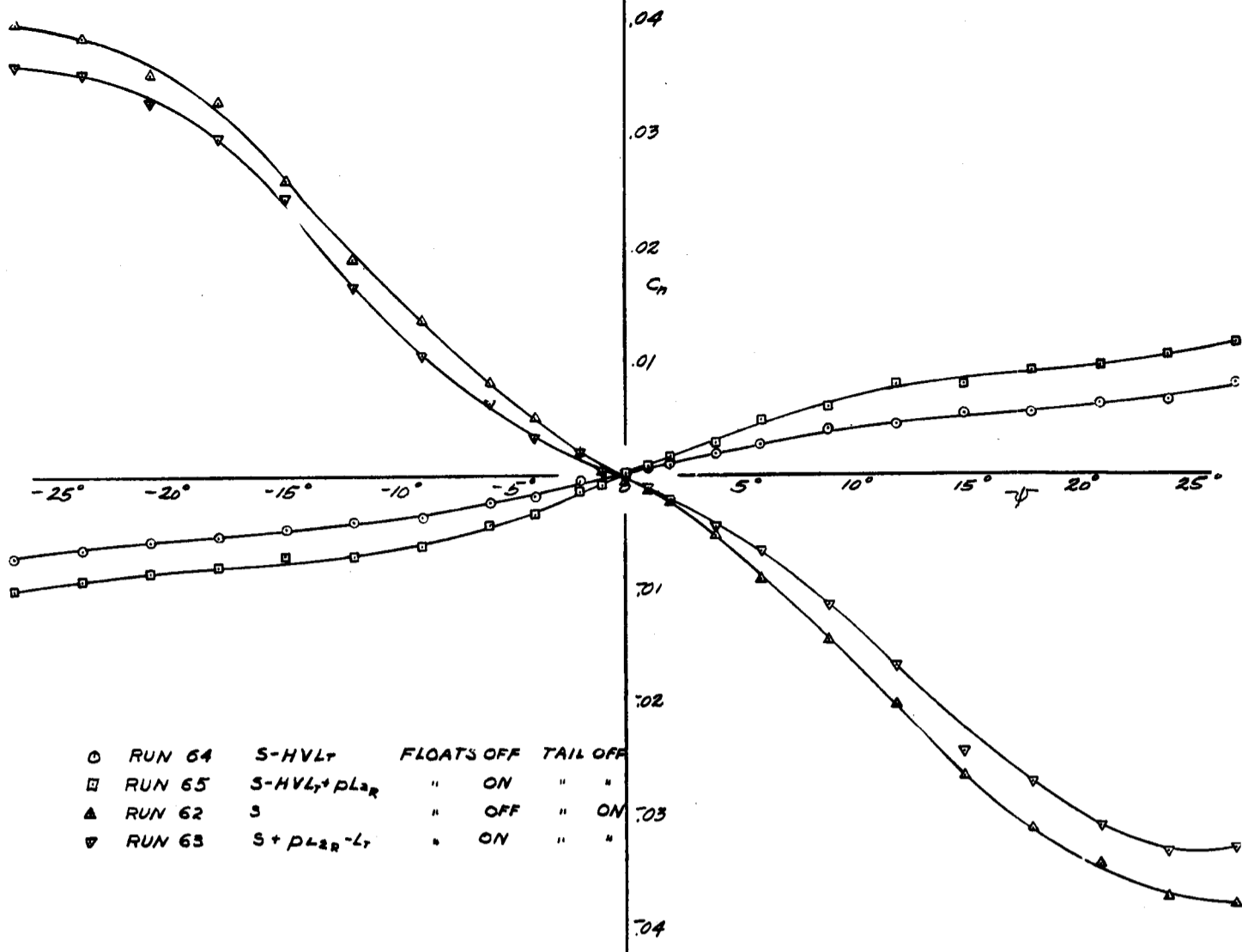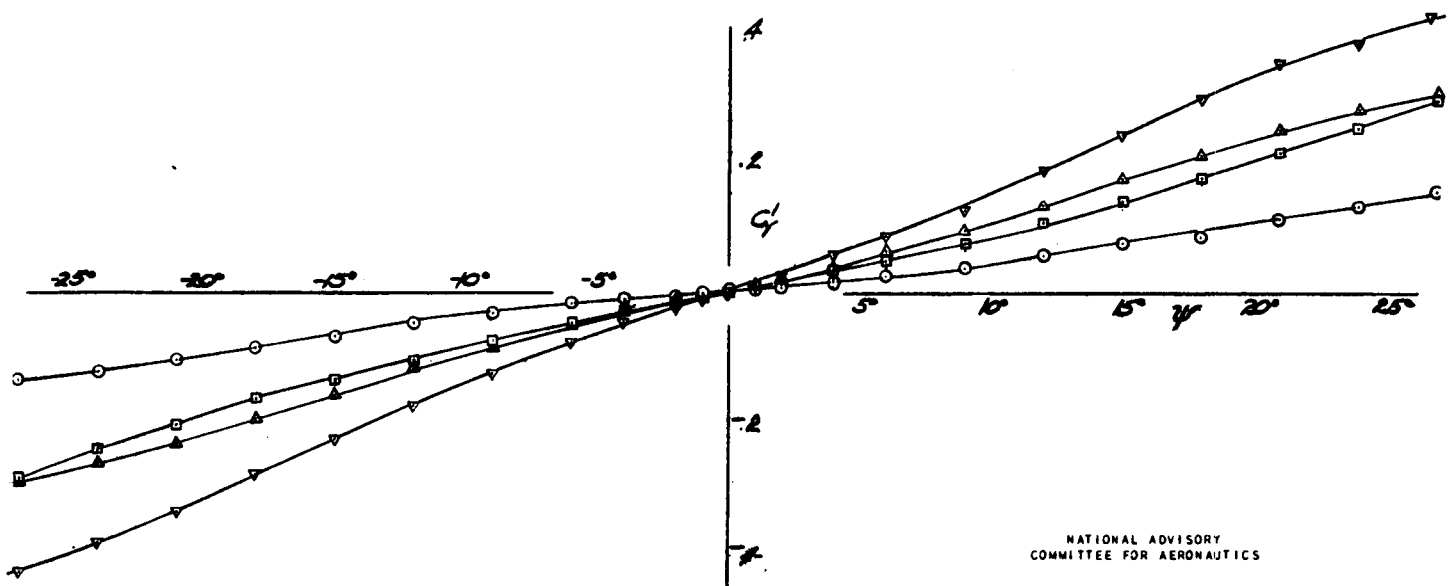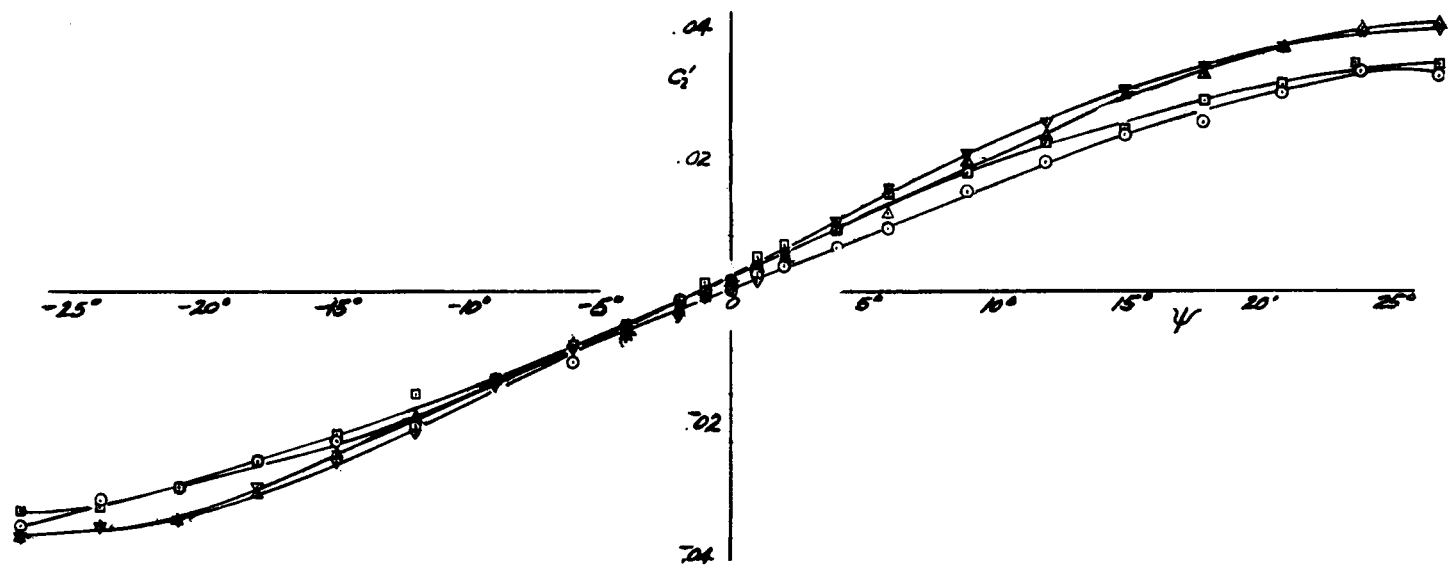FIG. 29 - ELEVATOR EFFECTIVENESS OF THE MODEL IN YAW,
FLOATS ON, FLAPS DOWN 45°, α_u = 6° , RUDDER NEUTRAL

			FLOATS		TAIL	
⊙	RUN 64	S-HVL$_T$		OFF		OFF
⊡	RUN 65	S-HVL$_T$+pL$_{a_R}$	"	ON	"	"
▲	RUN 62	S	"	OFF	"	ON
▽	RUN 63	S + pL$_{2_R}$-L$_T$	"	ON	"	"

NATIONAL ADVISORY
COMMITTEE FOR AERONAUTICS

FIG 30 – EFFECT OF FLOATS ON LATERAL-STABILITY CHARACTERISTICS OF
THE MODEL AT α₀=-1°, FLAPS UP, TAIL ON AND OFF
$C_L ≅ .25$, RUDDER AND ELEVATOR NEUTRAL
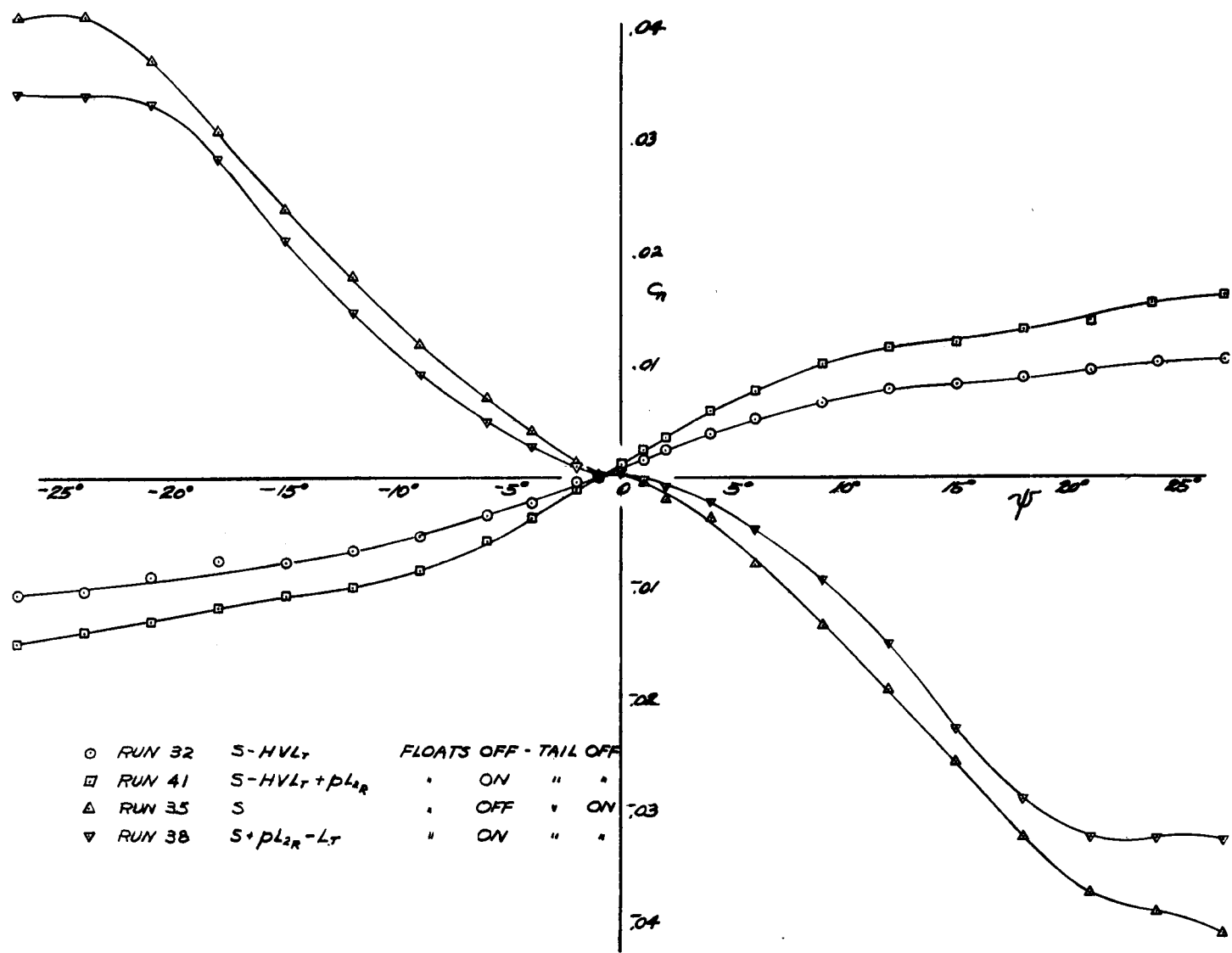
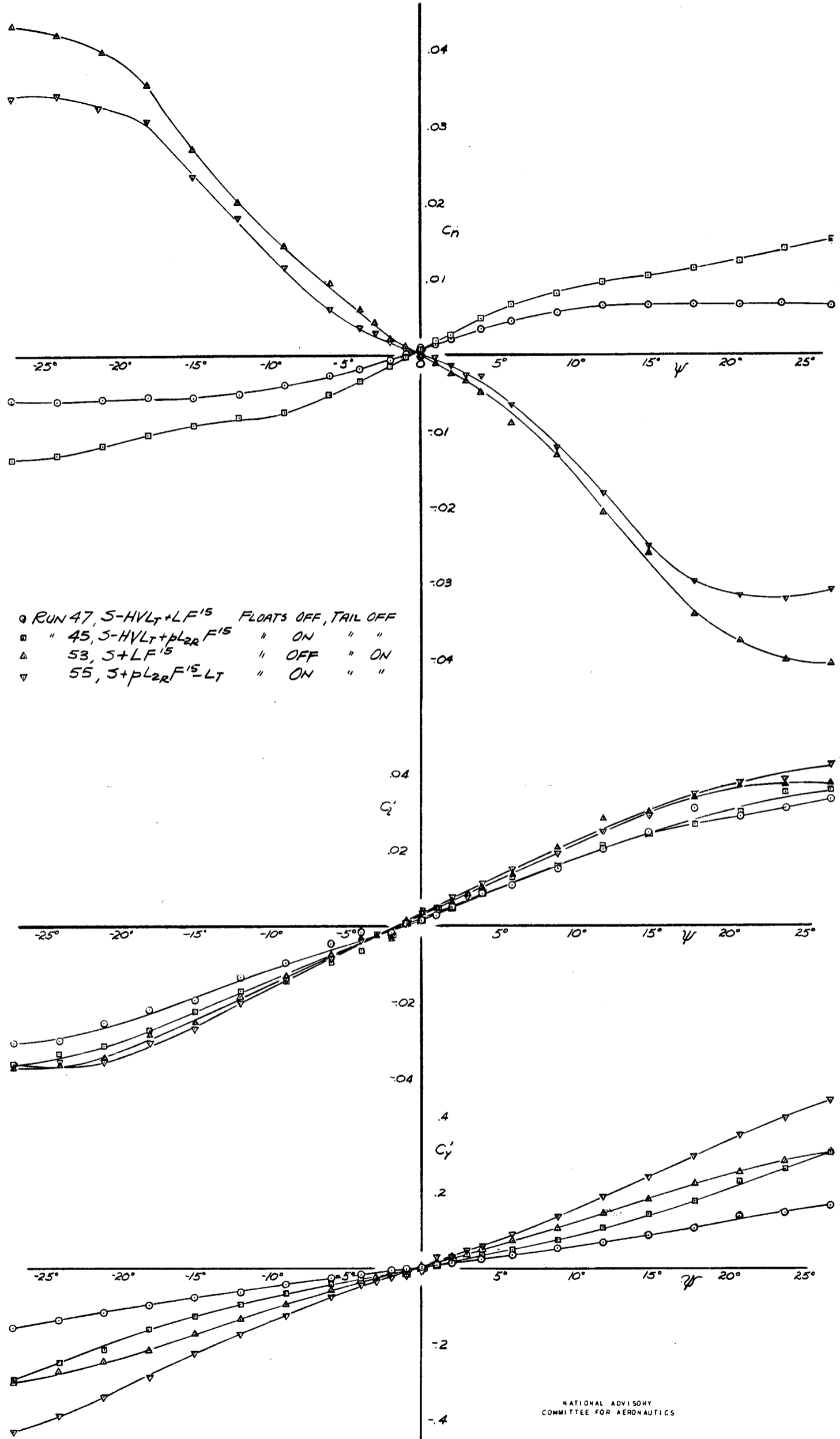| | RUN 32 | S-HVL_T | | FLOATS OFF | - | TAIL OFF |
⊙	RUN 32	$S-HVL_T$		FLOATS OFF	-	TAIL OFF
⊡	RUN 41	$S-HVL_T + pL_{2R}$		" ON	"	"
△	RUN 35	S		" OFF	"	ON
▽	RUN 38	$S + pL_{2R} - L_T$		" ON	"	"

FIG 31 — EFFECT OF FLOATS ON LATERAL STABILITY CHARACTERISTICS OF THE MODEL AT $\alpha_u = 6°$, FLAPS UP. TAIL ON AND OFF. $C_L \cong .9$ RUDDER AND ELEVATOR NEUTRAL.

Q RUN 47, S-HVL_T+LF^{15}   FLOATS OFF, TAIL OFF
▣ " 45, S-HVL_T+pL_{2R}F^{15}   "   ON   "   "
△ 53, S+LF^{15}   " OFF " ON
▽ 55, S+pL_{2R}F^{15}-L_T   " ON   "   "

FIG 32 — EFFECT OF FLOATS ON LATERAL-STABILITY CHARACTERISTICS OF
THE MODEL   AT d_u=6°, FLAPS DOWN 15°, TAIL ON AND OFF, C_L≅1.15
RUDDER AND ELEVATOR NEUTRAL

NATIONAL ADVISORY
COMMITTEE FOR AERONAUTICS

.04

.03

.02

C_n

.01

-25°   -20°   -15°   -10°   -5°   0   5°   10°   15° ψ 20°   25°

-.01

-.02

-.03

-.04

	RUN 49	$S-HVL_T+LF^{45}$	FLOATS OFF - TAIL OFF
⊙	RUN 43	$S-HVL_T+pL_{2_R}+F^{45}$	" ON " "
△	RUN 147	$S+LF^{45}$	" OFF " ON
▽	RUN 57	$S+pL_{2_R}+F^{45}-L_T$	" ON " "

.04

C'_l

.02

-25°   -20°   -15°   -10°   -5°   0   5°   10°   15° ψ 20°   25°

-.02

-.04

.4

C'_y

.2

-25°   -20°   -15°   -10°   -5°   0   5°   10°   15° ψ 20°   25°
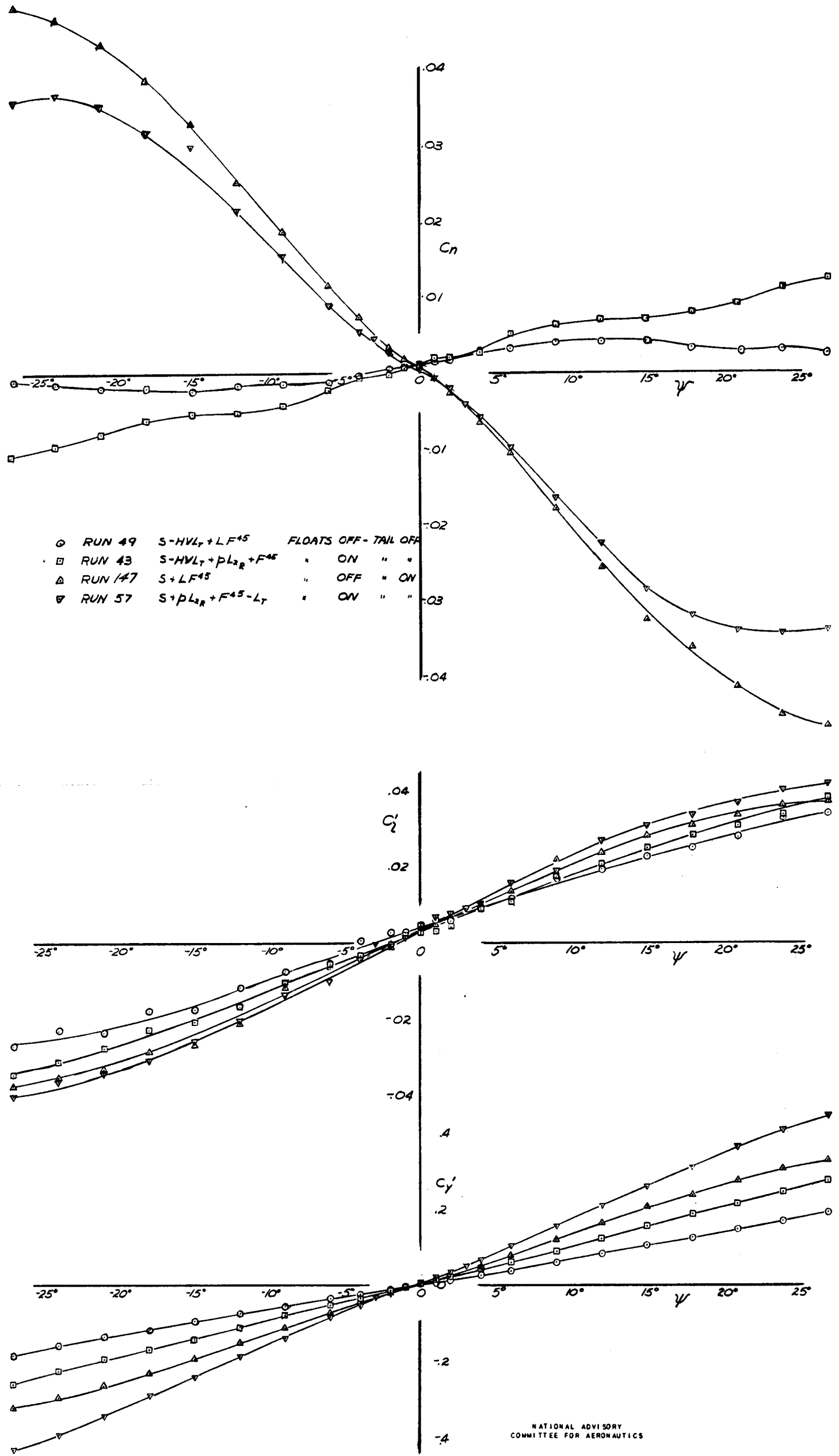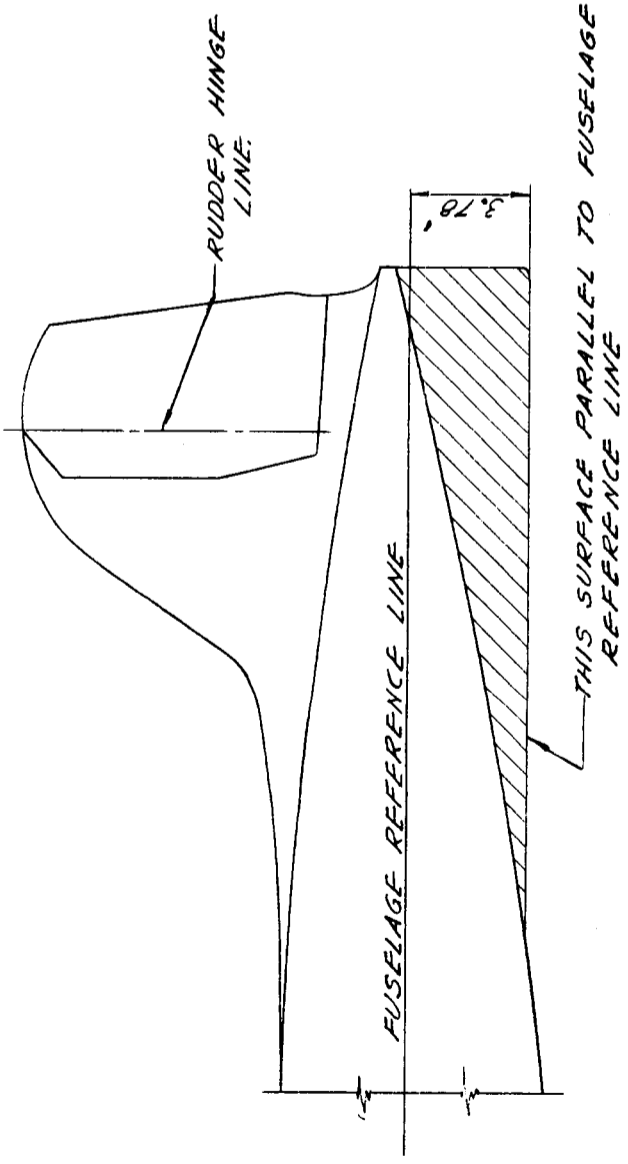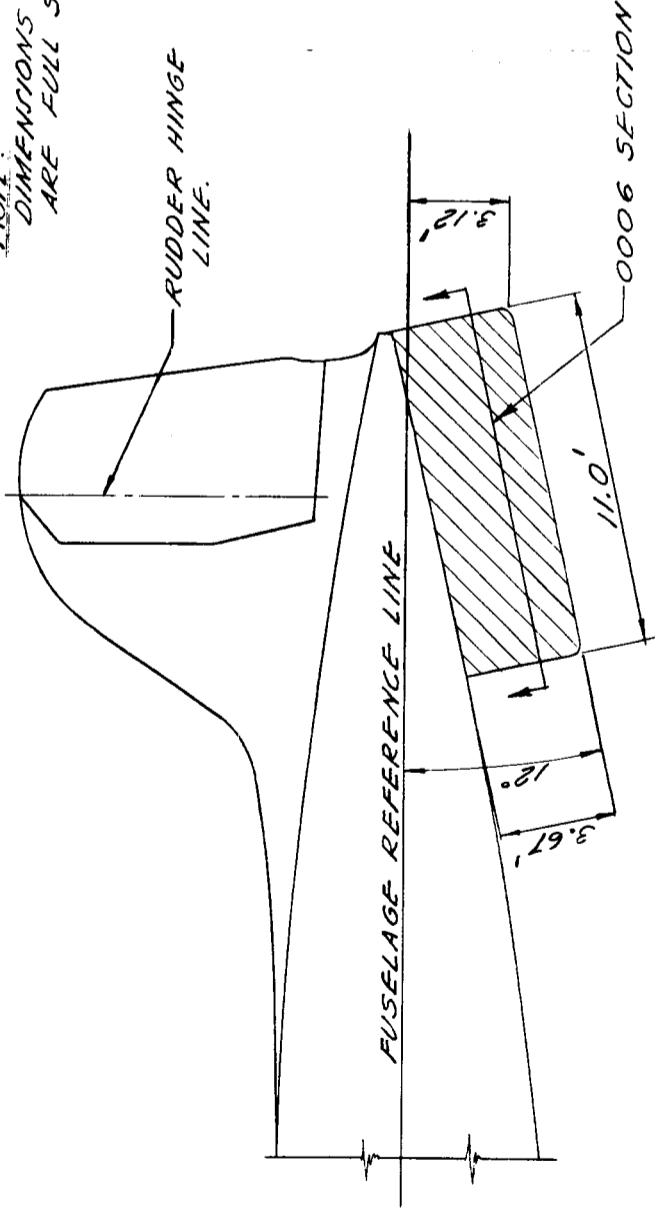
-.2

-.4

NATIONAL ADVISORY
COMMITTEE FOR AERONAUTICS

FIG. 33 — EFFECT OF FLOATS ON LATERAL-STABILITY CHARACTERISTICS OF THE MODEL AT $\alpha_u = 6°$, FLAPS DOWN 45°, TAIL ON AND OFF, $C_L \cong 1.4$ RUDDER AND ELEVATOR NEUTRAL.
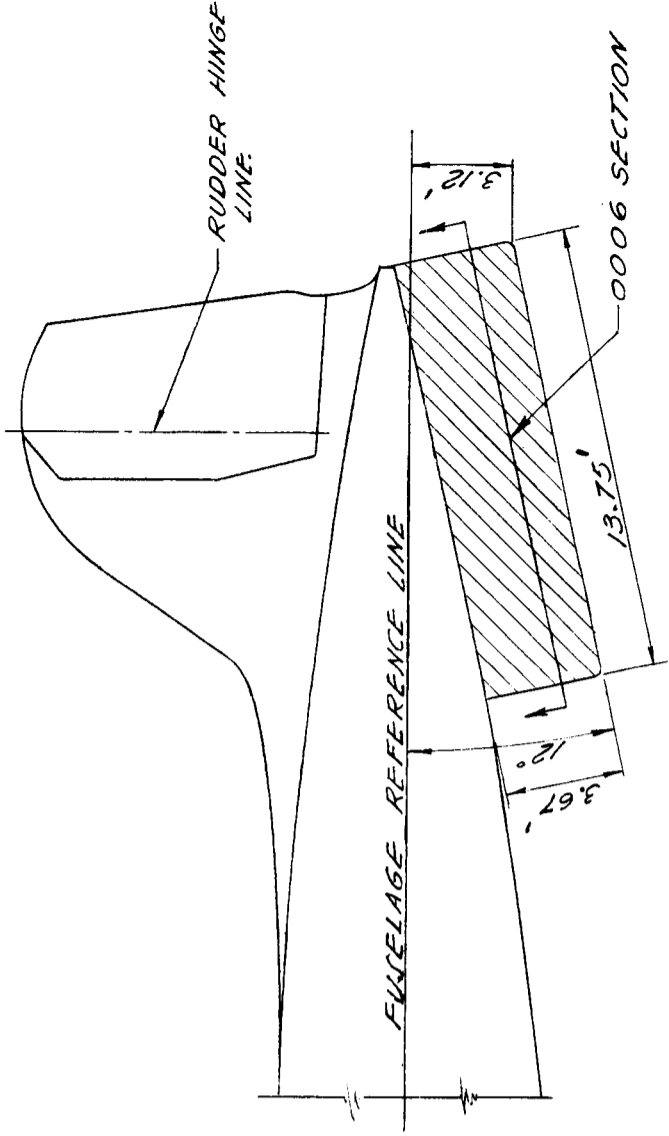
RUDDER HINGE LINE.

FUSELAGE REFERENCE LINE

0006 SECTION

3.12'

13.75'

12°

3.67'

V₃ LARGE RECTANGULAR SKID FIN
AREA = .46 Sᵥ

RUDDER HINGE LINE.

FUSELAGE REFERENCE LINE

3.81'

V₄ VERTICAL FIN EXTENSION
AREA = .38 Sᵥ

NATIONAL ADVISORY
COMMITTEE FOR AERONAUTICS

FIG. 34 TAIL MODIFICATIONS
TESTED ON THE MODEL

RUDDER HINGE LINE.

FUSELAGE REFERENCE LINE

3.78'

THIS SURFACE PARALLEL TO FUSELAGE REFERENCE LINE

V₁ TRIANGULAR SKID FIN
AREA = .41 Sᵥ

NOTE:
DIMENSIONS GIVEN ARE FULL SCALE.

RUDDER HINGE LINE.

FUSELAGE REFERENCE LINE

0006 SECTION

3.12'

11.0'

12°

3.67'

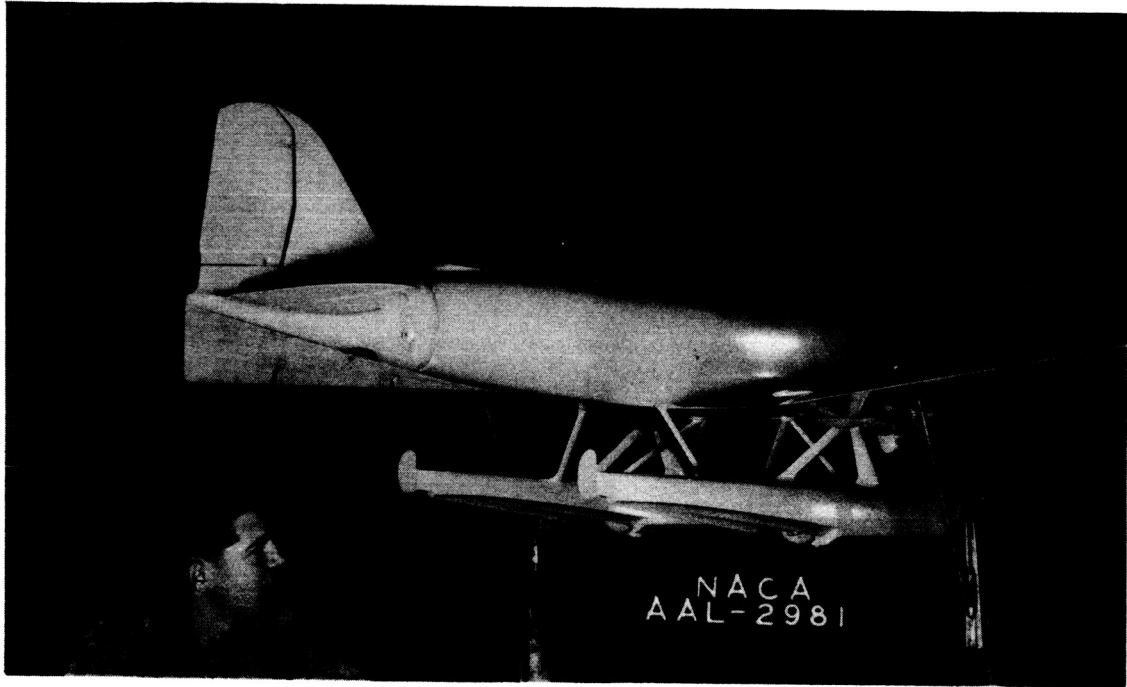V₂ SMALL RECTANGULAR SKID FIN
AREA = .37 Sᵥ

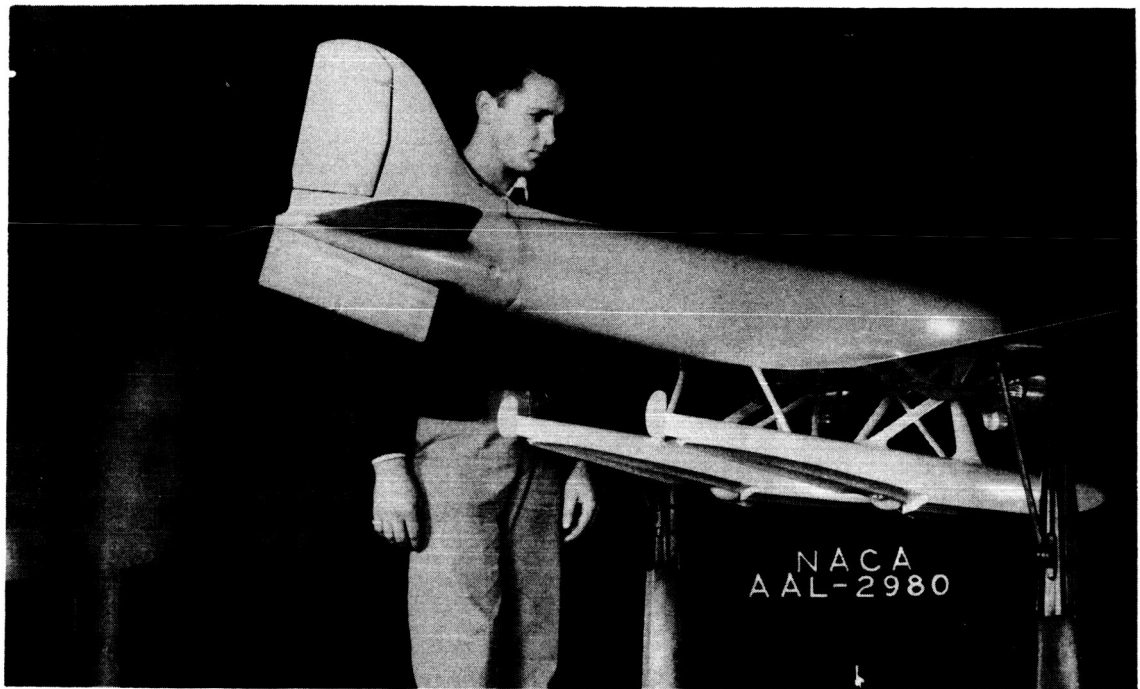Figure 35(a).- Model with triangular skid fin (V$_1$).

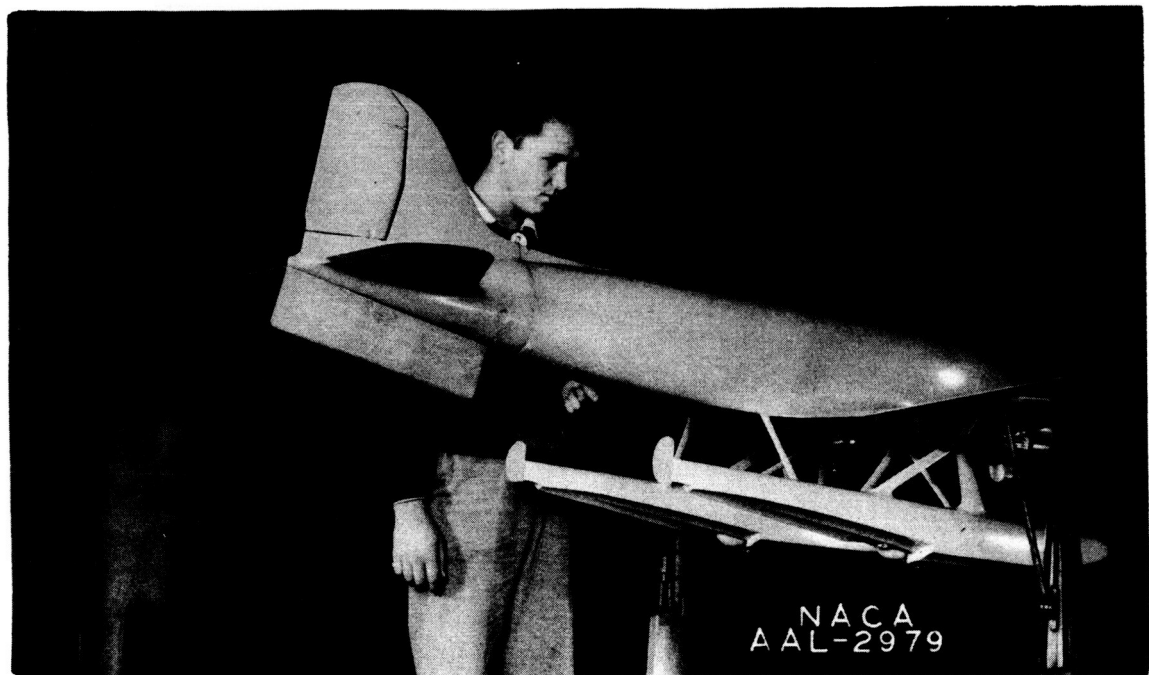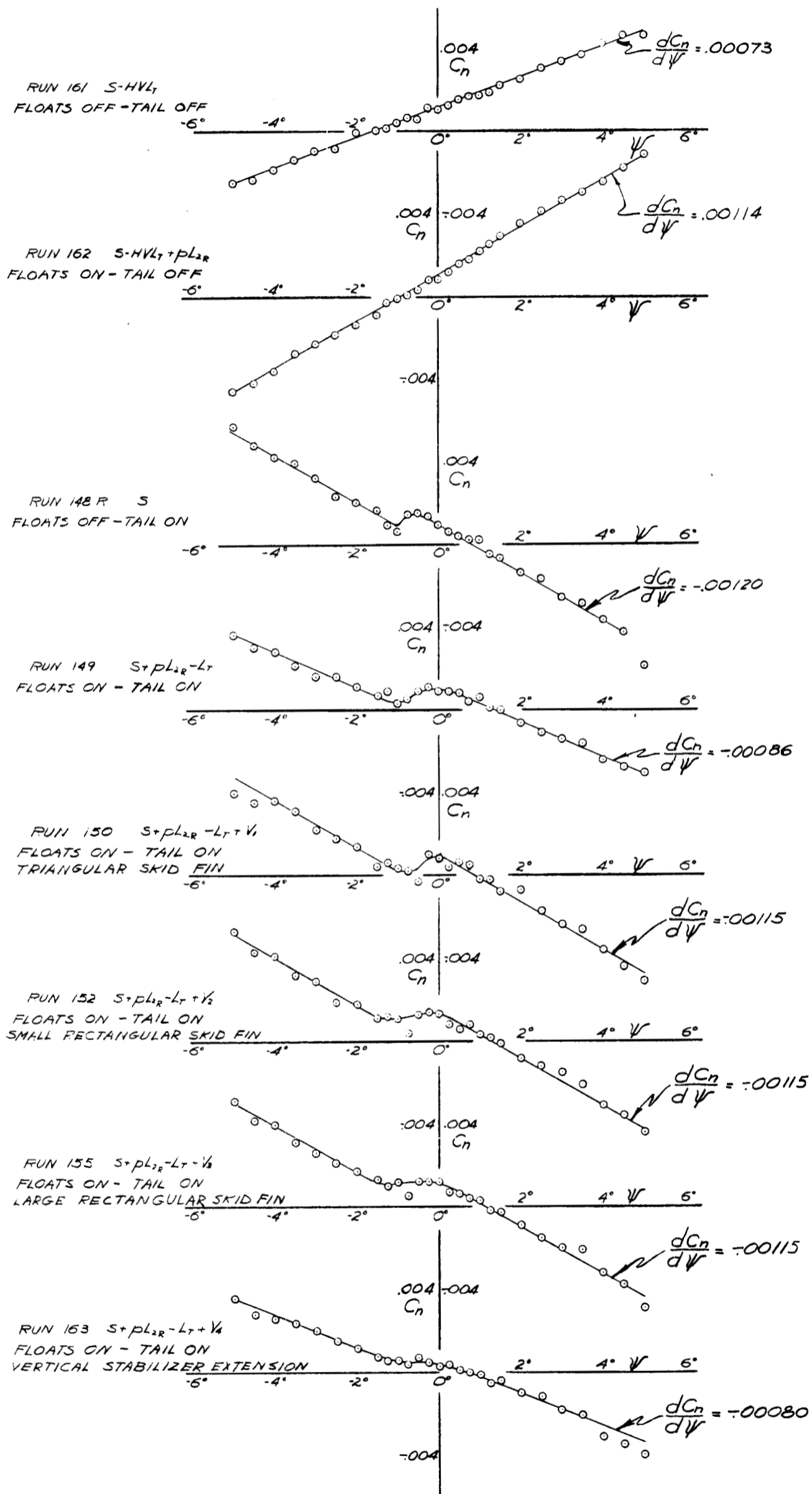Figure 35(b).- Model with small rectangular skid fin (V_2).

Figure 35(c).- Model with large rectangular skid fin (V_3).

Figure 35(d).- Model with vertical fin extension (V_4).

RUN 161 S-HVL_T
FLOATS OFF -TAIL OFF

$\frac{dC_n}{d\psi} = .00073$

RUN 162 S-HVL_T + pL_{2R}
FLOATS ON - TAIL OFF

$\frac{dC_n}{d\psi} = .00114$

RUN 148 R S
FLOATS OFF -TAIL ON

$\frac{dC_n}{d\psi} = -.00120$

RUN 149 S + pL_{2R} - L_T
FLOATS ON - TAIL ON

$\frac{dC_n}{d\psi} = -.00086$

RUN 150 S + pL_{2R} - L_T + V_1
FLOATS ON - TAIL ON
TRIANGULAR SKID FIN

$\frac{dC_n}{d\psi} = -.00115$

RUN 152 S + pL_{2R} - L_T + V_2
FLOATS ON - TAIL ON
SMALL RECTANGULAR SKID FIN

$\frac{dC_n}{d\psi} = -.00115$

RUN 155 S + pL_{2R} - L_T - V_3
FLOATS ON - TAIL ON
LARGE RECTANGULAR SKID FIN

$\frac{dC_n}{d\psi} = -.00115$

RUN 163 S + pL_{2R} - L_T + V_4
FLOATS ON - TAIL ON
VERTICAL STABILIZER EXTENSION

$\frac{dC_n}{d\psi} = -.00080$

FIG 36 - DIRECTIONAL STABILITY OF THE MODEL WITH VARIOUS
TAIL MODIFICATIONS. FLAPS UP, $\alpha_u = 6°$ $C_L \cong 0.9$
RUDDER AND ELEVATOR NEUTRAL.

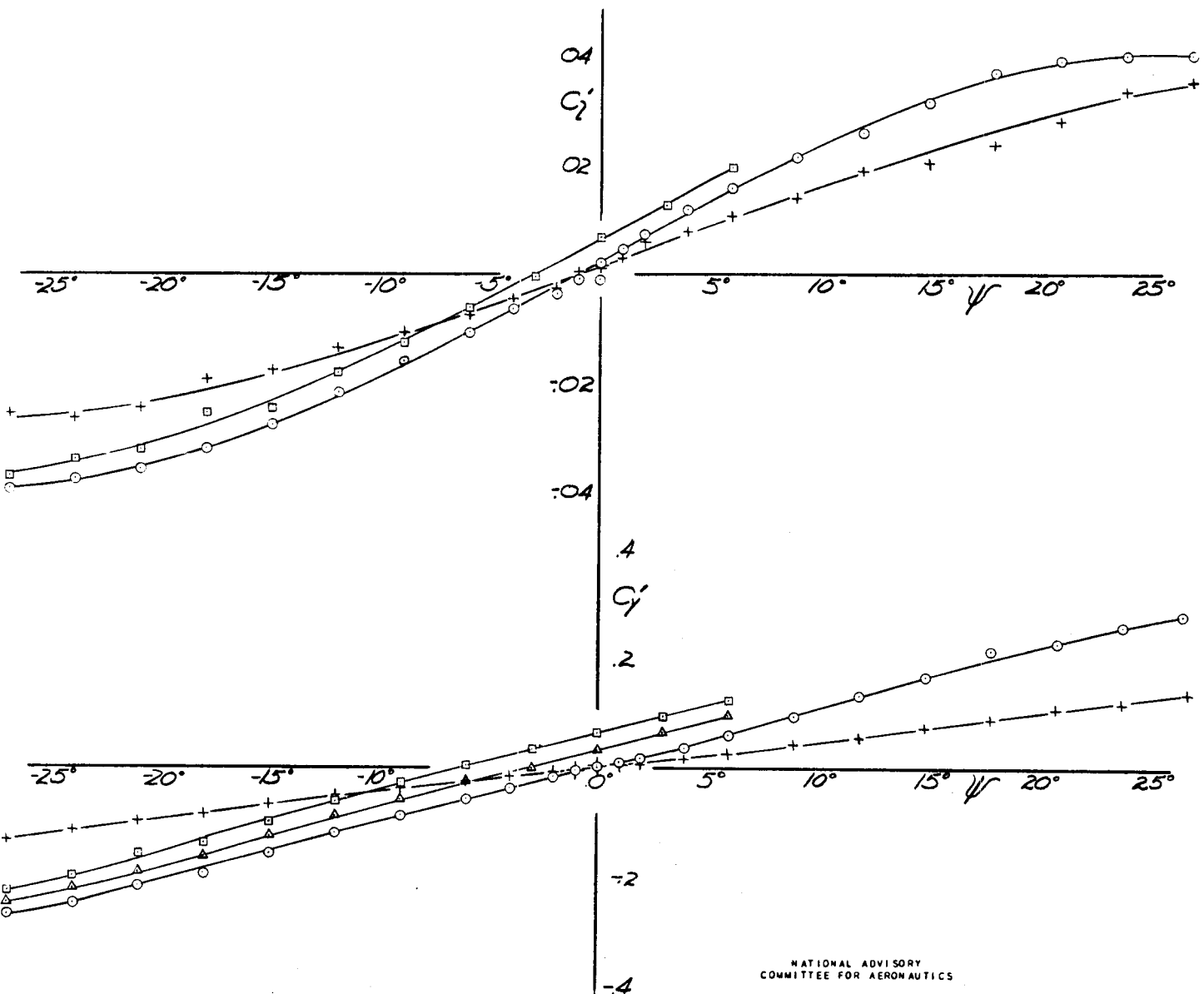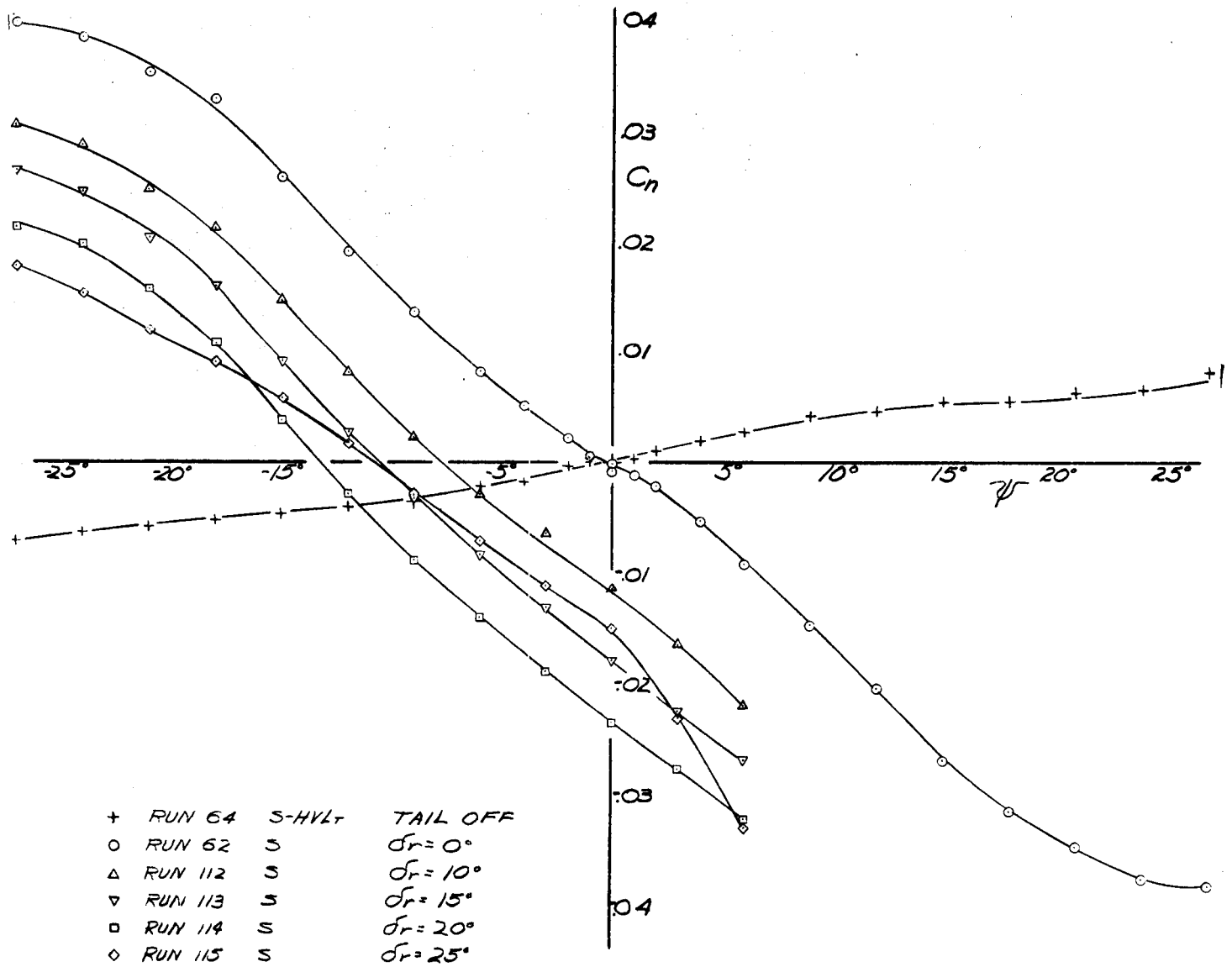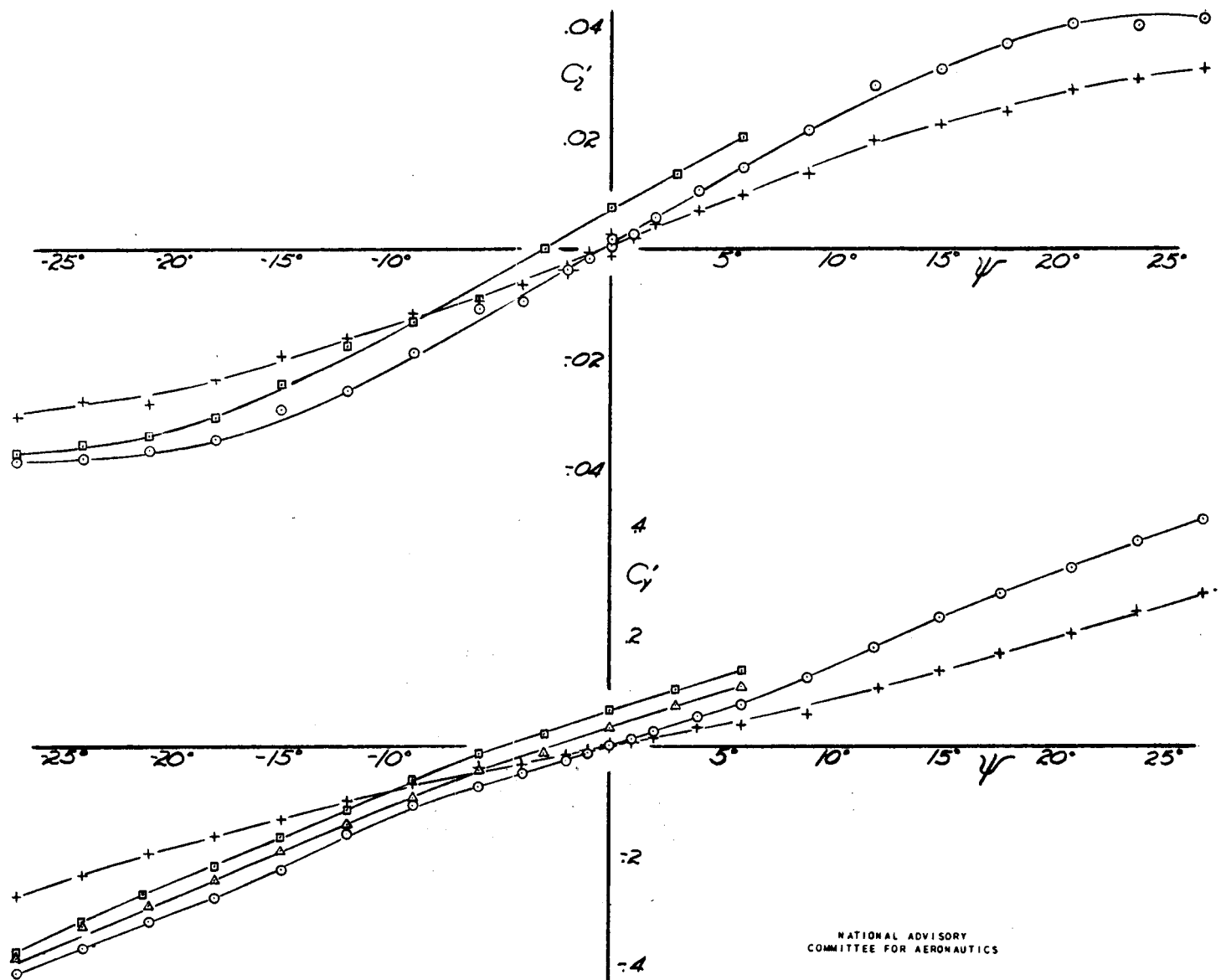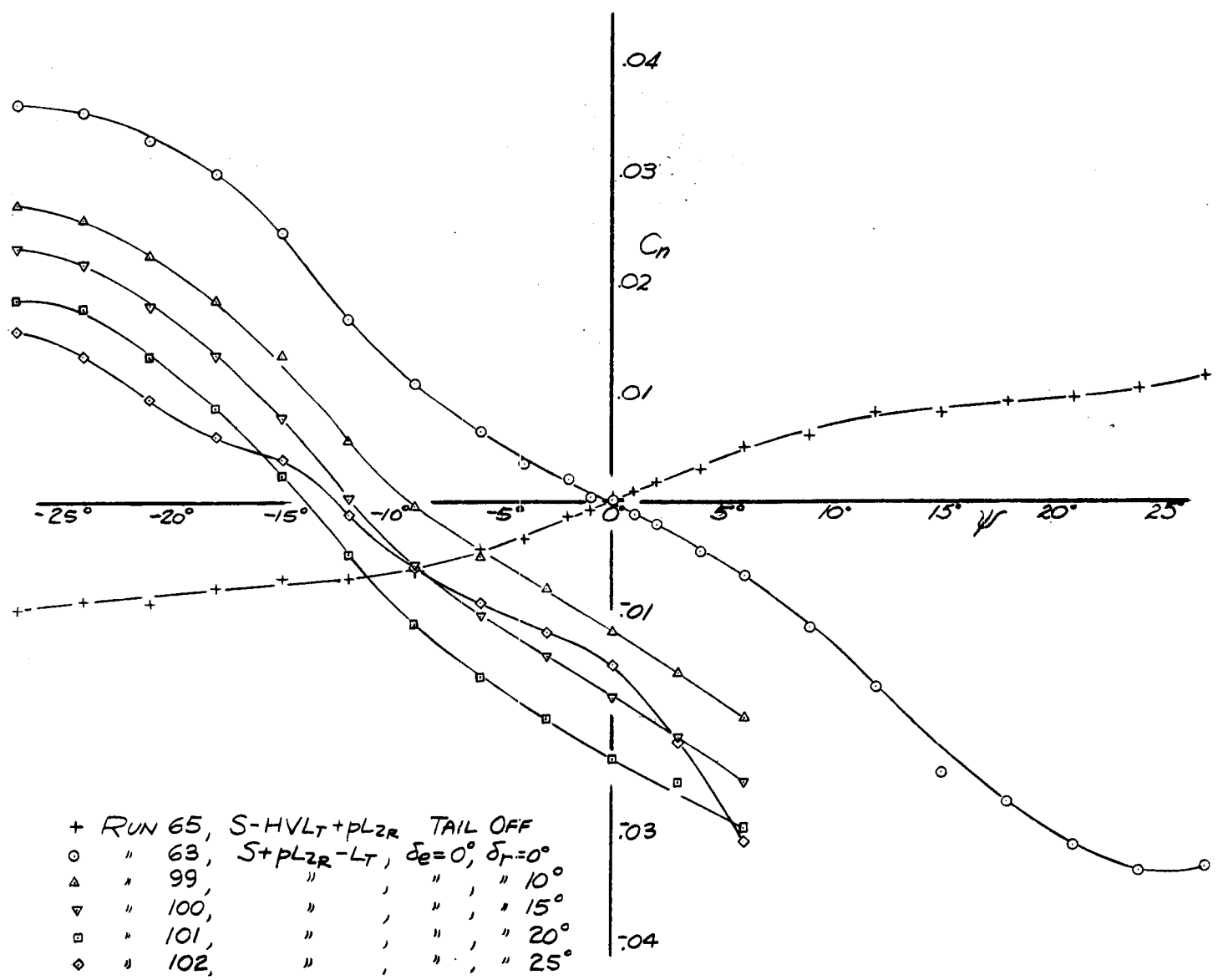|			
+	RUN 64	S-HVLт	TAIL OFF
O	RUN 62	S	$\delta_r = 0°$
△	RUN 112	S	$\delta_r = 10°$
▽	RUN 113	S	$\delta_r = 15°$
□	RUN 114	S	$\delta_r = 20°$
◇	RUN 115	S	$\delta_r = 25°$

FIG. 37 - RUDDER EFFECTIVENESS IN YAW, MODEL WITH
FLOATS OFF, FLAPS UP, $\alpha_u = -1°$, $C_L \cong .25$, ELEVATOR NEUTRAL

Cn

.04
.03
.02
.01
-.01
-.03
-.04

-25° -20° -15° -10° -5° 0 5° 10° 15° ψ 20° 25°

+ RUN 65, S-HVLT+pLZR TAIL OFF
⊙ " 63, S+pLZR-LT , δe=0°, δr=0°
△ " 99,   "   ,   "   , " 10°
▽ " 100,   "   ,   "   , " 15°
□ " 101,   "   ,   "   , " 20°
◇ " 102,   "   ,   "   , " 25°

C₂'

.04
.02
-.02
-.04

-25° -20° -15° -10° 5° 10° 15° ψ 20° 25°

Cy'

.4
.2
-.2
-.4

-25° -20° -15° -10° 5° 10° 15° ψ 20° 25°

NATIONAL ADVISORY
COMMITTEE FOR AERONAUTICS

FIG 38 - RUDDER EFFECTIVENESS IN YAW ,   MODEL WITH
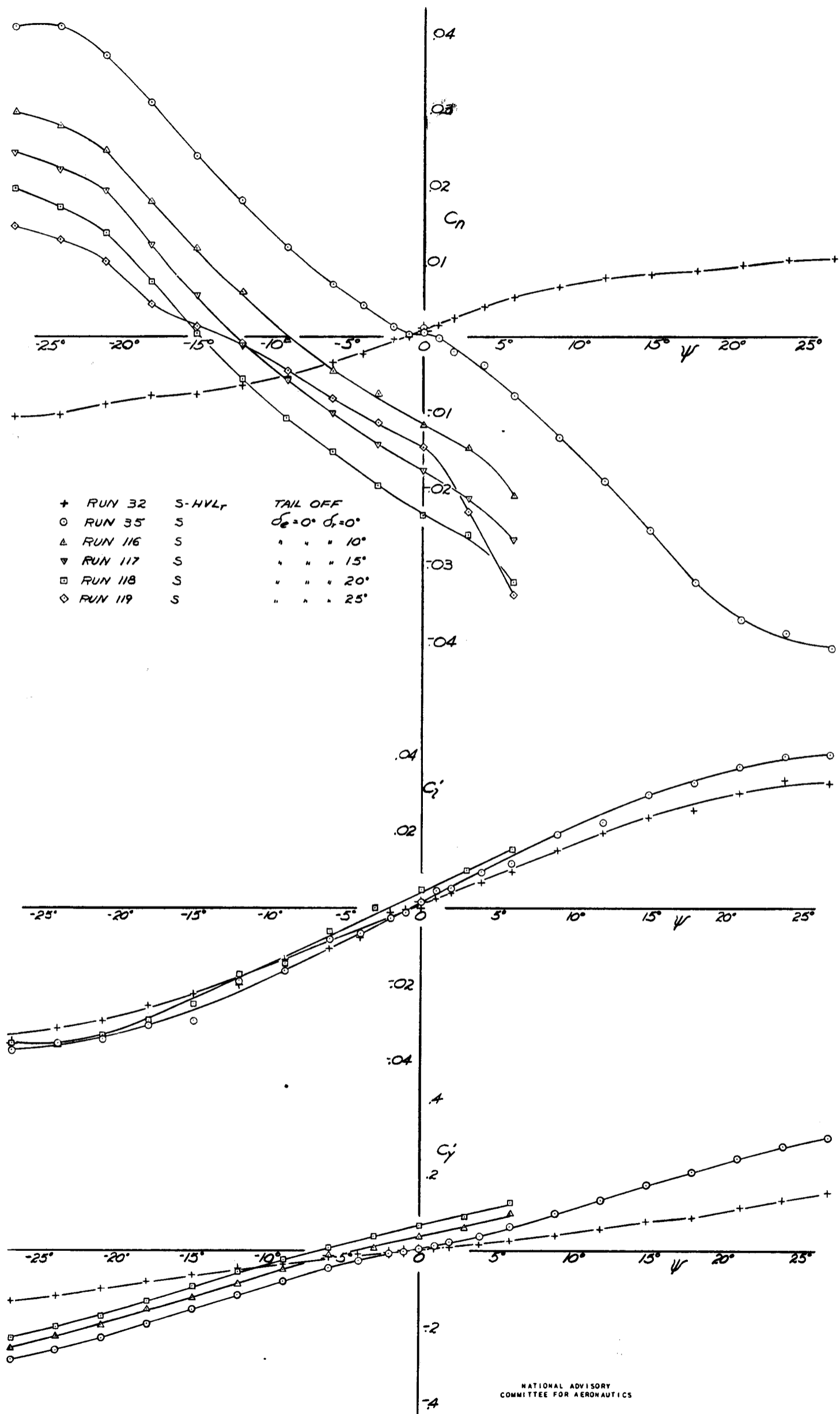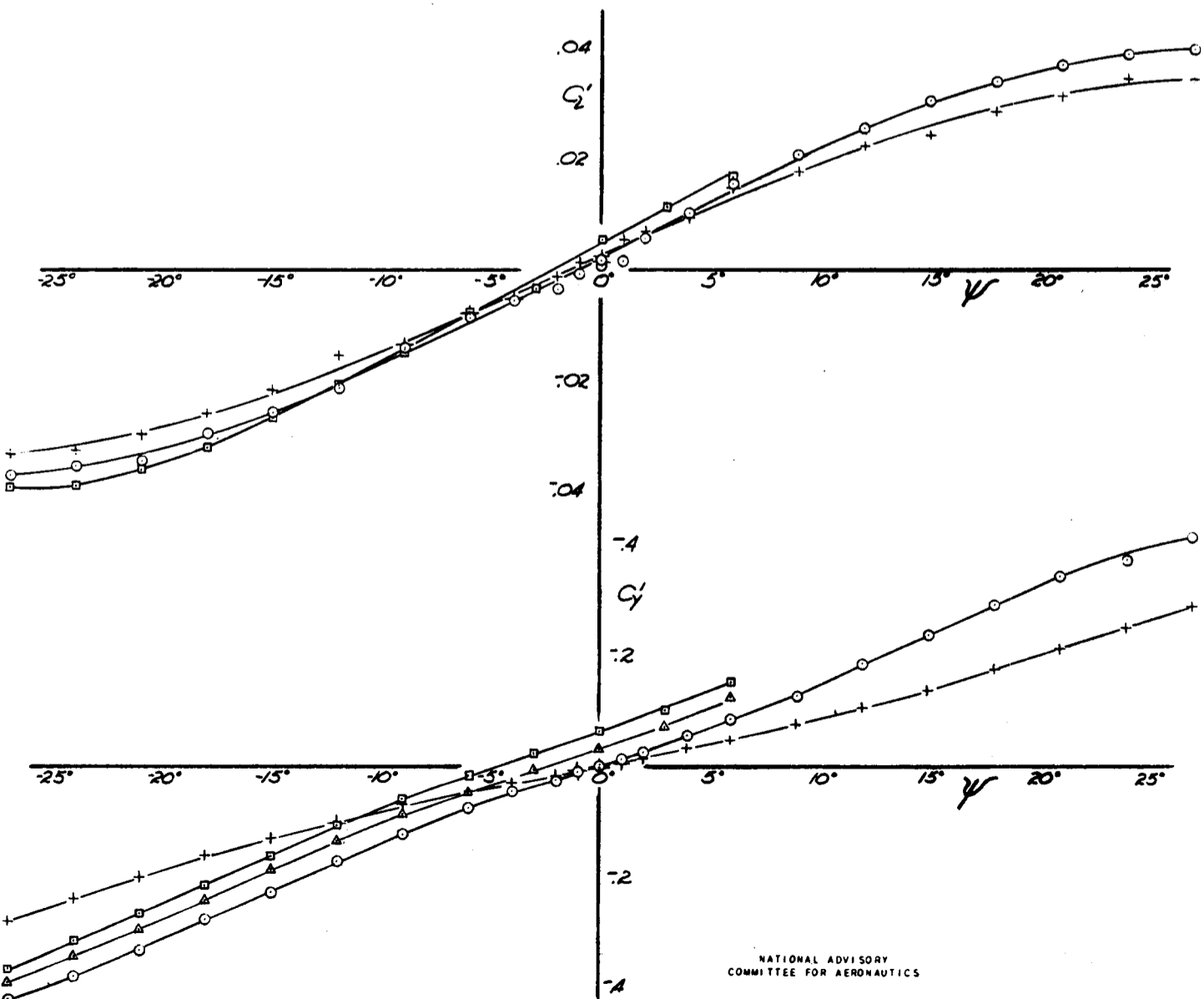FLOATS ON , FLAPS UP , αu =-1°, CL≅.25, ELEVATOR NEUTRAL

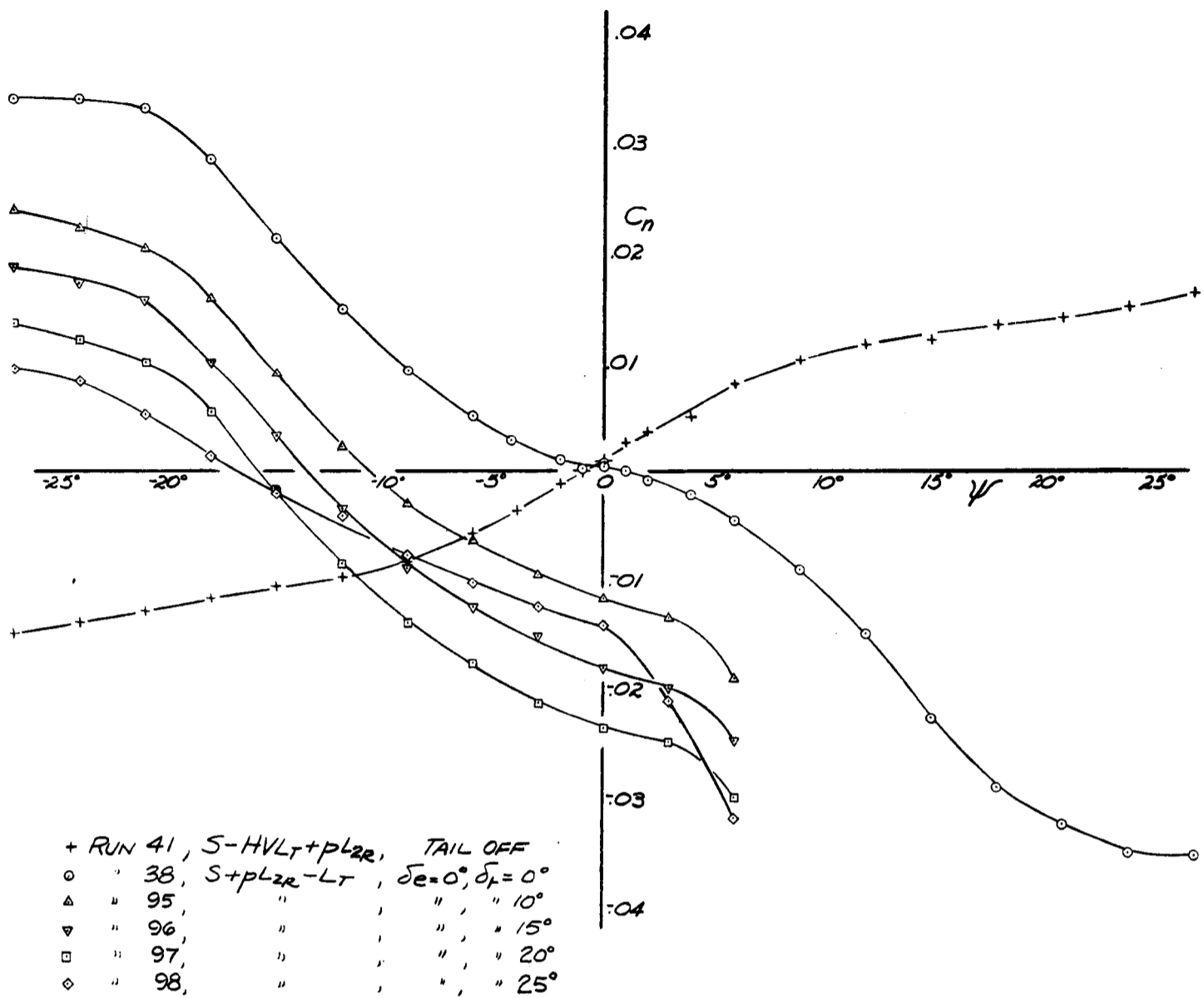|	RUN 32	S-HVL$_r$	TAIL OFF
+	RUN 32	S-HVL$_r$	TAIL OFF
⊙	RUN 35	S	$\delta_e = 0°$ $\delta_r = 0°$
△	RUN 116	S	" " " 10°
▽	RUN 117	S	" " " 15°
⊡	RUN 118	S	" " " 20°
◇	RUN 119	S	" " " 25°

FIG 39 - RUDDER EFFECTIVENESS IN YAW, MODEL WITH
FLOATS OFF, FLAPS UP, $\alpha_u = 6°$, $C_L \cong .9$, ELEVATOR NEUTRAL
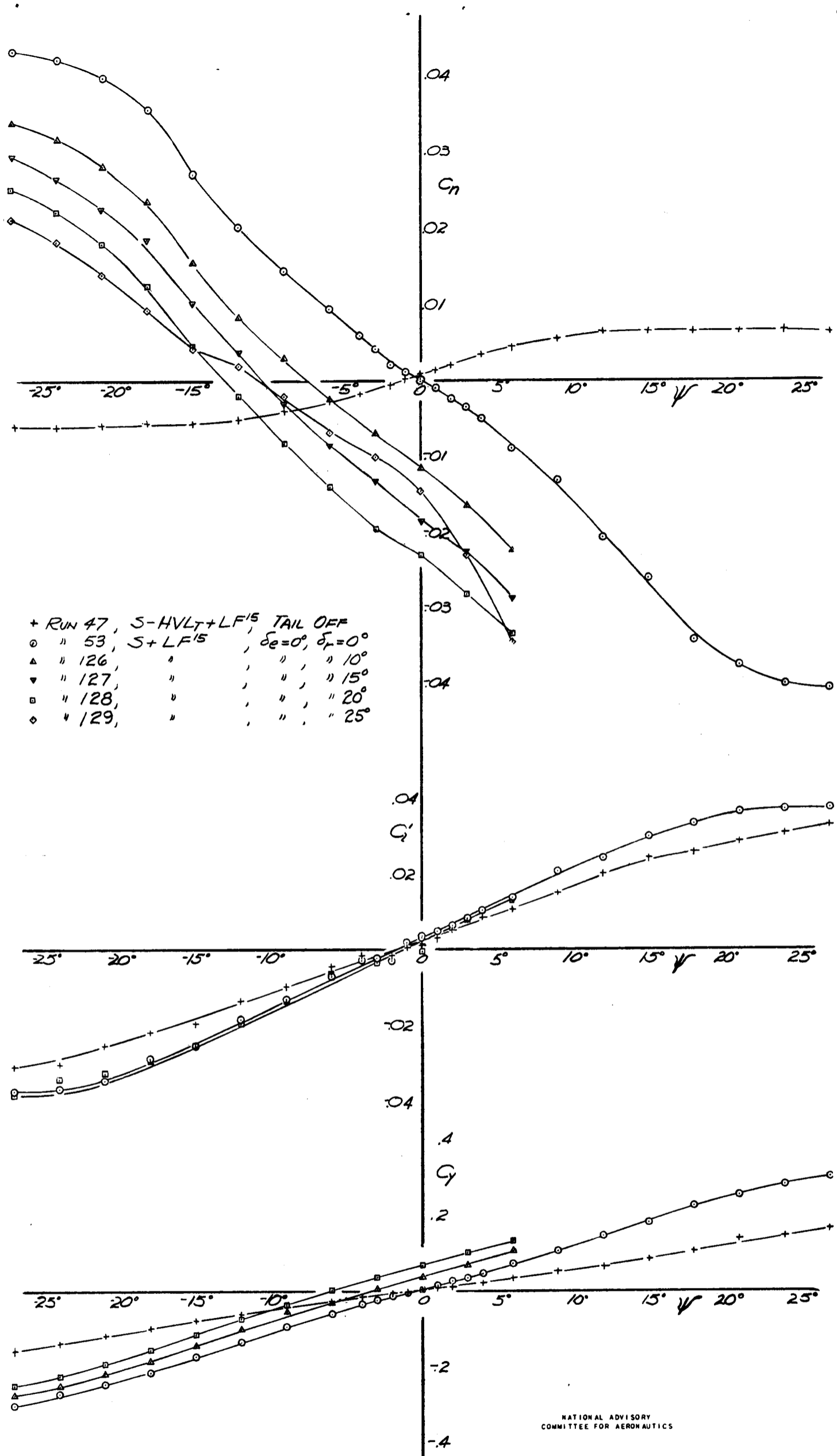
+ RUN 41 , S-HVL_T+pL_{2R}, TAIL OFF
○ " 38, S+pL_{2R}-L_T δe=0° δ_f=0°
△ " 95,   "   ,   " , " 10°
▽ " 96,   "   ,   " , " 15°
□ " 97,   "   ,   " , " 20°
◇ " 98,   "   ,   " , " 25°

FIG 40 - RUDDER EFFECTIVENESS IN YAW ,   MODEL WITH
FLOATS ON , FLAPS UP , α_u=6° , C_L ≅ .9 , ELEVATOR NEUTRAL

+ RUN 47 , S-HVL_T+LF'^{15} TAIL OFF
⊙ " 53 , S+LF'^{15} , δ_e=0°, δ_r=0°
▲ " 126 , " , " , " 10°
▼ " 127 , " , " , " 15°
▣ " 128 , " , " , " 20°
◇ " 129 , " , " , " 25°

FIG. 41 - RUDDER EFFECTIVENESS IN YAW, MODEL WITH
FLOATS OFF , FLAPS DOWN 15°, α_n=6°, C_L≅1.15 , ELEVATOR NEUTRAL

	RUN 45	$S-HYL_T + pL_{2_R} + F'^S$	TAIL OFF
+	RUN 45	$S-HYL_T + pL_{2_R} + F'^S$	TAIL OFF
o	RUN 55	$S + pL_{2_R} + F'^S - L_T$	$\delta_r = 0°$
△	RUN 136	" " " "	" = 10°
▽	RUN 137	" " " "	" = 15°
□	RUN 138	" " " "	" = 20°
◇	RUN 139	" " " "	" = 25°

FIG. 42 · RUDDER EFFECTIVENESS IN YAW, MODEL WITH FLOATS ON, FLAPS DOWN 15°, $\alpha_u = 6°$, $C_L \cong 1.15$, ELEVATOR NEUTRAL

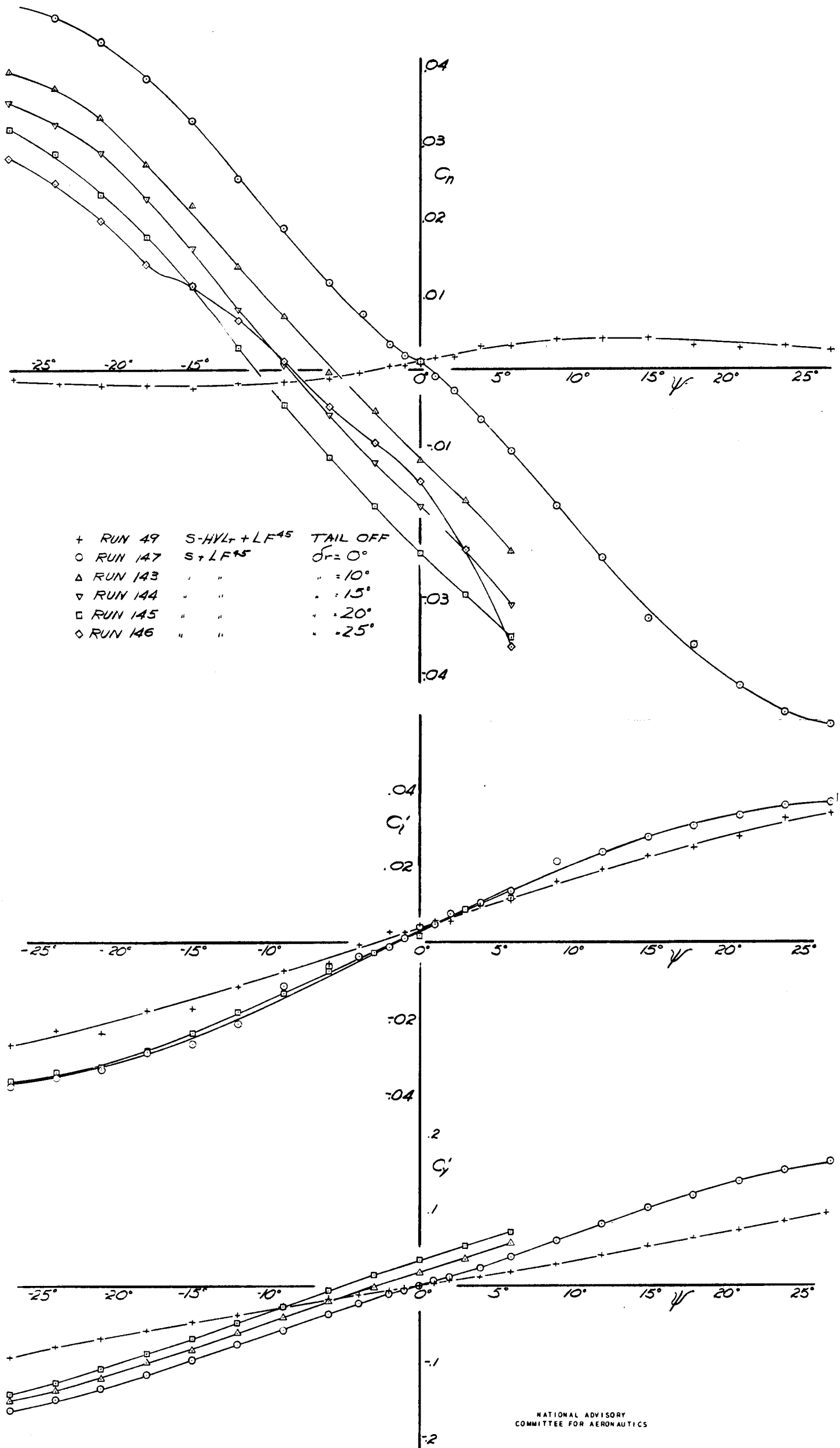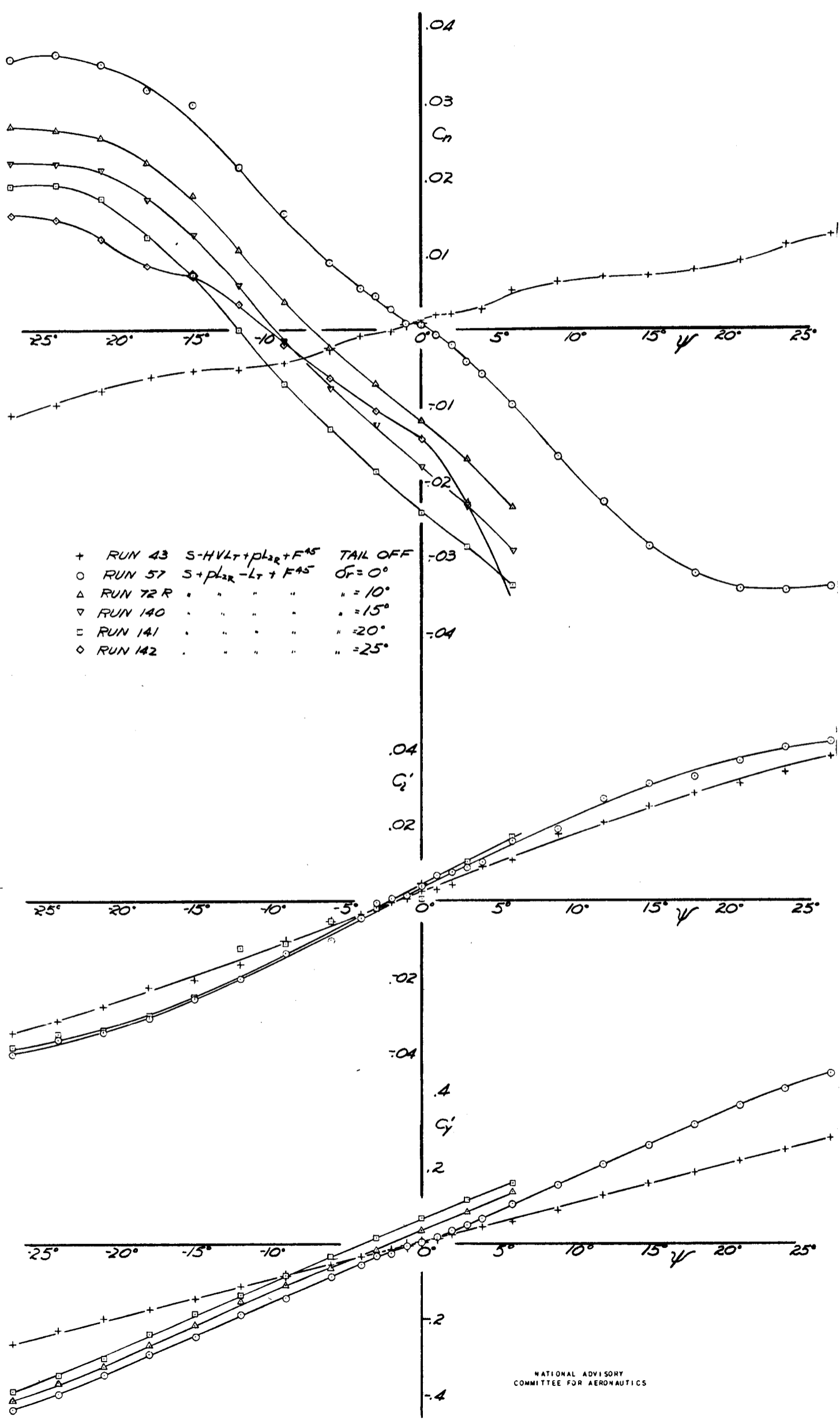| + | RUN 49 | $S\text{-}HVL_T + LF^{45}$ | TAIL OFF |
○	RUN 147	$S + LF^{45}$	$\delta_r = 0°$
△	RUN 143	,,	,, $= 10°$
▽	RUN 144	,, ,,	. $= 15°$
□	RUN 145	,, ,,	,, . $20°$
◇	RUN 146	,, ,,	. . $25°$

FIG 43 - RUDDER EFFECTIVENESS IN YAW, MODEL WITH
FLOATS OFF, FLAPS DOWN 45°, $\alpha_u = 6°$, $C_L \cong 1.4$
ELEVATOR NEUTRAL

C_n

.04
.03
.02
.01
-.01
-.02
-.03
-.04

-25° -20° -15° -10° -5° 0° 5° 10° 15° 20° 25° ψ

+	RUN 43	$S-HVL_T+pl_{2R}+F^{45}$ TAIL OFF
o	RUN 57	$S+pl_{2R}-L_T+F^{45}$ $\delta_r=0°$
△	RUN 72 R	" " " " " $=10°$
▽	RUN 140	" " " " " $=15°$
□	RUN 141	" " " " " $=20°$
◇	RUN 142	" " " " " $=25°$

C_l'

.04
.02
-.02
-.04

-25° -20° -15° -10° -5° 0° 5° 10° 15° 20° 25° ψ

C_Y'

.4
.2
-.2
-.4

-25° -20° -15° -10° -5° 0° 5° 10° 15° 20° 25° ψ
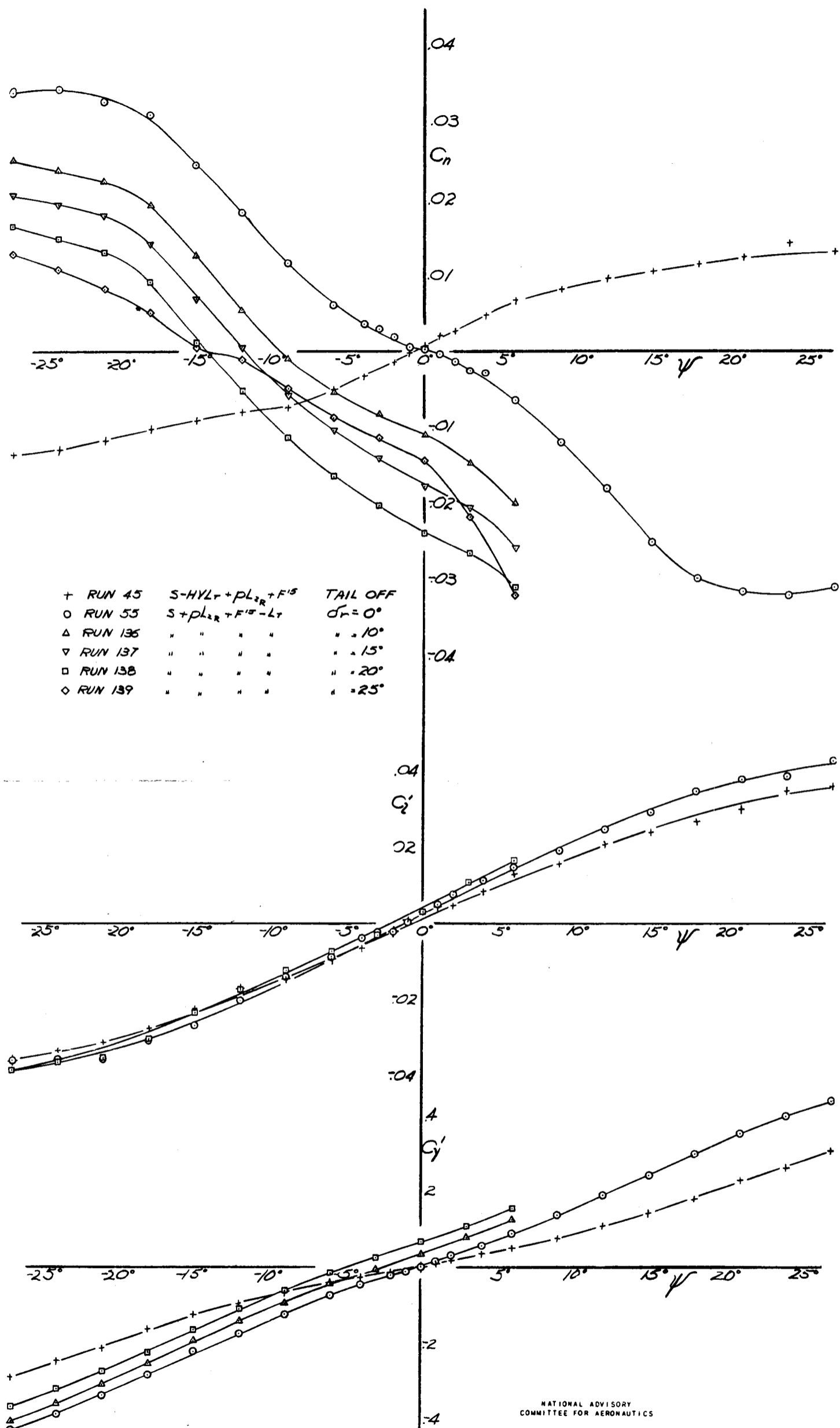
Fig. 44 - RUDDER EFFECTIVENESS IN YAW, MODEL WITH
FLOATS ON, FLAPS DOWN 45°, $\alpha_u=6°$, $C_L\cong1.4$,
ELEVATOR NEUTRAL

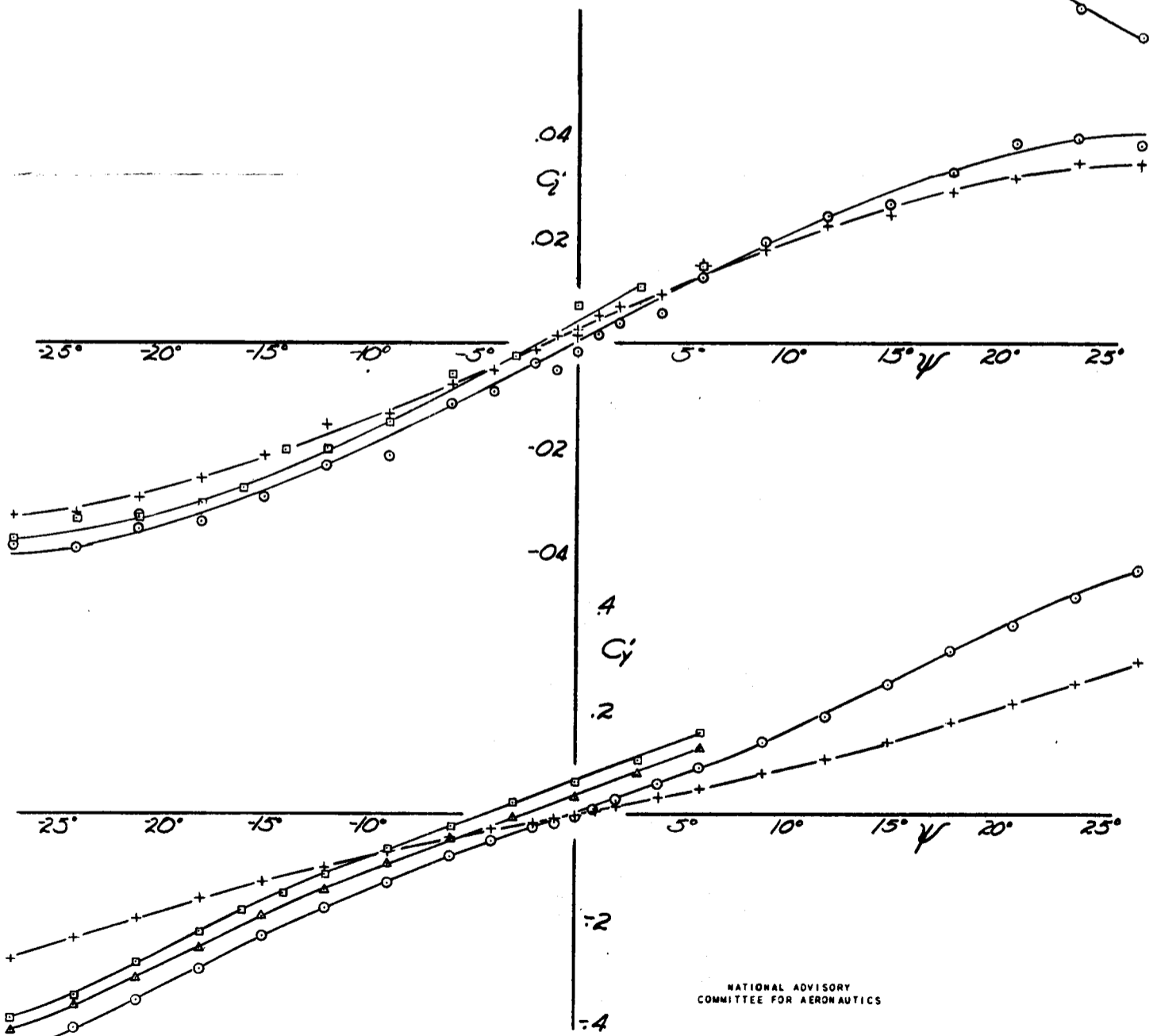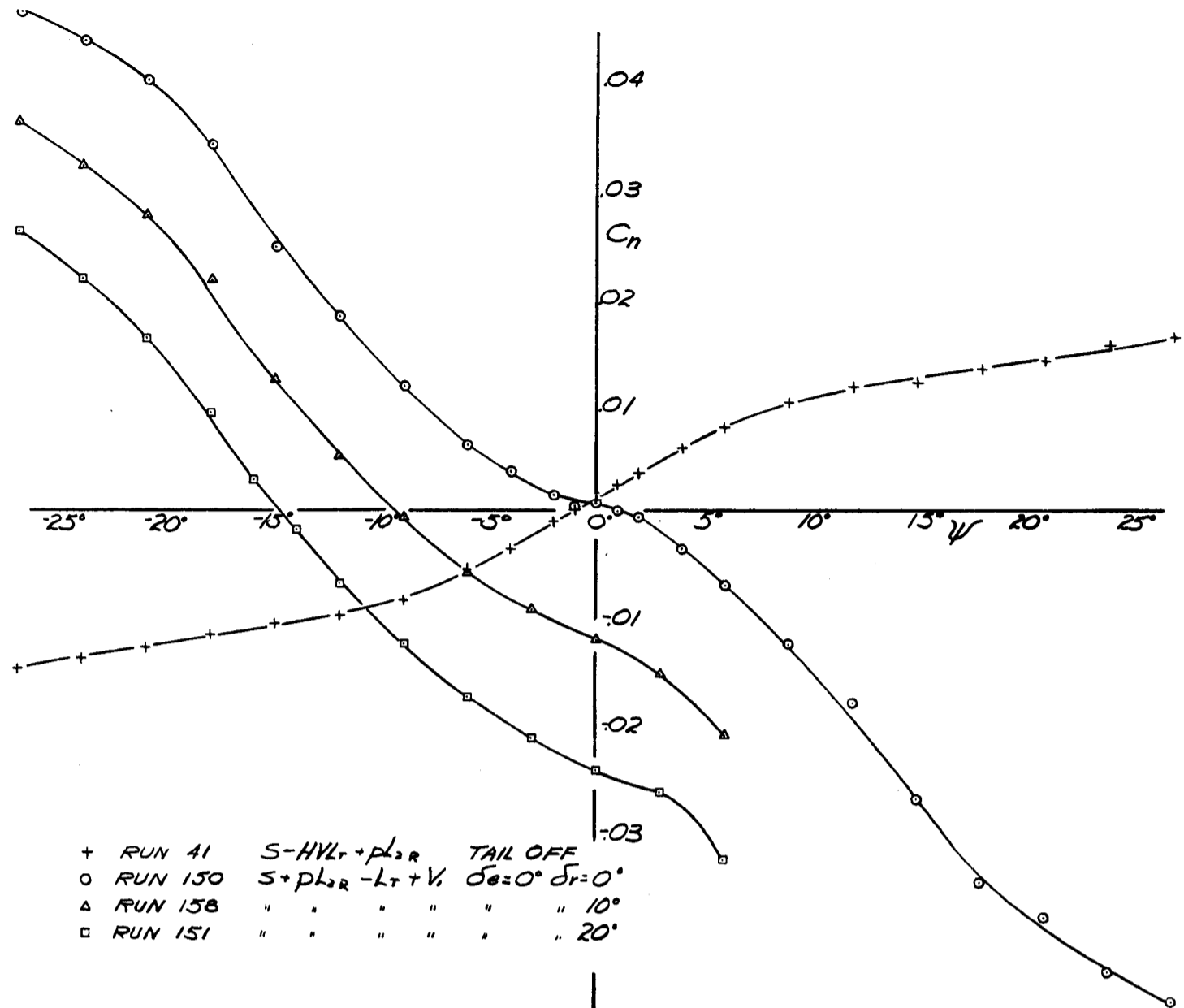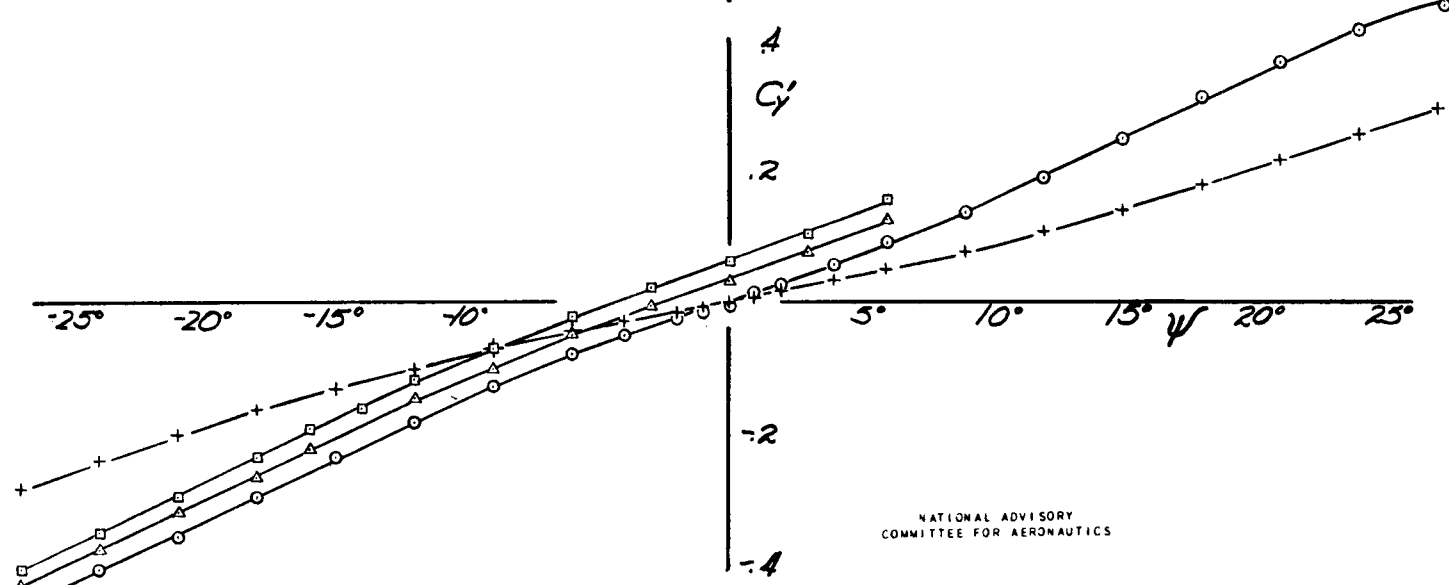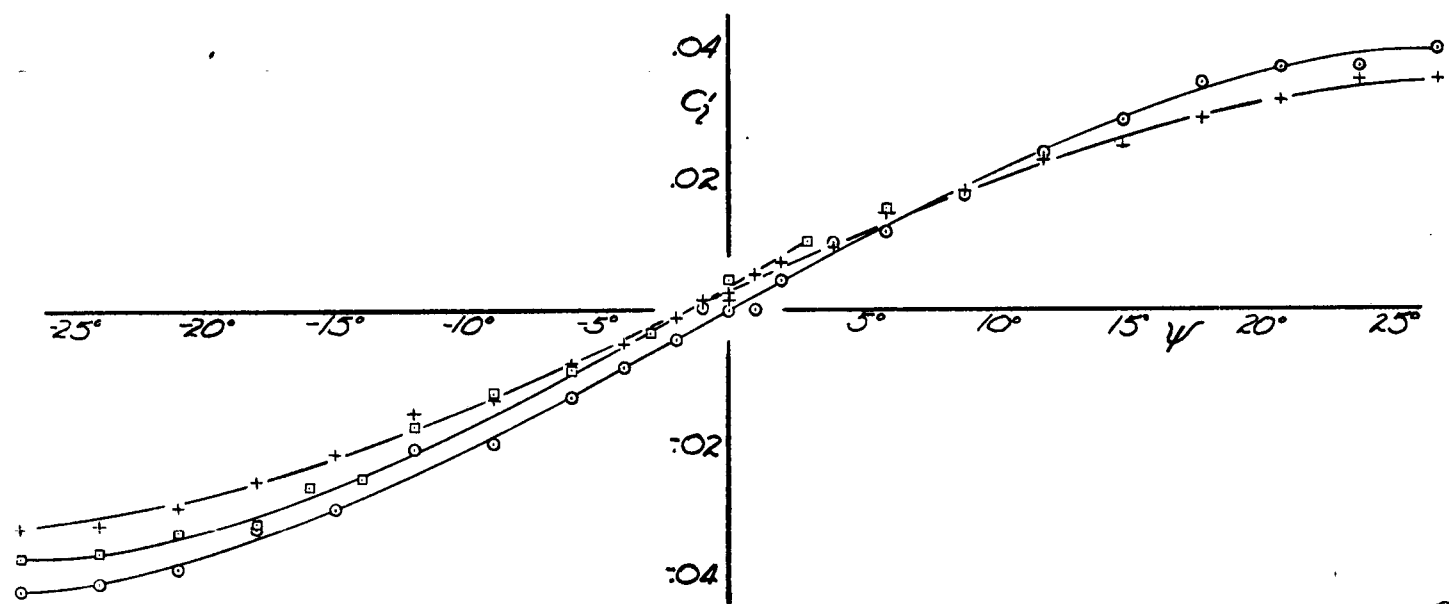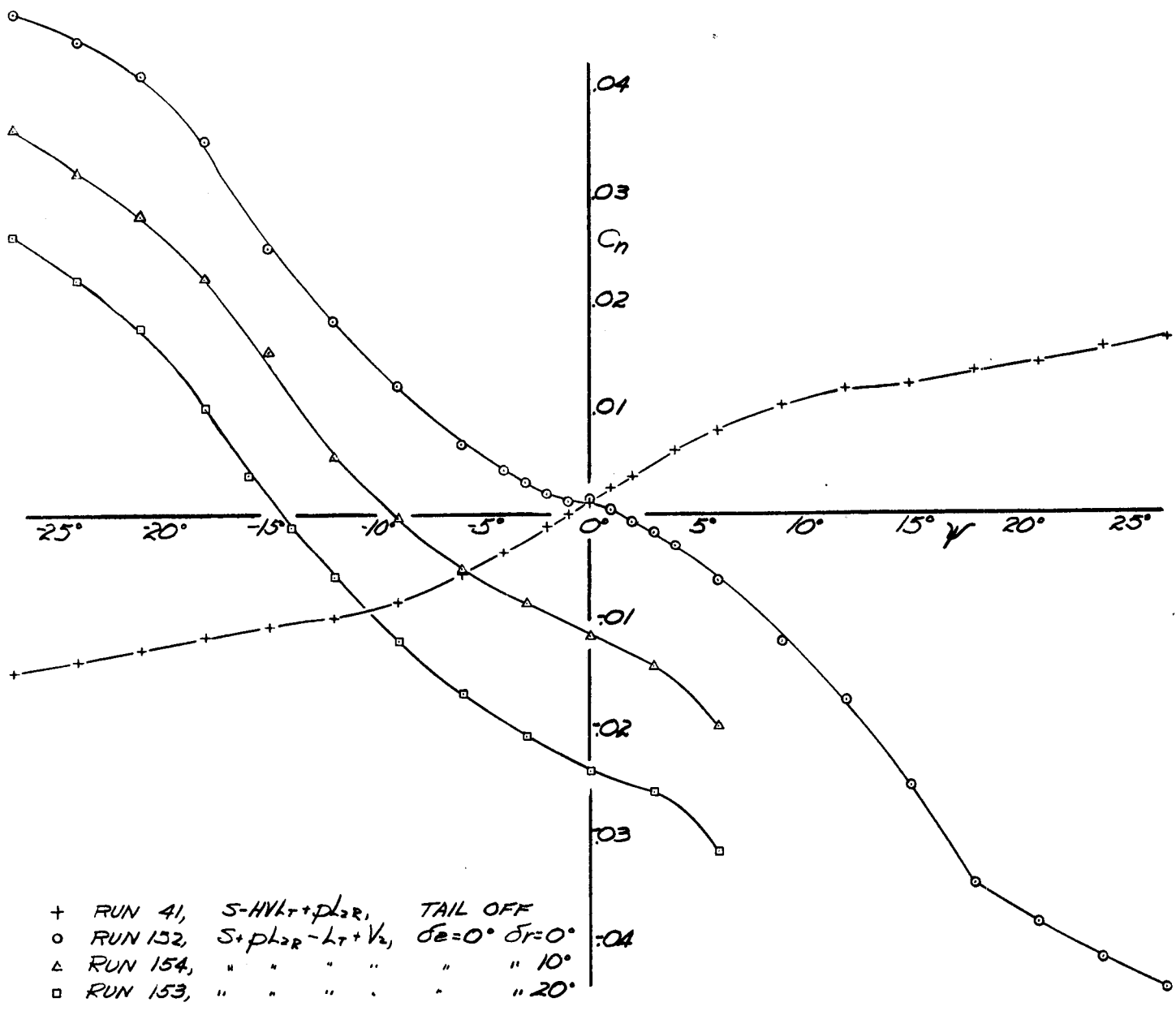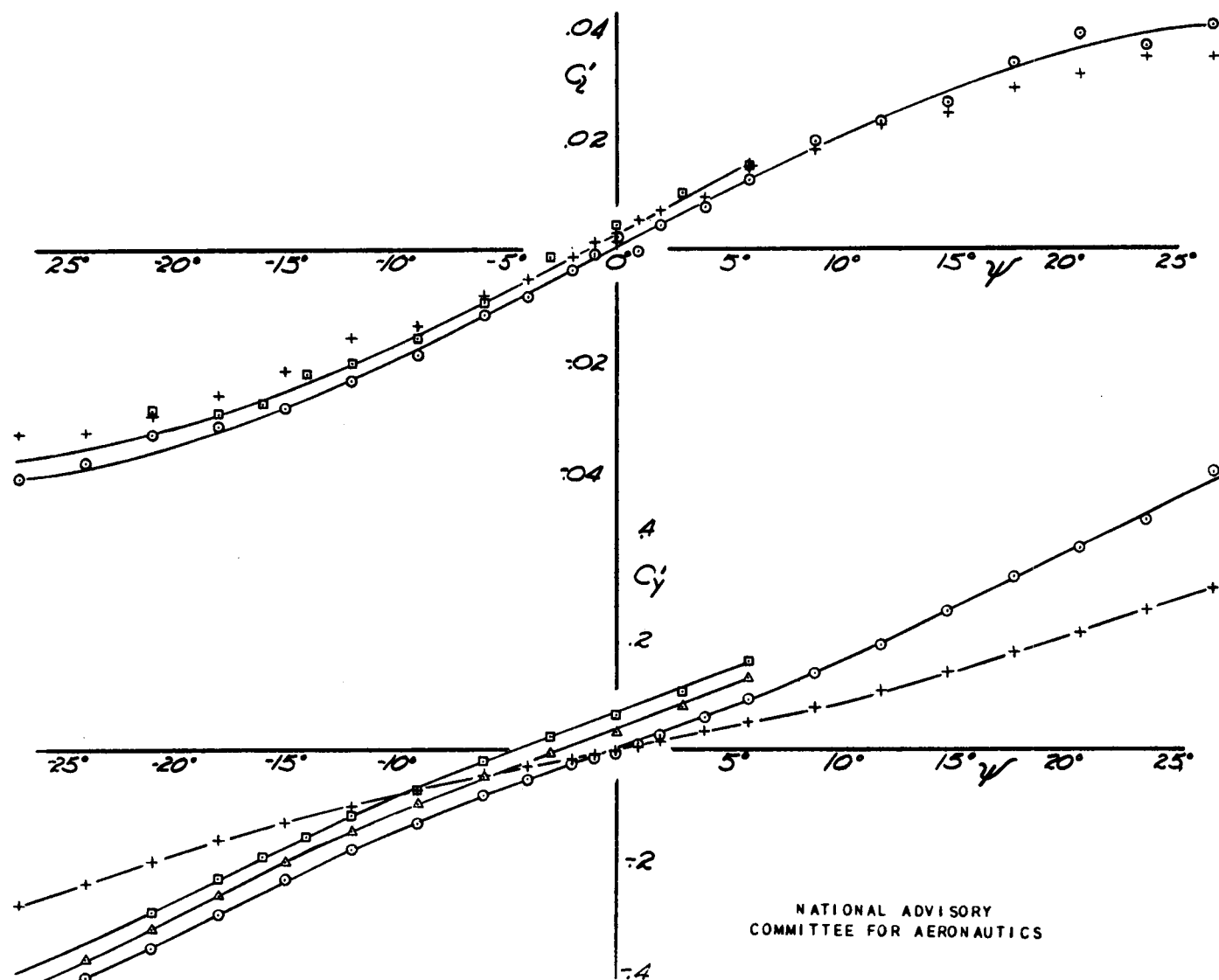FIG. 45- RUDDER EFFECTIVENESS IN YAW, MODEL WITH
TRIANGULAR SKID FIN (V₁), FLOATS ON, FLAPS UP, α_u=6°, C_L=.9
ELEVATOR NEUTRAL

+ RUN 41   S-HVL_T + ph_3R   TAIL OFF
o RUN 150   S+ph_3R -L_T + V.   δe=0° δr=0°
△ RUN 158   "   "   "   "   " 10°
□ RUN 151   "   "   "   "   " 20°

NATIONAL ADVISORY
COMMITTEE FOR AERONAUTICS

+ RUN 41,   S-HVl_T+pl_{2R},   TAIL OFF
o RUN 152, S+pl_{2R}-l_T+V_2,   δe=0° δr=0°
△ RUN 154, "   "   "   "   "   " " 10°
□ RUN 153, "   "   "   "   "   " " 20°
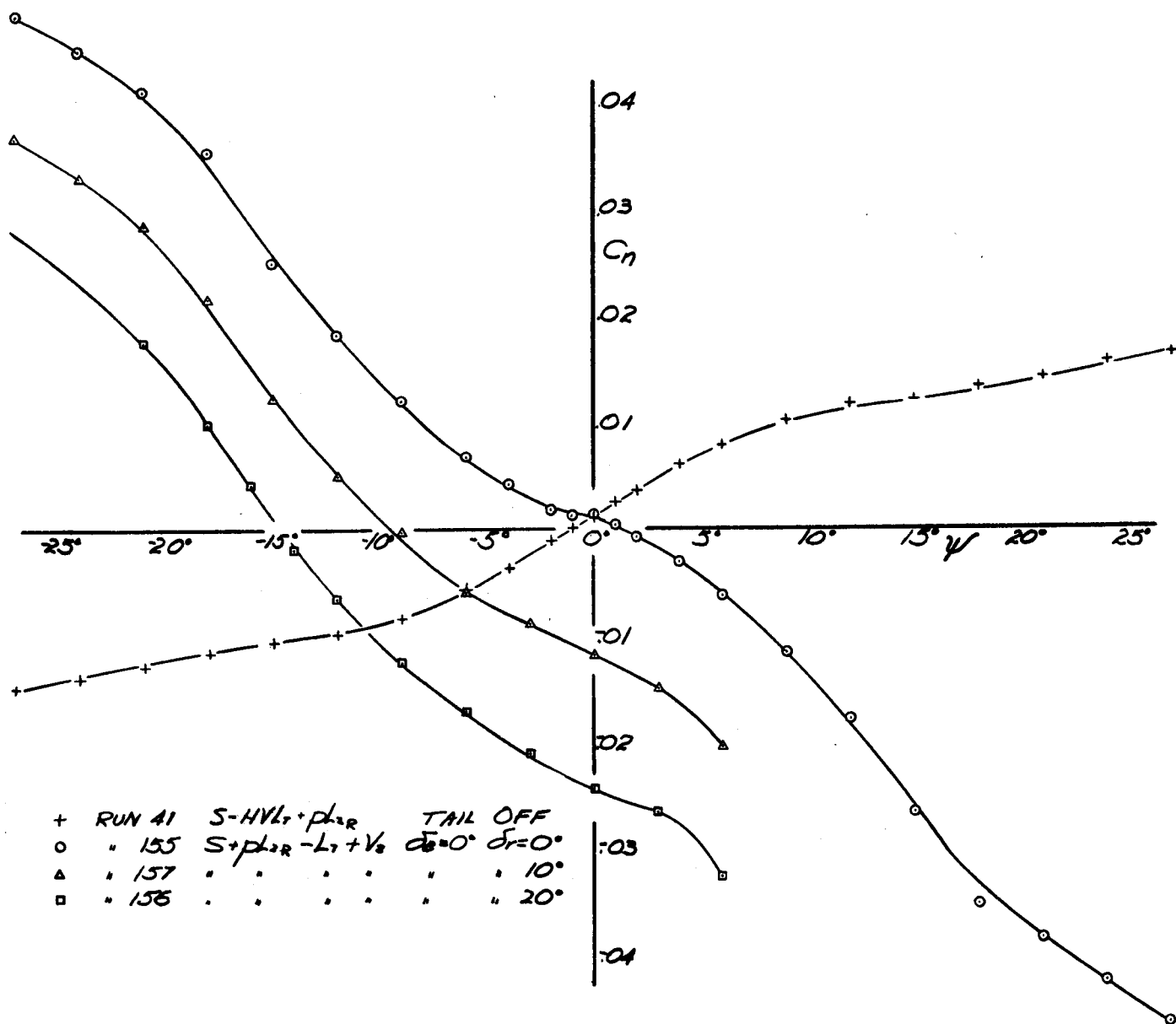
FIG. 46 - RUDDER EFFECTIVENESS IN YAW,   MODEL WITH
SMALL RECTANGULAR SKID FIN (V_2), FLOATS ON, FLAPS UP, α_u=6°, C_L=.9
ELEVATOR NEUTRAL

+ RUN 41 S-HVl_T+pl₂R TAIL OFF
○ " 155 S+pl₂R-L₇+V₈ δ_e=0° δ_r=0°
△ " 157 " " " " " " 10°
□ " 156 " " " " " " 20°

FIG. 47- RUDDER EFFECTIVENESS IN YAW, MODEL WITH
LARGE RECTANGULAR SKID FIN (V₈), FLOATS ON, FLAPS UP, α_u=6°, C_L=.9
ELEVATOR NEUTRAL

.04

.03

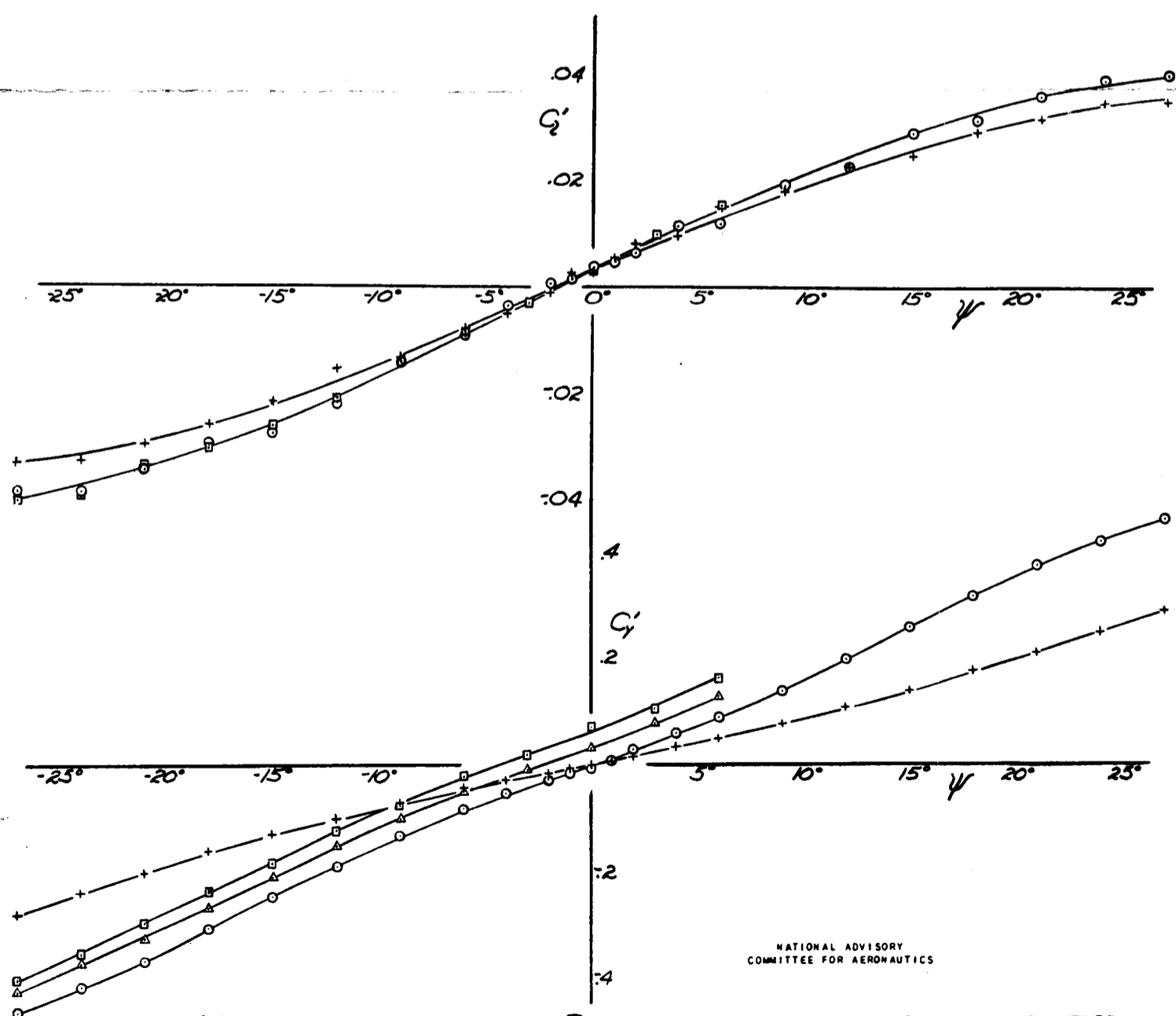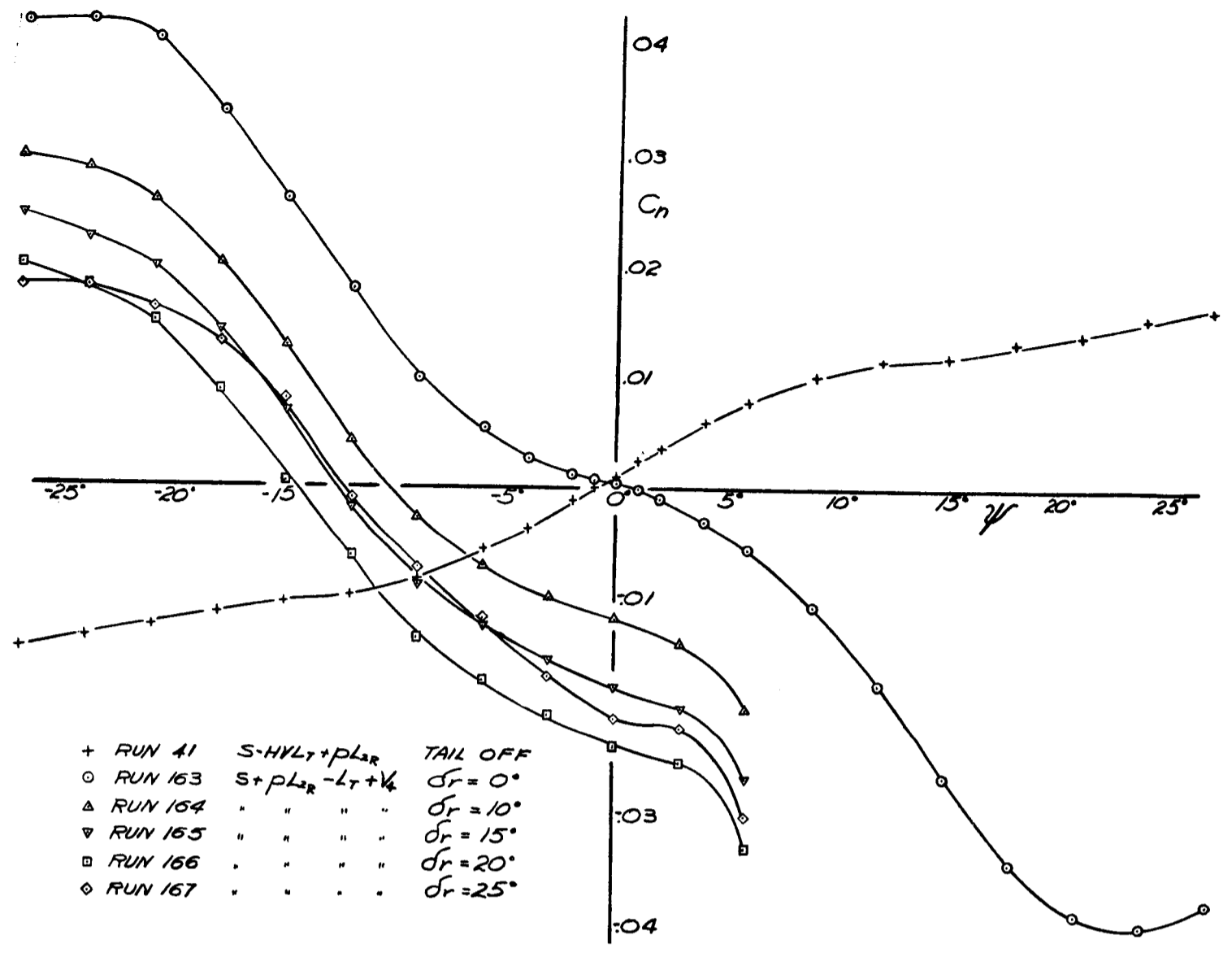C_n

.02

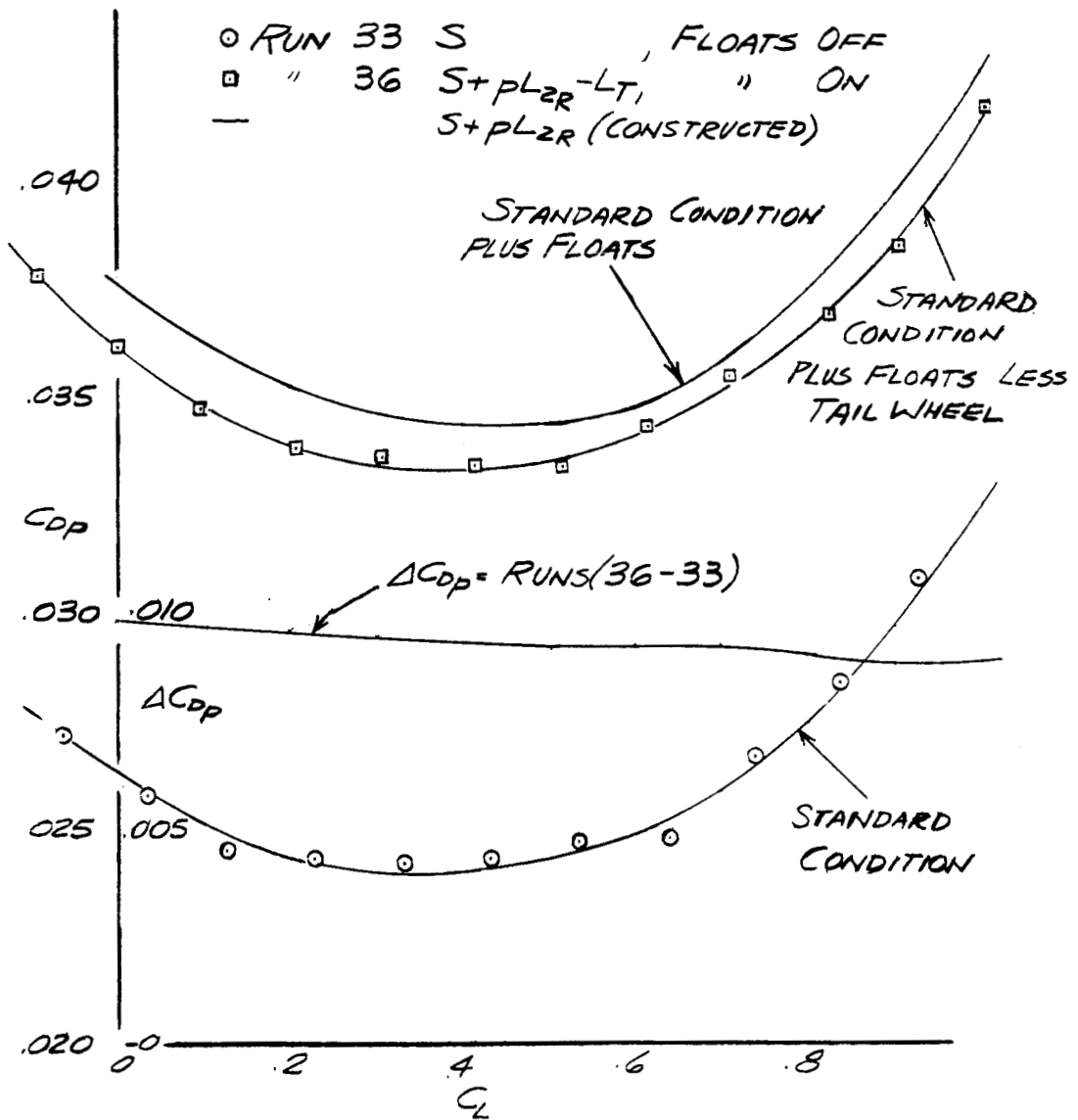.01

-25° -20° -15° -5° O 5° 10° 15° ψ 20° 25°

-.01

-.02

+ RUN 41   S·HVL$_T$ +pL_{2R} TAIL OFF
⊙ RUN 163   S + pL_{2R} -L_T + V$_4$ δ_r = O°
△ RUN 164   "   "   "   " δ_r = 10°
▽ RUN 165   "   "   "   " δ_r = 15°
▢ RUN 166   "   "   "   " δ_r = 20°
◇ RUN 167   "   "   "   " δ_r = 25°

-.03

-.04

.04

C_l'

.02

-25° -20° -15° -10° -5° O° 5° 10° 15° ψ 20° 25°

-.02

-.04

.4

C_Y'

.2

-25° -20° -15° -10° -5° 5° 10° 15° ψ 20° 25°

-.2

-.4

NATIONAL ADVISORY
COMMITTEE FOR AERONAUTICS

FIG 48- LATERAL STABILITY AND RUDDER EFFECTIVENESS CHARACTERISTICS
OF THE MODEL WITH A LEADING EDGE FIN EXTENSION (V$_4$) α_u = 6°,
FLOATS ON, FLAPS UP, ELEVATOR NEUTRAL, C_L ≅ 0.9.

○ RUN 33 S , FLOATS OFF
□ " 36 S+pL₂R−LT₁ " ON
— S+pL₂R (CONSTRUCTED)

STANDARD CONDITION PLUS FLOATS

STANDARD CONDITION PLUS FLOATS LESS TAIL WHEEL

ΔC_{Dp} = RUNS (36−33)

STANDARD CONDITION

C_{Dp}

ΔC_{Dp}

.040
.035
.030   .010
.025   .005
.020   0
       0   .2   .4   .6   .8

C_L

FIG. 49 − MINIMUM DRAG CHARACTERISTICS, MODEL WITH FLOATS ON AND OFF, TAIL ON, FLAPS UP.